Jacob – an activity-regulated morphogenetic factor for synapto-dendritic cytoarchitecture

DISSERTATION

zur Erlangung des akademischen Grades

doctor rerum naturalium

(Dr. rer. nat.)

genehmigt durch die Fakultät für Naturwissenschaften
der Otto-von-Guericke-Universität Magdeburg

von Diplom-Physiologin Irina Zdobnova
geboren am 15.07.1977 in Ryzan, Russia

Gutachter: Prof. Dr. E. D. Gundelfinger
Prof. Dr. D. Kuhl

eingereicht am: 24.10.2007
verteidigt am: 07.07.2008

Acknowledgments

This work was performed from July 2002 till April 2007 at the Leibniz Institute for Neurobiology, Department of Neurochemistry and Molecular Biology headed by Prof. Dr. Eckart D. Gundelfinger, The study was supported by graduate program "Biologische Grundlagen von Erkrankungen des Nervensystems", Otto von Guericke University, Magdeburg.

Here, I would like to thank all colleagues and friends who have helped during my studies for making my experience in the lab both educational and pleasurable.

First of all I would like to thank my supervisor Dr. Michael R. Kreutz, for giving me the opportunity to do my PhD in his group. I sincerely appreciate his suggestions, help and support.

I sincerely appreciated Prof. Dr. Eckart D. Gundelfinger for the scientific suggestions and endless scientific discussions during numerous seminars, and also for his interest in my work and constructive critic.

I would like to acknowledge the enthusiasm and critic of Prof. Dr. G. Reiser, head of Graduiertenkolleg. I thank also all students of Graduiertenkolleg for support and friendship.

Special thanks to my collaborator Dr. Heiner Sann for his experimental contribution to this work.

I would like to express my large gratitude to Dr. Anna Karpova for her interest in this work, invaluable assistance in confocal laserscan microscopy and friendly support.

Special thanks are dedicated to Dr. Christina Spilker for critically reading this thesis, helpful suggestions and constructive comments.

My appreciation also goes to Dr. Peter Landgraf for his kind help in solving technical problems, helpful suggestions and encouragement.

I would like to thank for technical support from Dr. Werner Zuschratter, Monica Marunde and Corinna Borutzki as well as all other colleagues in The Leibniz Institute for Neurobiology for the good atmosphere and their friendly cooperation.

I want to thank Martin Kreutz for introducing me to the secrets of cell cultures. I also sincerely appreciated the scientific suggestions and endless scientific discussions of my Ph.D. fellows, especially Daniela Dieterich, Marco Landwehr, Marina Mikhaylova, Imbritt Konig, Jale Sahin.

And many thanks to everyone who helped in any way contributing to this Ph.D. thesis.

Finally, I want to thank my parents, my brother, and my husband as well as my best friends, who supported and encouraged me during all this time, they deserve my deep gratitude.

Erklärung

Hiermit erkläre ich, dass ich die von mir eingereichte Dissertation mit dem Thema **”Jacob – an activity-regulated morphogenetic factor for synapto-dendritic cytoarchitecture„** selbständig verfasst, nicht schon als Dissertation verwendet habe und die benutzten Hilfsmittel und Quellen vollständig angegeben wurden.

Weiterhin erkläre ich, dass ich weder diese noch eine andere Arbeit zur Erlangung des akademischen Grades doctor rerum naturalium (Dr.rer.nat.) an anderen Einrichtungen eingereicht habe.

_____ _____

(Ort, Datum) (Irina Zdobnova)

Index:

Summary

N-methyl-D-aspartate (NMDA) receptor-mediated calcium signaling plays an essential role in many processes in neurons such as nuclear gene transcription and synaptic plasticity. Calcium-dependent signaling from the synapses to the nucleus can result in long-lasting changes of synaptic input and dendritic cytoarchitecture. Moreover, the site of calcium entry can determine the biological outcome of the signal and therefore calcium channel-associated signaling complexes might have a key role in mediating the selective activation on gene transcription programs in response to calcium influx.

The neuronal calcium-sensor protein Caldendrin is highly enriched in dendrites including dendritic spines and tightly associated with the postsynaptic density (PSD). At elevated calcium levels Caldendrin binds to Jacob – a newly identified brain-specific protein. Jacob displays a distribution similar to that of Caldendrin in the PSD and dendritic spines but, in contrast to Caldendrin, is also found in neuronal nuclei. Jacob harbors a bipartite nuclear localization signal (NLS) in its central α-helical region and translocates to the nucleus in response to NMDA receptor activation. Immunofluorescence studies in primary hippocampal neurons demonstrate that the presence of the NLS sequence is essential for Jacob's nuclear transport. Moreover, after enhanced synaptic activation Caldendrin binds Jacob and masks Jacob's NLS, and thereby interferes with Jacob's nuclear recruitment. Furthermore, nuclear accumulation of Jacob is mainly initiated by calcium flux through extrasynaptic NMDA receptors, triggers the Ca2+/cAMP-responsive element binding protein (CREB) shut-off pathway and in consequence, negatively regulates CREB target gene expression, which results in cell death. Nuclear knockdown of Jacob prevents CREB shut-off after extrasynaptic NMDA receptor activation. Moreover, overexpression experiments show that nuclear accumulation of Jacob has a drastic negative effect on synapto-dendritic architecture, whereas overexpression of extranuclear Jacob leads to an increased number of dendrites and the formation of PSD-like structures that eventually promote formation of dendritic protrusions with multiple active synaptic contacts. It could be proposed that Jacob in the nucleus either blocks an essential nuclear signaling pathway required to prevent the removal of synaptic input or regulates the expression of genes that will destabilize synapses. On the other hand, overexpression of extranuclear Jacob triggers the formation of huge PSD-like structures in neurons suggesting that the presence of Jacob in synapses could be a stabilizing factor for the synaptic PSD and prevents spine dismantling. Altogether these data suggest that Jacob can be recruited via Caldendrin binding only in the extensively activated synapse and this recruitment leads to stabilization of the existing PSD or recruitment of new PSD-proteins and therefore strengthening of the synapse, whereas less activated synapses could not recruit Jacob and will be removed by a mechanism that involves the nuclear accumulation of Jacob. These findings are discussed in the context of homeostatic plasticity mechanisms that must exist to keep the system functional throughout live.

1 Introduction

The human brain contains about 100 billion nerve cells, each forming as many as thousand connections with other neurons. Alteration in the number and nature of the interconnections between individual neurons is widely assumed to be the mechanism by which memory traces are encoded and stored in the central nervous system (Martin, et al., 2000; Daoudal and Debanne, 2003). Nerve cells communicate with each other through contact points called synapses. The efficiency of information flow through synapses – synaptic transmission – determines the activity patterns of neuronal networks. Synapses are highly dynamic 'plastic' structures, and corresponding dynamic changes in the efficiency of synaptic transmission are thought to represent the physiological basis of learning and memory (Antonova, 2001; Engert and Bonhoeffer, 1999). Synaptic activity can induce a variety of changes within postsynaptic neurons, ranging from transient posttranslational modifications to altered programs of gene expression, and it is thought that synaptic activity by itself triggers signaling pathways to the nucleus that will eventually control transcriptional regulation. This indicates that signals generated at the synapse must be transported to the nucleus, where they are converted into changes in gene expression. First, a signal from distal synapse must travel along the length of the axon or dendrite to reach the nucleus and this distance can be extremely large. If translocation of molecules to the nucleus can be initiated at a single synapse and does not result from the net activity, the second problem arises: the amount of protein needed in the nucleus to be relevant for gene transcription is relatively high as compared to protein concentration in single dendritic spines (Deisseroth et al., 2003). Moreover, the translocation to the nucleus would dilute this concentration at least 2000-fold with respect to the much larger nuclear volume (Lodish et al., 2001). On the other hand, it is assumed that activity-dependent synaptic plasticity is induced at synapses that originally evoked the activity. This is necessary for the formation of privileged pathways of activity between appropriate nerve cells during memory formation. It evokes the next very important questions: which type of gene transcription is necessary for long-term plasticity processes and how does altered gene expression feed back to the activated synapses that originally induced it?

1.1 The neuron : structure, dynamics and regulation

Neurons are highly polarized cells with distinct subcellular compartments, including one or multiple dendritic processes arising from the cell body, and a single, extended axon.

The dendritic tree grows by the addition and elongation of branches. Primary dendrites emerge from the cell body, and branch to form secondary and then tertiary dendrites. However, the branching patterns of neurons are not random; rather, they are unique to each cell type in the central nervous system (CNS) (Jan and Jan, 2003). Neurons with distinct dendritic morphology typically perform different signal processing and computations for their particular physiological functions (Euler and Denk, 2001; Hausser and Mel, 2003; Wong and Ghosh, 2002). Communication between neurons involves synapses formed between axons of the presynaptic neurons and dendrites of the postsynaptic neurons. The transmission of the synaptic signal to the soma is affected by the branching pattern of the dendritic tree, and the striking variations in dendritic morphology in the CNS therefore have important consequences for neuronal information processing (Häusser et al., 2000). Thus, a neuron's dendrite does not develop in isolation but dendrites are surrounded by neighbouring neurons and glia. The acquisition of a mature dendritic morphology depends on the coordinated action of a number of different intra- and extracellular factors (Cline, 2001; Gao and Bogert, 2003; Jan and Jan, 2001; McAllister, 2000; Scott and Luo, 2001; Whitford et al., 2002; Wong and Ghosh, 2002).

One of the most important factors, which influence dendritic remodeling during development, is neuronal activity (Wong and Wong, 2001; McAllister, 2000; Whitford et al., 2002), although it is still not known how activity exerts its effects. The timing of afferent innervation and synapse formation coincides with the period of maximum growth and dendritic remodeling, and recent studies underscore the importance of afferent activity in regulating dendritic development (Wong and Ghosh, 2002). However, there are controversial data about the influence of neuronal activity on dendritic remodeling. Rocha and Sur (1995) and later Luthi and colleagues (2001) showed that blockade of NMDA receptors *in vivo* and in organotypic slice cultures resulted in a more complex arborization of the dendritic tree and a substantial increase in synapse number. On the other hand, it was shown that pharmacological blockade of NMDA receptors markedly reduces dendritic growth in the *Xenopus* tectum (Rajan and Cline, 1998), in spinal motor neurons (Kalb, 1994) and in the supraoptic nucleus (Chavaleyre et al., 2002). An interesting observation in this regard was reported by Lohmann and colleagues (2002): they demonstrated that chick retinal ganglion cells displayed two patterns of spontaneous calcium increases in their dendrites, one global and the second involving neurotransmitter-mediated local 'flashes' of calcium. By differentially inhibiting these increases, they were able to show that blockade of local, but not global activity caused rapid dendritic retraction, supporting the idea that sustained neurotransmitter evoked calcium-mediated signals locally stabilize dendritic

arbors. A similar observation was made by Vaillant and coworkers (2002) when they found that in cultured sympathetic neurons activity was sufficient to induce dendrite formation, and withdrawal of the activity led to complete dendritic retraction.

Although afferent activity can shape dendritic arborizations, it is not well understood how neurotransmission can locally regulate dendritic structure, allowing or causing retraction of some processes, but promoting stability and even growth of others. What are the signaling mechanisms underlying these effects?

1.2 Signaling from synapse to nucleus

Long-lasting structural changes in a dendrite require *de novo* protein synthesis and mRNA formation. Accordingly, synaptic activity has to be signaled to the nucleus to regulate gene transcription. Signals from the cytoplasm to the nucleus can be conveyed in several different ways (Fig. 1). First, the transcription factor itself can move to the nucleus upon changes in its phosphorylation state. For example, nuclear factor of activated T-cells c4 (NFATc4), which is expressed in hippocampal neurons, undergoes a translocation from the cytosol to the nucleus upon the opening of L-type calcium channels. The translocation step is dependent upon calcineurin-mediated dephosphorylation of NFATc4, which causes the unmasking of multiple nuclear localization signals and the active transport of the transcription factor through the nuclear pore complex (Graef et al., 1999).

Second, some transcriptional regulators are modulated by directly sensing calcium-levels that can arise in the nucleus after neuronal excitation (Lipscombe et al., 1988). The transcription factor downstream regulatory element antagonistic modulator (DREAM), a calcium-binding protein that contains three active calcium-binding motifs (EF-hands) (Carrion et al., 1999; Osawa et al., 2001), is abundant in the nucleus. It has been proposed that nuclear DREAM remains bound to a downstream regulatory element (DRE) that acts as a gene silencer when nuclear calcium is low, but dissociates upon elevation of calcium causing DRE derepression and activation of downstream genes (Carrion et al., 1999).

The other well characterized Ca^{2+}-activated transcriptional event is the synaptic-activity dependent phosphorylation of the transcription factor Ca^{2+}/cAMP responsive element binding protein (CREB). In this case, the translocating message is not conveyed by free Ca^{2+}-moving from the ion channels to the nucleus, or by the transcription factor CREB by itself, but by Ca^{2+}-dependent activation of signaling cascades. In fact, CREB remains constitutively bound to CRE (Ca^{2+}/cAMP responsive element) regulatory sites controlling

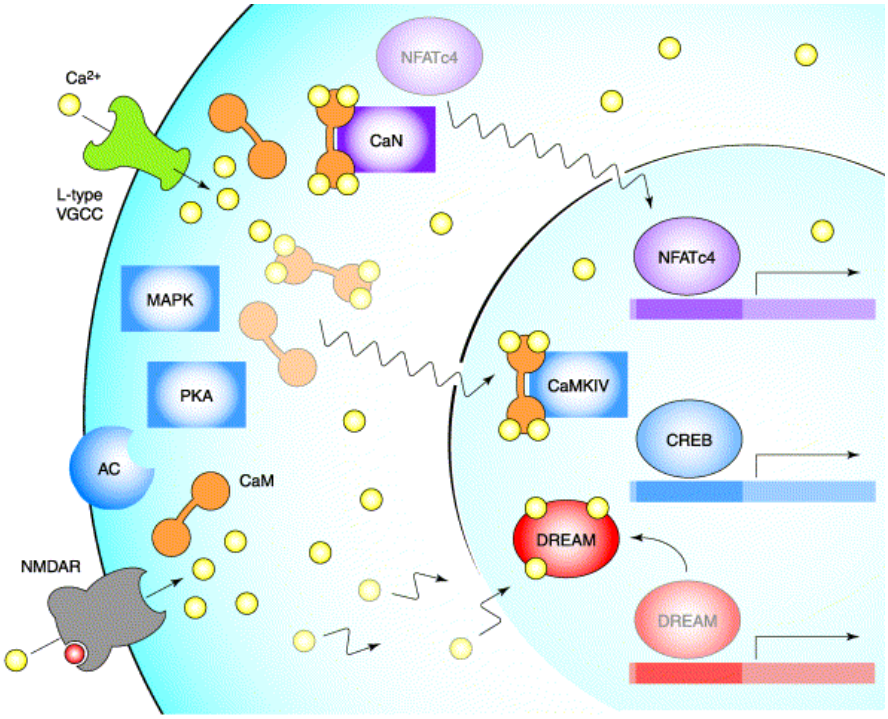

Fig. 1 Signaling from the membrane to the nucleus: multiple strategies for information transfer. A snapshot image of the early stages (0–5 min) of activity-dependent gene expression. Following rises in intracellular calcium (Ca^{2+}), DREAM dissociates from DNA resulting in the lifting of transcriptional repression. Within seconds of calcium entry through L-type calcium channels and NMDA receptors, CaM translocates to the nucleus, supporting CREB phosphorylation through activation of CaMKIV. Nearly as rapid, NFATc4 also undergoes translocation to the nucleus following its dephosphorylation by calcineurin (CaN) (from ref. Deisseroth et al., 2003).

target genes, and becomes activated by phosphorylation on its Ser-133 residue. A fast Calmodulin (CaM) -dependent kinase cascade and a slow mitogen-activated protein kinase (MAPK) cascade (likely to be cAMP-modulated) converge on Ser-133 following surface membrane depolarization and calcium influx, and work together to promote CREB-dependent gene expression (West et al., 2002; Wu et al., 2001a).

There are many signaling molecules that mediate the transduction of synaptic signals to transcriptional regulation in the nucleus at different levels, but calcium seems to be a key component of synapse-to-nucleus communication. Calcium levels can be altered locally in neurons in several ways. First, NMDA receptors, AMPA receptors (AMPARs) and neuronal nicotinic cholinergic receptors (nAChRs) are permeable to calcium. Second, the opening of voltage-gated calcium channels (VGCC) in response to membrane depolarization leads to an influx of calcium from the extracellular environment. Third, calcium is released from intracellular stores by the binding of inositol-1,4,5-triphosphate ($Ins(1,4,5)P_3$) and ryanodine, or by calcium-induced calcium release (CICR) from the endoplasmic reticulum. The endoplasmic reticulum is present in dendritic shafts and spines,

and it is strategically positioned adjacent to the plasmalemma to sense local changes in the environment (Berridge 1998; Bootman et al., 2001; Spacek and Harris 1997).

The influx of calcium through different types of channels differs in its ability to activate gene transcription (Bading, 1993). Calcium influx through L-type VGCCs and NMDA receptors in particular is tightly coupled to CREB activation. The localized elevation of calcium just beneath sites of calcium entry is sufficient to trigger the phosphorylation of CREB at Ser-133 even when the global cytoplasmic calcium rise is blocked, consistent with the hypothesis that signaling pathways are activated close to or at calcium channels (Deisseroth et al., 1996, 2003; Dolmetsch et al., 2001; West et al., 2002). Interestingly, rise of intracellular calcium-levels from other sources like intracellular calcium-stores or P/Q- and N-type calcium-channels are ineffective to trigger the crucial phosphorylation of CREB at Ser-133.

The special role of the NMDA receptor and the L-type channel may be attributable to their selective ability to directly bind CaM and therefore, recruit CaM signaling (Deisseroth et.al., 1998), both are also specifically localized at or near synapses, in which additional pools of CaM are present for recruitment. Therefore, either or both mechanisms may underlie the selective ability of these channels to initiate locally Ca^{2+}/CaM-activated MAP kinase signaling or fast CaM-dependent kinase cascade converging on Ser-133 of CREB in the cell nuclei (Deisseroth et al., 1998; Dolmetsch et al., 2001; Mermelstein et al., 2001; Hardingham et al., 2001a; Wu et al., 2001a, b). All these studies indicate that channel-associated signaling complex might have a key role in mediating the selective activation on gene-transcription programs in response to calcium influx.

1.3 The calcium-binding protein Caldendrin and its binding partner Jacob

CaM is the prototype of a ubiquitously expressed calcium-sensor protein. In its calcium-bound state it alters the properties of several other proteins and signaling cascades that have been implicated in diverse functions (Berridge, 1998; Ikura, 1996). However, a large variety of other EF-hand proteins have been identified, among them neuronal calcium-sensor (NCS) proteins, which are present exclusively in neurons and are therefore supposed to serve more specific functions in neuronal cells (Braunewell and Gundelfinger, 1999; Burgoyne and Weiss, 2001; Burgoyne et al., 2004).

One of these NCS proteins is the exclusively neuronal EF-hand protein Caldendrin (also termed CaBP1) (Seidenbecher et al., 1998; Haeseleer et al., 2000). Caldendrin is the

closest relative of CaM in brain. It contains in its C-terminal half four EF-hand sequence motifs, the second of which is cryptic and incapable to bind calcium (Fig. 2) (Seidenbecher et al., 1998, 2002). This non-functional EF-hand of Caldendrin is highly conserved in different species during vertebrate evolution. The unique N-terminal half of Caldendrin exhibits no similarity to other known proteins (Seidenbecher et al., 1998).

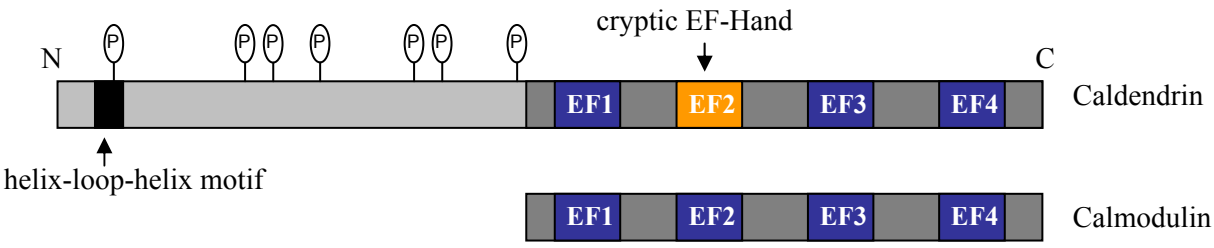

Fig. 2 Schematic illustration of the Caldendrin and Calmodulin primary structures.
Schematic drawing of the Caldendrin (top) and Calmodulin (bottom) domain organisation. Phosphorylation sites (ellipses with 'P'), functional (blue rectangles) and non-functional (orange rectangle) EF-hands are depicted.

Caldendrin is tightly associated with the cortical cytoskeleton and the PSD fraction of synaptic proteins. It is, however, only present in a subset of synapses and seems to be exclusively associated with the somatodendritic cytoskeleton of mature principal neurons in brain regions with a laminar organization (Seidenbecher et al., 1998; Laube et al., 2002). As Caldendrin has evolved relatively late during vertebrate evolution (Seidenbecher et al., 2002) and because of its unique features Caldendrin might exert distinct cellular functions associated with specific requirements for somato-dendritic calcium signaling of principal neurons. In search for Caldendrin binding partners, a novel brain-specific protein, termed Jacob (Fig. 3), was identified using a Yeast-2-Hybrid-Assay (by Dr. Michael R. Kreutz).

The Jacob gene displays a complex organization with 16 exons, most of which are smaller than 120 bp and separated by relatively small introns (Daniela Dieterich, Ph.D. thesis, 2003). Different splice variants were identified resulting in different Jacob isoforms with different molecular weights. Sequence alignment of human, rat and murine Jacob revealed a high degree of conservation between these species (98% identity at the amino acid level between rat and mouse; 95% rat or mouse versus human). Searches in public databases of lower vertebrates, *Drosophila, Caenorhabditis elegans, Escherichia coli*, yeast and plants did not reveal any significant sequence similarities suggesting that Jacob has appeared late during evolution.

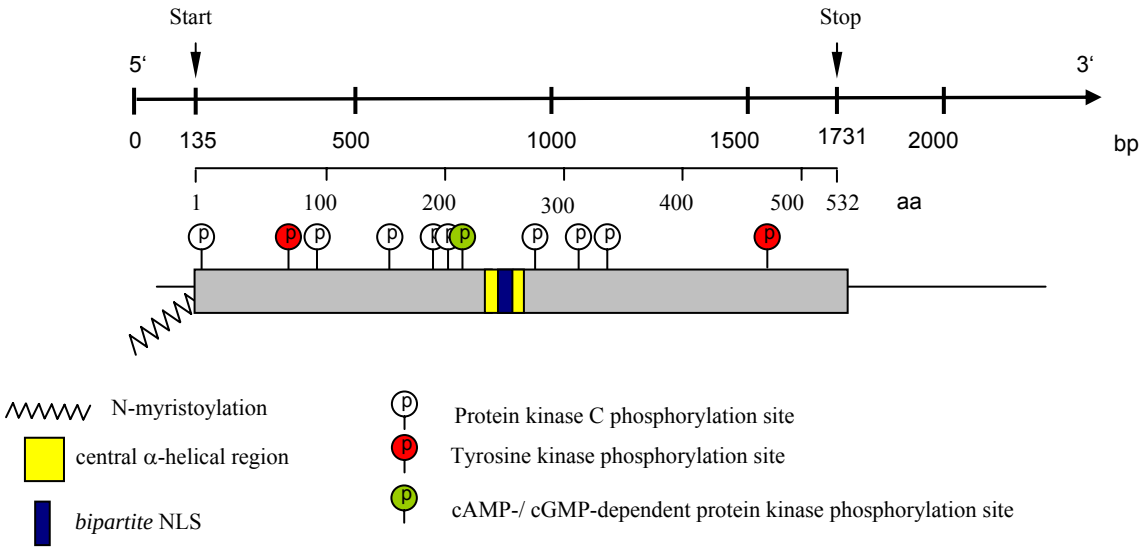

Fig. 3 Schematic illustration of the Jacob primary structure.
Schematic drawing of the protein (bottom) encoded by the Jacob cDNA (top). N-myristoylation motif, bipartite nuclear localization signal (NLS), central α-helical region and phosphorylation sites are depicted.

In situ hybridization experiments revealed a strikingly restricted expression of Jacob transcripts in the limbic brain and cortical areas similar to that of Caldendrin (Laube et al., 2002). The highest levels of Jacob mRNA are present in cerebral cortex, hippocampus, olfactory bulb, thalamus and amygdala and this distribution almost identical for all splice variants of Jacob (Daniela Dieterich, Ph.D. thesis, 2003). The distribution of the Jacob protein revealed a similar pattern as the *in situ* hybridization studies: Jacob is abundant in cortex and limbic brain structures including amygdala, thalamus and hippocampus. At the cellular level, particularly intense staining was observed in the somato-dendritic compartment of pyramidal cells in cortex and hippocampus. Jacob and Caldendrin distribution demonstrate significant overlap in dendritic processes and spines (Laube et al., 2002; Seidenbecher et al., 1998; Daniela Dieterich, Ph.D. thesis, 2003).

Moreover, Jacob and Caldendrin were only present in a subset of ProSAP2/Shank3-positive synapses (Daniela Dieterich, Ph.D. thesis, 2003). In contrast to Caldendrin, intense Jacob immunoreactivity (IR) was also seen in neuronal nuclei. Moreover, it was found that Jacob translocates to the nucleus in response to NMDA receptor activation. Jacob IR increases significantly in neuronal nuclei within 30 min after NMDA receptor activation with highest levels following 2h. Nuclear Jacob IR returned to control levels within 4h. No recruitment of Caldendrin to the nucleus was observed (Daniela Dieterich, Ph.D. thesis, 2003). Due to this synapto-nuclear localization and the NMDA-receptor-activation driven nuclear import, Jacob is well suited for the coupling of signals from excitatory synapses to nuclear gene

transcription, moreover, the time course of Jacob's nuclear accumulation is in favor for a role in the regulation of gene transcription that could be responsible for the induction of protein synthesis underlying neuronal plasticity processes (Bading, 2000).

Analysis of the primary structure of Jacob revealed a putative myristoylation motif at the N-terminus end of the protein (Daniela Dieterich, Ph.D. thesis, 2003). Myristoylation is a post-translation modification by which myristic acid is covalently attached to the amino-group of an N-terminal glycine residue. It can loosely tether the modified protein to the plasma membrane, endoplasmatic reticulum, mitochondrion or other membrane systems (Resh, 1999). Jacob also harbors a bipartite nuclear localization signal in the middle part of the protein (between amino acids 250-265). A nuclear localization signal is a short stretch of amino acids that mediates the transport of nuclear proteins into the nucleus, which is necessary for the active import through the nuclear pore complex (Boulikas, 1993). Therefore, the presence of both of these motifs - myristoylation and nuclear localization – can play a very important role in protein subcellular localization.

To prove this possibility regarding two Jacob mutants were generated: a deletion mutant in which the six basic amino acid residues between 247-252 were deleted (ΔNLS-Jacob-GFP); and second, a construct in which the crucial glycine at position 2 was mutated to an alanine (ΔMyr-Jacob-GFP). Expression of ΔNLS-Jacob-GFP in COS7 cells led to an extranuclear localization of the mutant protein; in opposite, expression of ΔMyr-Jacob-GFP construct led to an exclusive nuclear localization of the mutant protein. In support of the view that the bipartite NLS is responsible for the nuclear import of Jacob we also found that the cellular localization of the double mutant ΔNLS/ΔMyr-Jacob-GFP is extranuclear in COS7 cells (Daniela Dieterich, Ph.D. thesis, 2003). It was shown previously, that the central part of Jacob containing the NLS is the Caldendrin binding region and that Caldendrin interacts with Jacob in a calcium-dependent manner and this interaction can not be competed by CaM (Daniela Dieterich, Ph.D. thesis, 2003). Therefore, binding of Caldendrin to Jacob can be predicted to reduce or inhibit the accessibility of the Jacob's NLS possibly mediate its association with the dendritic and synaptic cytoskeleton. Since, Jacob binds Caldendrin only in the presence of elevated calcium-levels, increased synaptic activation and the presence or absence of Caldendrin in the respective synapto-dendritic compartment could be important factor controlling Jacob's subcellular localization. Therefore, the Caldendrin-Jacob interaction might play an important role in the transformation of dendritic calcium-signals into morphogenetic signals for the synapto-dendritic cytoarchitecture.

1.4 Aims of the work

Calcium is the pivotal messenger coupling synaptic activity to nuclear gene transcription and calcium-dependent signaling from the synapses to the nucleus can result in long-lasting changes of synaptic inputs and dendritic cytoarchitecture. However, the mechanisms that underlie calcium-dependent synapse-to-nucleus communication remain unclear. Therefore, the major aim of the study was to investigate the possible role of Jacob in the signaling processes underlying activity-dependent nuclear gene transcription involved in structural remodeling of synapto-dendritic cytoarchitecture and therefore determine the new synapse-to-nucleus pathway that underlying long-lasting synapto-dendritic remodeling. Since, Jacob was found in synapto-dendritic compartments and also in neuronal nuclei, the first step was to investigate physiological consequences of the nuclear and extranuclear localization of Jacob. For this purpose primary neuronal cultures were transfected with different mutants and wt-Jacob cDNA. Since, Jacob is recruited to the nucleus in response to NMDA receptor activation (Daniela Dieterich, Ph.D. thesis, 2003), a pharmacological approach was used to investigate the effect of endogenous Jacob redistribution after NMDA receptor activation on synaptogenesis in primary hippocampal neurons.

2 Materials and Methods

2.1 Materials

2.1.1 Chemicals

All chemicals were obtained from Roche, Calbiochem, Clontech, Gibco Life Technologies, Invitrogen, Merck, Roth, Serva and Sigma-Aldrich. Special chemicals and solutions utilized are detailed in the corresponding method descriptions. Solutions were prepared with water purified on a Milli-Q® System, Millipore.

2.1.2 Antibody

2.1.2.1 Primary Antibody

Table 1 Primary antibodies used.

Antibody	Species	Dilution	Firm/Manufacturer
anti-MAP2	mouse, monoclonal	IF: 1:500	Sigma
anti-GFP (rb290)	rabbit, polyclonal	IF: 1:2000	Abcam
anti-Bassoon (mAB7f)	mouse, monoclonal	IF: 1:1000	Dr. W. Altrock
anti-Bassoon (sap7f)	rabbit, polyclonal	IF: 1:1000	Dr. W. Altrock
anti-JB 150	rabbit, polyclonal	IF: 1:200	Dr. Pineda antibody-service/ Dipl.-Biochem. B.Hoffman, Dr. C.I. Seidenbecher
anti-NMDAR 2a	rabbit, polyclonal	IF: 1:500	Chemicon
anti-NMDAR 2b	rabbit, polyclonal	IF: 1:500	Chemicon
anti-GluR 2	mouse, monoclonal	IF: 1:500	Chemicon
anti-ProSAP2	guinea pig, polyclonal	IF: 1:1000	Bockmann et al., 2002, J.Neurochem
anti-PSD95	mouse, monoclonal	IF: 1:1000	clone K28/43 Upstate
anti-pCREB	rabbit, polyclonal	IF: 1:500	Upstate

2.1.2.2 Secondary Antibody

Table 2 Secondary antibodies used.

Antibody	Species	Dilution	Firm/ Manufacturer
anti-mouse IgG, Alexa Fluor™ 488/568-conjugated	goat	1:1000	Molecular Probes

anti-rabbit IgG, Alexa Fluor™ 488/568- conjugated	goat	1:1000	Molecular Probes
anti-guinea pig IgG, Alexa Fluor™ 488/568- conjugated	goat	1:1000	Molecular Probes
anti-mouse IgG, Cy5™-conjugated	goat	1:500	Molecular Probes
anti-rabbit IgG, Cy5™-conjugated	goat	1:500	Dianova
anti-guinea pig IgG, Cy5™-conjugated	goat	1:500	Dianova

2.1.3 Bacterial Nutrient Mediums

Table 2 Media used for growth of bacteria. All media were autoclaved at 121ºC for 15 min.

LB-medium	5 g/l yeast-extract, 10 g/l Bacto-Trypton, 5 g/l NaCl
LB-plate	1000 ml LB-medium, 15 g agar
SOC-medium	20 g/l Bacto-Trypton, 5 g/l yeast-extract, 10 mM NaCl, 2,5 mM KCl, 10 mM Mg_2SO_4, 10 mM $MgCl_2$, 20 mM glucose

2.1.4 Expression constructs

Table 3 Vectors and constructs used in the present study. Rat Jacob (cDNA accession number: AJ293697); rat Caldendrin (cDNA accession number: CAD20347).

Construct (Name)	**Amino acids**	**Vectors**
wt-Jacob-GFP	1-532	pEGFP-N
ΔNLS-Jacob-GFP	1-247 + 252-532	pEGFP-N
ΔMyr-Jacob-GFP	1-532 mutation G2A	pEGFP-N
ΔMyr/ΔNLS-Jacob-GFP	mutation G2A; 1-247 + 252-532	pEGFP-N
Δexon9-Jacob-GFP	1-339	pEGFP-N
C-term-Jacob-GFP	238-532	pEGFP-N
wt-Caldendrin-GFP	1-298	pEGFP-N
ΔMyr/Δexon9-Jacob-GFP	mutation G2A; 1-339	pEGFP-N
siRNA-pRNAt-GFP		pRNAT-H1.1/Hygro

2.1.5 Cell strains

Table 4 Cell strains used in the present work.

Bacteria	E. coli XL1-Blue MRF' (Stratagene)

2.1.6 Animals

Rats *(Rattus Rattus norvegicus*) from the strain Wistar, bred in the Leibniz Institute for Neurobiology, were used for the biochemistry assays and for the preparation of primary neuronal cultures.

2.2 Methods

2.2.1 Molecular biological methods

All molecular biological methods used during the work correspond to standard protocols described by Ausubel et al. (1999) and are outlined in this chapter. All modifications in the standard protocols are described in detail.

2.2.1.1 Polymerase chain reaction (PCR)

PfuTurbo® DNA Polymerase: **Stratagene**
Oligonucleotide (Primer): **Invitrogen**
Deoxynucleoside triphosphate (NTPs): **Roche**

PCR was used for amplification of specific segments of DNA and insertions of restriction sites at the termini of the amplified fragments for further subcloning. Primers that were used in the PCR are listed in Table 5. A reaction mixture (25 µl) included 10-25 ng plasmid-DNA as a template (or DNA which was extracted with Phenol/Chloroform from a chromatin-immunoprecipitate), 10 pM of each primer (forward and reverse) (or hexanucleotide primers), 1mM desoxynucleotidephosphate d(A, C, G, T)TPs, 10 times concentrated reactions buffer, 0,25 U thermostable PfuTurbo®-DNA-Polymerase. Heating reaction tubes to 95ºC for 5 min to denature the double-stranded DNA always preceded PCR temperature cycles. 30-40 cycles were done as following: a) DNA denaturanion (45 sec-1 min 95ºC); b) primer annealing to their complementary sequences in the target DNA (45 sec-1 min 55-60ºC); c) extension (2-3 min 72ºC).

Table 5 Primers used to clone C-term-Jacob. Underlined sequences correspond to restriction sites used for cloning.

Name	Position	Primer sense	Sequence (5'→ 3')	Restriction site
C-term-Jacob	816-836	forward	GCGCGAATTCATG TTCCAGACGGCAA CCACAACT	*EcoRI*
	1707-1730	reverse	GCGCGGATCCCAG GACGTCATCAAAG TCCAGCAG	*BamHI*

2.2.1.2 DNA Restriction

Restriction enzymes: **New England Biolabs, Gibco, Roche**

Restriction enzymes (*EcoRI, BamHI*) were used for digestion of DNA-fragment or plasmid DNA in ratio: 1 U per 1 µg DNA. The reaction mixture was incubated for 1 hour at recommended temperature (37ºC).

2.2.1.3 Agarose-Gel electrophoresis and DNA Elution

Agarose:	**UltraPure, Gibco**
50 x TAE buffer:	**2 M Tris-Acetat, 0.05 M EDTA**
Ethidium bromid solution:	**1 mg/ml, Roth**
6x DNA-loading buffer:	**30 % (volume %) Glycerol, 0.25 % (weight %)**
Xylencyanol:	**50 mM EDTA, pH 8.0**
DNA Molecular Weight Markers:	**MBI Fermentas**
QIAEX II Gel Extraction Kit:	**Qiagen**
GENECLEAN II, BIO 101:	**Q-Biogene**

Agarose gel electrophoresis was used to control the size and purity of DNA fragments. 1 % (volume to weight) agarose gel for high size DNA fragment (0.5 -10 kb) was prepared. For this purpose 1 x TAE buffer and agarose were mixed by melting in a microwave oven, 0.5 µg/ml ethidium bromide was added to facilitate visualization of DNA fragments during the run. The desired DNA fragments were cut out from the gel with a scalpel under UV-light and then eluted and purified using GENECLEAN II Gel Extraction Kit for fragments less than 6kb and using QIAEX II for bigger fragments.

2.2.1.4 Subcloning of DNA fragments

T4-DNA-Ligase:	**Promega**
T4-DNA-Ligase Buffer	**Promega**

For subcloning plasmid vector and DNA fragments were cleaved with appropriate endonucleases. Then the desired DNA segments were isolated by agarose gel electrophoresis and purified. T4-DNA-ligase was used for ligation in a concentration 1 U per 10 µl reaction mixture. The reaction mixture was incubated at 23ºC for 3 hours and then overnight at 16ºC.

2.2.1.5 Bacteria transformation

Electroporation cavity: **0,2 cm electrode distance (Equibio)**

Electrocompetent *E.coli* bacteria prepared according to Sambrook *et al*., (1989) were transformed with plasmid-DNA, than plated on LB agar plate containing appropriate antibiotics and incubated over night at 37ºC.

2.2.1.6 Plasmid DNA preparation (Mini- and Maxi-preparation)

P1 buffer:	**50mM Tris-HCl, pH 8.0, 10 mM EDTA, 100 µg/ml RNase A**
P2 buffer:	**200 mM NaOH, 1% (weight %) SDS**
P3 buffer:	**3 M Potassium acetate, pH 5.5**
EndoFree Plasmid Maxi Kit:	**Qiagen**

DNA mini-preparations were used to select positive transformants. Each single colony was cultured for 16 hours in 2 ml LB-medium containing the appropriate selective antibiotic. Then the bacterial cells were harvested by centrifugation, resuspended in 300 µl P1 buffer, lysed by 300 µl P2 buffer for 5 min and neutralized by 300 µl chilled P3 buffer. After 5 min incubation samples were centrifuged (14000 x g, 7 min) and then washed with 70 %-ethanol (vol. %), air dried and redissolved in 50µl water. Plasmid DNA purification for the transfection of the hippocampal primary cultures was carried out with material supplied by the EndoFree Plasmid Maxi Kit and was performed according to the recommendations of the manufacturer.

2.2.1.7 DNA Sequencing

To check for possible mutations during PCR and subcloning all used DNA constructs were sequenced by SEQLAB Company (Göttingen). Sequence alignment of cloned DNA fragments was done using computer program 'Basic Local Alignment Search Tool' (BLAST; NCBI: http://www.ncbi.nlm.nih.gov/BLAST/).

2.2.2 Cell culture

2.2.2.1 Hippocampal primary cell culture preparation

Medium 1:	**DMEM, 10% fetal calf serum, 2 mM L-glutamine, 100 U/ml Penecillin, 100 µg/ml Streptomycin**
Medium 2:	**Neurobasal™, 1 x B27 (Gibco), 100 U/ml Penecillin, 100 µg/ml Streptomycin, 0,5 mM L-glutamine**
Trypsin:	**0,1% in HBSS**
Dnase I:	**(Roche) 0,01% (200U) in HBSS, 2,4 mM $MgSO_4$**

Hippocampal primary cultures were prepared according to Goslin and Banker (1998) with some modifications (Dresbach et al., 2003). Rat embryos E19 were decapitated and the hippocampi were taken out and collected in chilled HBSS. The hippocampi were washed 3 times with HBSS, and then trypsinated for 20 min at 37ºC. After 5 washing steps with HBSS, hippocampi were treated with DNase I and passed 3 times through a needle with a width of 0.9 mm x 40 mm and 3 times through needle with a width of 0,43 mm x 23 mm. The cell solution was poured through nylon net with an aperture size of 125 µm to remove larger cell groups. The neurons were plated onto poly-D-lysine-coated glass coverslips in 24-well-plates in Medium 1. Twenty-four hours after plating, Medium 1 was exchanged for Medium 2. The cell cultures were kept in a humidified 95% air, 5% CO_2 incubator (Heraeus).

2.2.2.2 Transfection of hippocampal primary cultures

Opti-MEM:	**(Gibco)**
Lipofectamine™ 2000:	**(Invitrogen™)**
Medium 3:	**Neurobasal™, 1 x B27 (Gibco), 0.5 mM L-glutamine**

For all transfection experiments medium density hippocampal primary cultures (40,000 cells/coverslip) were used 11 to 13 days after plating. The cells were transfected using Lipofectamine 2000 according to the manufacturer's instructions. Prior to transfection growth medium was exchanged for 1 ml Medium 3. To prepare the transfection mix, Lipofectamine 2000 was diluted in Opti-MEM (1µl Lipofectamine 2000 + 50µl Opti-MEM per 1 well) and after 5 min incubation at room temperature mixed with diluted DNA (1µg DNA + 50µl Opti-MEM per 1 well). The resulting mix was incubated for 20 min at room temperature; 100 µl of the mix was then added per well, and neurons were placed in the incubator for 4h. Medium was then exchanged for 500 µl 37ºC prewarmed Medium 2 and the cells were kept in the incubator until fixation.

2.2.2.3 Stimulation of the primary hippocampal cultures

1 x ON:	**20mM Na-HEPES, pH 7.4, 15 mM $MgHCl_2$, 1.5 mM $CaCl_2$, 135 mM NaCl, 5mM KCl, 6 g/l glucose**
NMDA-stock solution:	**100 mM in H_2O**
Actinomycin D-stock solution:	**20 mg/ml in DMSO**
MK-801 (Sigma) stock solution:	**10mM in H_2O**
4-AP (Sigma) stock solution:	**1M in H_2O**
Bicuculline methiodide (Tocris) stock solution:	**10 mM in H_2O**
DAPI (Sigma) stock solution:	**1 mg/ml in H_2O**

PI (Sigma) stock solution: **1.25 mM in H_2O**

Cultured hippocampal cells were preincubated for at least 10 min at 37ºC in 1 x ON buffer before all stimulation experiments and 1 x ON buffer was used for all washing steps and chemical dilutions. Then cells were stimulated with NMDA (final concentration, 50 or 100 μM) and washed 3 times. Gene transcription inhibitor actinomycin D (final concentration, 10 μg/ml) was added 30 min before NMDA stimulation. Then cells were kept in 1 x ON buffer with or without actinomycin D in the incubator until fixation.

For stimulation of synaptic NMDA receptors primary hippocampal cultures were simultaneously treated with 50 μM bicuculline and 2.5 mM 4-aminopyridine (4-AP) for 30 min. For activation of extrasynaptic fraction of NMDA receptors synaptic NMDA receptors were selectively inactivated using 5 μM MK-801 in conjunction with bicuculline and 4-AP. After 30 min the cultures were washed 3 times and extrasynaptic NMDA receptors were then activated by 100 μM NMDA for 3 min and kept in the incubator until fixation. Cell viability was determined by nuclei staining with 100 ng/ml 4',6-diamidino-2-phenylindole (DAPI) and propidium iodide (PI) (10 μM), respectively. After 30 min incubation with DAPI and PI neurons were fixed and the ratio between dead and total number of cells was determined.

2.2.2.4 Immunocytochemistry

Blocking solution:	**10 mM PBS, 10% (volume %) horse serum, 5% (weight %) sucrose, 2% (weight %) BSA, 0.3% (vol.%) Triton X-100**
Mowiol:	**10% (weight %) mowiol, 25% (volume %) glycerol, 100mM Tris-HCl, pH 8.5, 2.5% (weight %) DABCO**
VectaShield + propidium iodide:	**(Vector)**
VectaShield + DAPI:	**(Vector)**
ApopTag ® Red Apoptosis Detection Kit	**(Chemicon)**

Cells were fixed for 10 min with 4% paraformaldehyde (PFA) or for 20 min with 100% methanol at -20°C. In case of methanol fixation after washing with PBS, cells were re-hydrated in PBS for 50 min. After fixation cells were incubated in blocking solution for 30 min at RT. The primary antibodies were diluted in blocking solution and incubated overnight at 4°C. After washing (3x 10 min PBS) cells were incubated with secondary fluorescent antibodies (diluted in blocking solution) for 2 h at RT, washed again (3x 10 min PBS) and embedded in Mowiol or VectaShield mounting medium with propidium iodide or DAPI for nuclear staining.

To determine the number of apoptotic cells neurons were fixed in 2% PFA and then stained by using the ApopTag® Red Apoptosis Detection Kit: the DNA strand breaks were detected

by enzymatically labeling the free OH termini with modified (digoxigenin conjugated) nucleotides. Incorporated digoxigenin-dNTPs then were detected by using anti-digoxigenin conjugated-rhodamine antibodies.

2.2.2.5 Sample preparation for scanning electron microscopy (SEM)

SEM experiments were performed in collaboration with Dr. Heiner Sann, from the Special laboratory for electron- and laserscanning microscopy, at the Leibniz Institute for Neurobiology, Magdeburg. For SEM analysis hippocampal primary neurons were fixed in a solution of 1% glutaraldehyde in 20 mM PBS for 30 min for visualizing the morphology of the cells; for PSDs quantification neurons were fixed with 4% PFA for 10 min and immunostained as described above (2.2.3.4) and the region of interest was scanned with confocal laser scanning microscope (see 2.4). Then samples were dehydrated in solutions of increasing ethanol concentration, and critical-point dried and sputtered with a thin layer of gold. Digital images were made at 4 kV using a DSM 942 Zeiss SEM.

2.2.3 Imaging and Quantification

Images were viewed using a Zeiss axioplan microscope equipped with a Spot RT camera (Visitron Systems) or with a confocal laser scanning microscope (Leica TCS 4D, Leica Bensheim, Germany) equipped with a Krypton-Argon-Ion laser (488/568/647 nm). To exclude bleeding of the dyes across channels all images were scanned sequentially. Labeled transfected neurons were chosen randomly for quantification from two to six coverslips from two to four independent experiments for each construct. Changes in fluorescence intensity level were quantified from averaged confocal image stacks acquired using ImageJ software in the regions of interest. The number of neurons used for quantification is indicated in the figure legends. Statistical significance was determined by Student's t-test. Data are presented as mean ± SE. A level of $p<0.05$ was considered statistically significant. $p< 0.1$; $**p< 0.01$; $*** p< 0.001$.

3 Results

3.1 Myristoylation and NLS motifs are crucial for the subcellular localization of Jacob

Jacob harbors at its N-terminus a myristoylation motif and a bipartite nuclear localization signal in its central α-helical region. Myristoylation at the N-terminus of proteins serves as a lipid anchor to membranes (Resh, 1999), whereas nuclear localization signals are crucial for the protein transport into the cell nucleus (Boulikas, 1993). Therefore the presence of both motifs can potentially play an important role for Jacob's subcellular localization. In fact, transient transfection of COS-7 cells with the Jacob deletion mutant construct of a protein lacking the nuclear localization signal (ΔNLS-Jacob-GFP) leads to an exclusive extranuclear localization of overexpressed Jacob protein. In contrast, a myristoylation mutant, ΔMyr-Jacob-GFP, in which the crucial glycine at position 2 was mutated to an alanine, showed an exclusive nuclear accumulation in transfected COS-7 cells (unpublished data from Dr. Michael R. Kreutz).

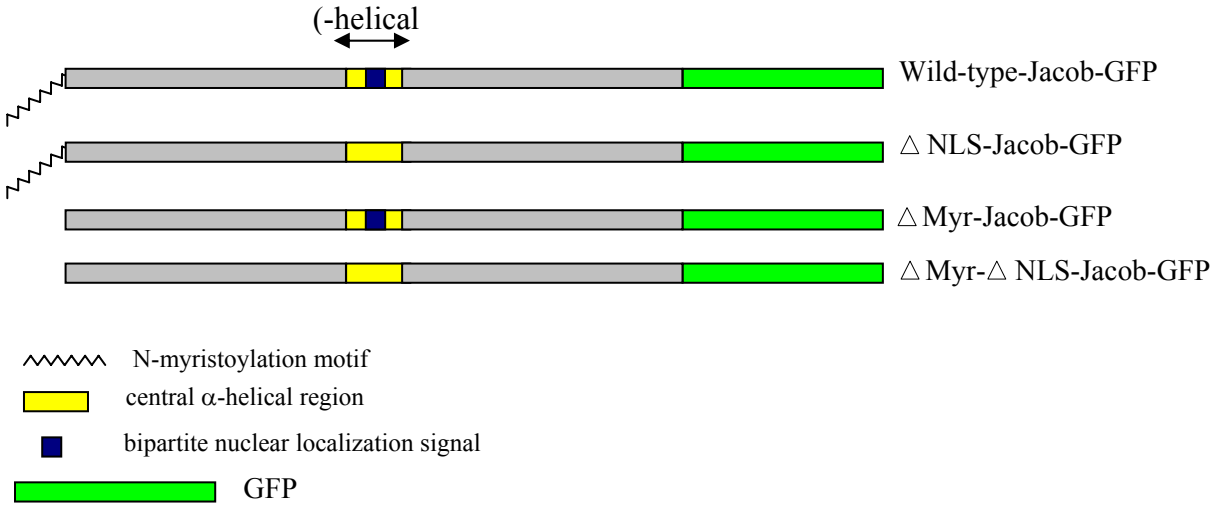

Fig. 4 Schematic representation of the Jacob cDNA constructs.
N-myristoylation motif, bipartite nuclear localization signal (NLS), central α-helical region are depicted. Green lines represent the GFP-tag.

To check whether the presence of the N-myristoylation motif and the nuclear localization signal also plays a crucial role in Jacob's subcellular localization in mature hippocampal neurons, neuronal cultures were transfected with different Jacob mutants at day in vitro 11 (Fig. 4).

Already 6 hours following transfection, expression of all used constructs was clearly visible. Transfected neurons were fixed 6, 12 and 24 hours after transfection and their

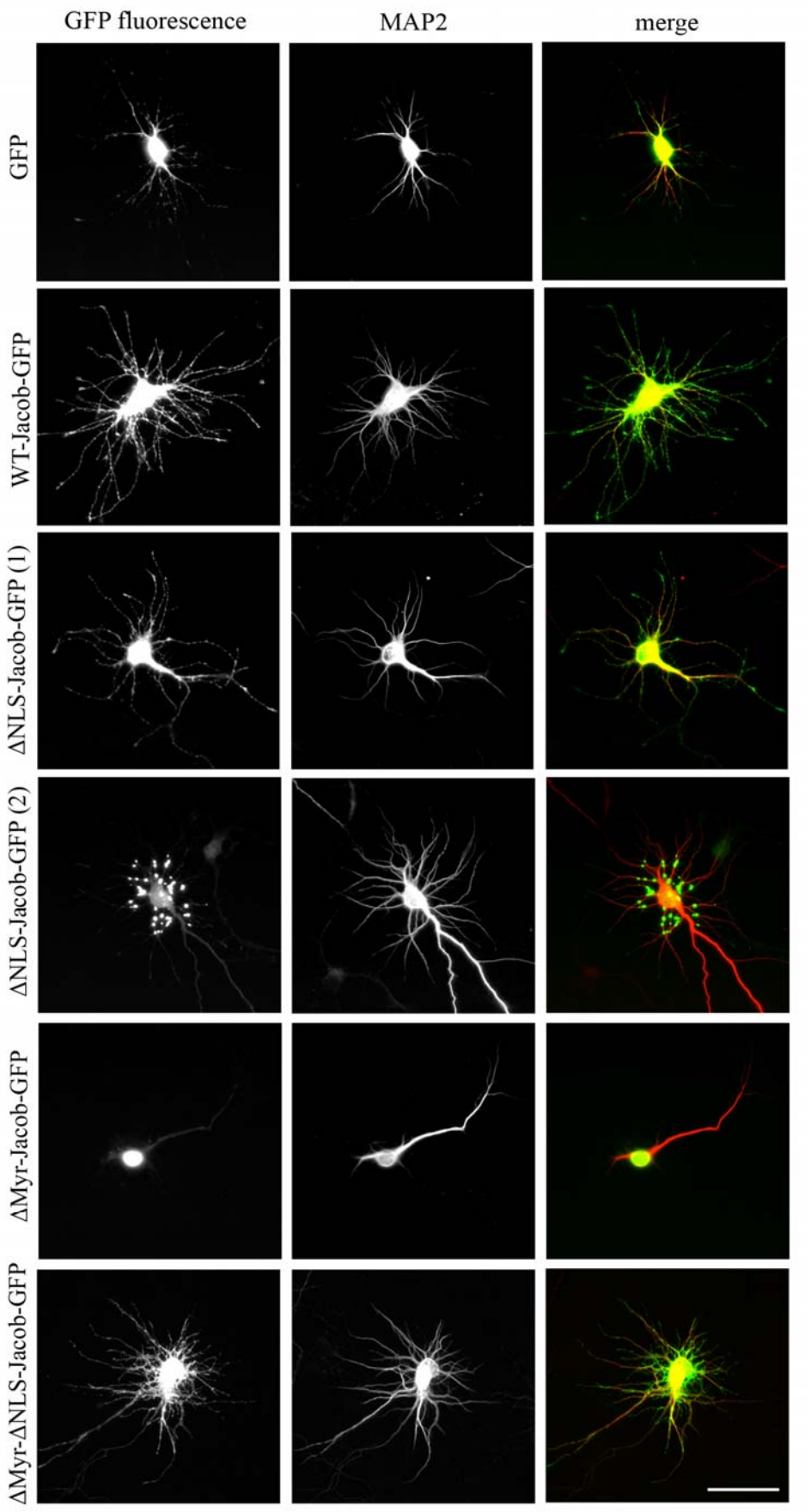

Fig. 5

See next page for legend

Fig. 5 Subcellular localization of different GFP-tagged Jacob mutants in transfected primary hippocampal neurons. DIV-11 primary hippocampal neurons were transfected with different Jacob-GFP constructs (as indicated to the left) or with pEGFP-vector without insert (control) and fixed 6 hours after transfection. Transfected neurons were immunolabeled for MAP2 (red in merge) to confirm their neuronal identity. Scale bar: 50 μm.

neuronal identity was confirmed by immunofluorescence staining for Microtubule-associated protein 2 (MAP2).

After overexpression, wt-Jacob-GFP filled the whole cytoplasm and was also present in the cell nuclei similar to the control GFP protein (Fig. 5). Transfection of neuronal cells with the ΔMyr-Jacob-GFP construct led to an exclusive nuclear localization of the mutant protein. In contrast, overexpression of ΔNLS-Jacob-GFP resulted in an extranuclear localization of the protein. Interestingly, in 70% of cells transfected with ΔNLS-Jacob-GFP the mutant protein diffusely filled the whole cell cytoplasm, whereas in 30% of the cells the overexpressed protein was concentrated in huge protrusions disposed around the cell body and along dendrites (Fig. 5).

These data indicate that the NLS is essential for nuclear import of Jacob whereas N-myristoylation seems to be crucial for its extranuclear localization. In support of this view it was also found that the cellular localization of the double mutant ΔMyr-ΔNLS-Jacob-GFP was exclusively extranuclear in transfected hippocampal neurons (Fig. 5).

3.2 Jacob affects the synapto-dendritic cytoarchitecture

3.2.1 Extranuclear and nuclear Jacob have different effects on dendritic cytoarchitecture

To elucidate the functional consequences of the nuclear and extranuclear localization of Jacob, hippocampal primary neurons were transfected with different mutants (ΔNLS-Jacob-GFP, ΔMyr-Jacob-GFP) and wild-type Jacob cDNA constructs. Neurons transfected with GFP vector without insert were used as a control (Fig. 6). Morphological analysis of the transfected hippocampal neurons was done at 6, 12, and 24 hours after transfection. Immunofluorescence staining against the dendrite-specific cytoskeletal protein MAP2 was used for visualizing of the dendritic processes. To analyze the dendritic topology all MAP2-immunopositive neurites outgoing from the cell soma and all visible branch points were quantified (Fig. 6 II-A, B). The percentage of neurites that are longer than 25 or 50 μm was quantified to estimate a possible effect of Jacob-mutants

I.

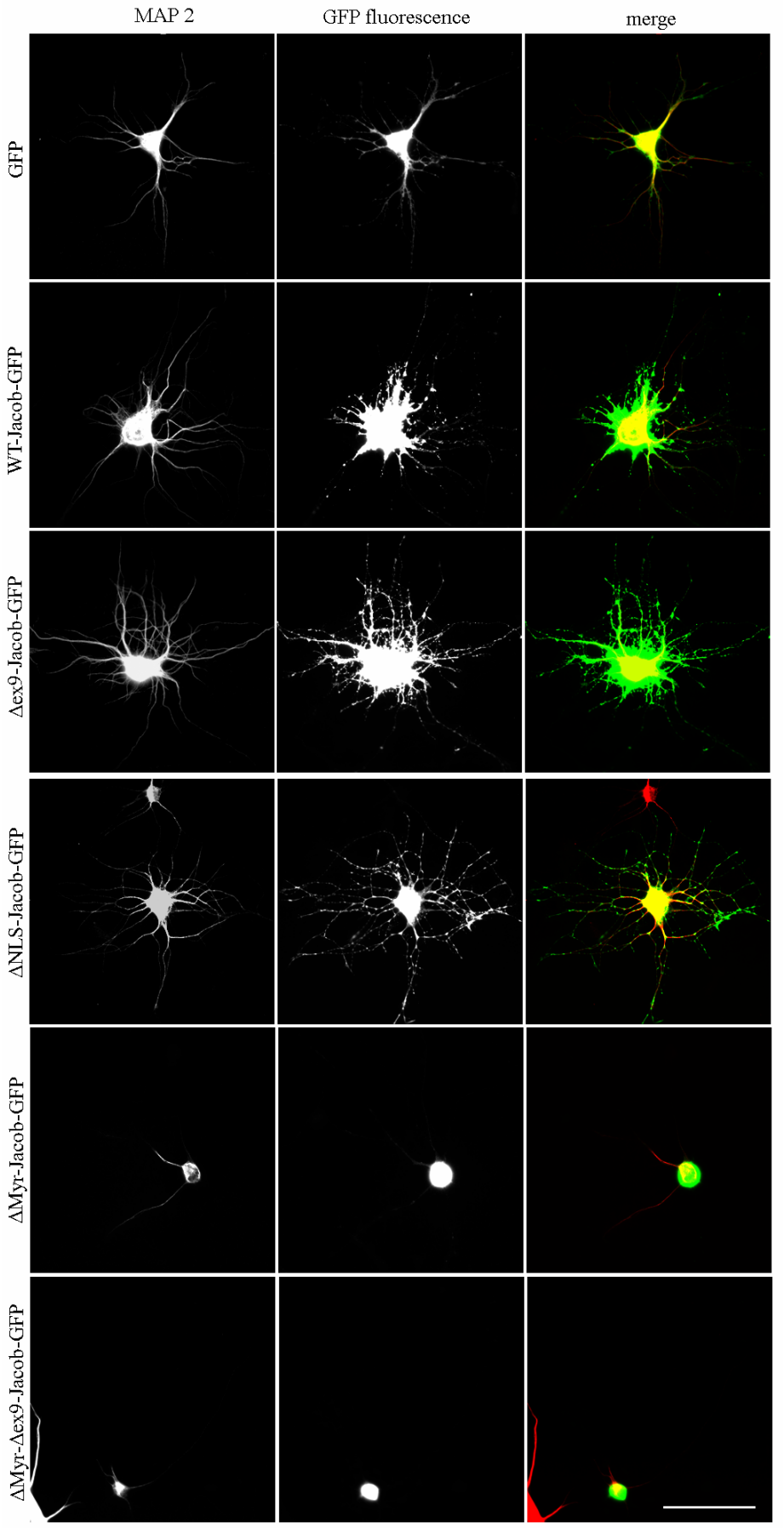

Fig. 6-I

See next page for continuance

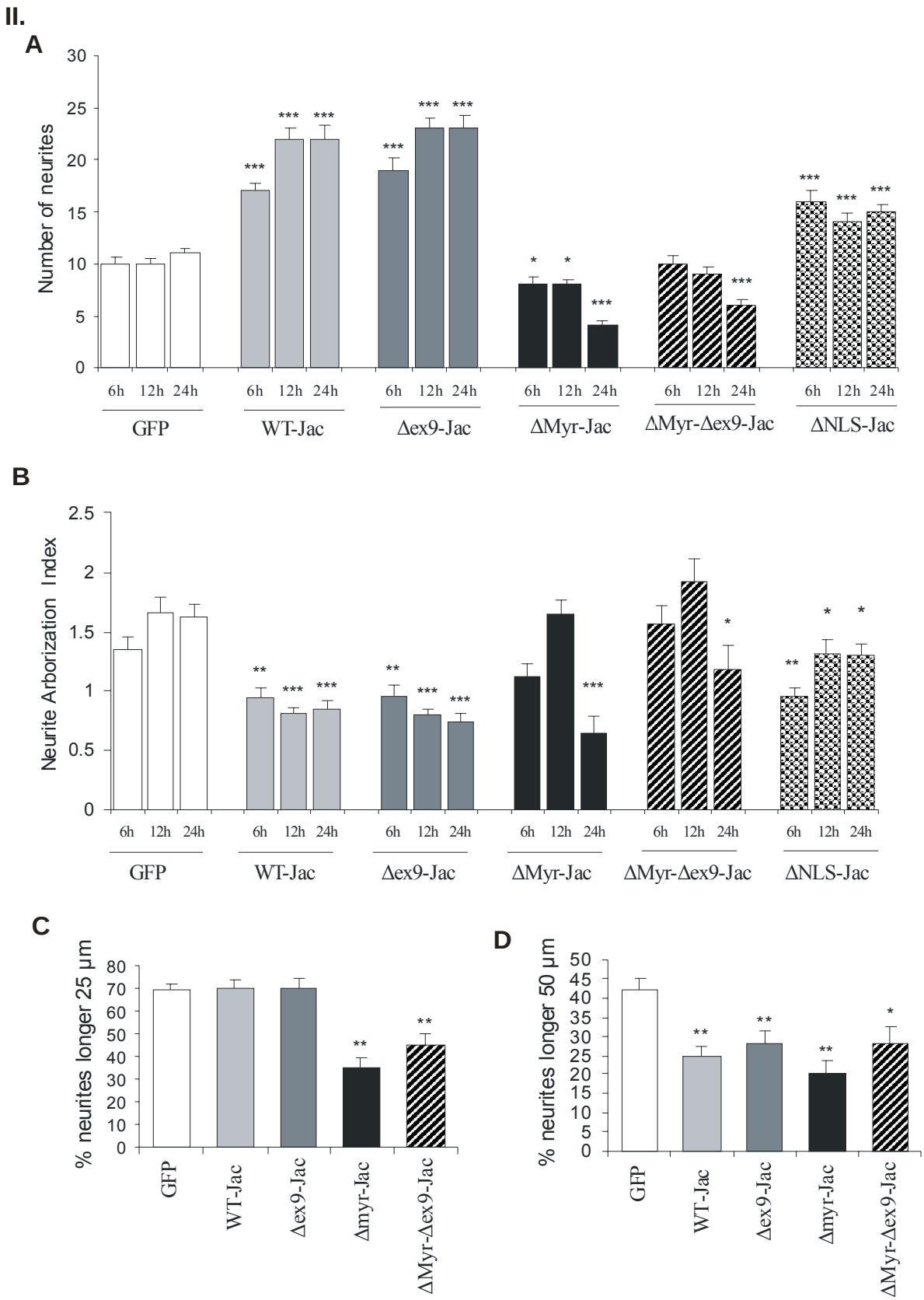

Fig. 6-II

See next page for legend

Fig. 6 Overexpression of different Jacob cDNA constructs leads to drastic changes in dendritic cytoarchitecture in primary hippocampal neurons.
Primary hippocampal neurons after 11 DIV were transfected with different Jacob-GFP constructs or with pEGFP-vector without insert (control) and fixed 6, 12 and 24 hours after transfection. Dendritic morphology was assessed by immunostaining with anti-MAP2 antibody.
I. Micrographs depicting MAP2 labeled (red in merge) hippocampal neurons 24 hours after transfection with different Jacob-constructs (as indicated to the left). Scale bar: 50 μm.
II. Morphological analysis of primary neurons after Jacob overexpression in primary hippocampal neurons. Diagram (**A)** represents quantification of MAP2-immunopositiv neurites outgoing from the cell soma. Neurons transfected with wt-Jacob-GFP (light-gray columns) showed significant increase in neurite number in comparison to GFP-control neurons (white columns) already 6 hours after transfection. Δexon9-Jacob-GFP (dark-gray columns) and ΔNLS-Jacob-GFP (latticed columns) overexpression also cause an increase in neurites number, whereas neurons transfected with ΔMyr-Jacob-GFP (black columns) and ΔMyr-Δexon9-Jacob-GFP (hatched columns) have significantly less neurites than GFP transfected neurons.
Diagram (**B)** shows a quantification of dendritic complexity by determination of the average number of dendritic branch points for each MAP2-immunopositive dendrite (dendrite arborization index). wt-Jacob-GFP, Δexon9-Jacob-GFP and ΔNLS-Jacob-GFP overexpression resulted in drastic simplification of the dendritic tree already 6 h following transfection. Statistically significant decreases of the dendrite arborization index were observed after 24 h in ΔMyr-Jacob-GFP and ΔMyr-Δexon9-Jacob-GFP transfected neurons. (**C, D)** Neurons transfected with different Jacob cDNA constructs have shorter dendritic processes. Neurons transfected with different Jacob-mutants have significantly less neurites which are longer than 50 μm (C) or longer than 25 μm (D) in comparison to GFP-transfected neurons. Quantification was done 24 h after transfection. Data are presented as a mean ± SEM. * $p < 0,1$; ** $p < 0,01$; *** $p < 0,001$. 50 neurons were quantified per each time point in each group.

overexpression on dendritic length (Fig. 6, II-C, D). All transfected neurons survived for at least 48 hours after transfection.

Overexpression of Jacob mutants resulted in drastic changes in dendritic cytoarchitecture in primary hippocampal neurons (Fig. 6). Full-length Jacob-GFP overexpression led to a dramatic increase in neurite number in comparison to GFP transfected controls. This effect was very rapid and could be observed already 6 hours following transfection. Another 6 hours later neurons transfected with wt-Jacob-GFP had already 2.5 times more dendritic protrusions than GFP transfected cells. Moreover, neurons overexpressing wt-Jacob-GFP protein showed almost 50 % decrease in the neurite arborisation index and the percentage of neurites which are longer than 50 μm. ΔNLS-Jacob-GFP overexpression caused similar changes in the dendritic cytoarchitecture though changes in dendritic number and complexity was not as prominent as in case of wt-Jacob-GFP overexpression.

Both wt-Jacob-GFP and ΔNLS-Jacob-GFP proteins localize extranuclearly after overexpression and cause similar changes in dendritic cytoarchitecture whereas ΔMyr-Jacob-GFP protein accumulates exclusively in the cell nuclei and has an opposite effect on neurite number. Already 6 hours following transfection neurons transfected with ΔMyr-

Jacob-GFP had 25% less dendritic processes than control GFP cells, and after 24 hours this difference was already 75% (Fig. 6, II-A). Therefore, overexpression of ΔMyr-Jacob-GFP resulted in retraction of almost all dendritic processes within 24 hours.
Neurites, which were present after 24 hours following transfection were also less complex and much shorter than in case of GFP-control cells: a 2 times reduction in neurite arborization index and more than 2 times reduction in percentage of neurites which are longer than 50 μm and 25 μm was visible. These data suggest that the intranuclear accumulation of Jacob has a strong negative effect on dendritic cytoarchitecture.

3.2.2 Nuclear Jacob has negative effects on the number of synaptic contacts

Dendritic morphology has a profound impact on neuronal information processing. The overall extent and orientation of dendrites determines the kinds of input a neuron receive (Whitford et al., 2002; Whong and Ghosh, 2002). On the other hand, changes in synaptic input and neuronal activity can greatly influence dendritic morphology. However, there are controversial data about influence of neuronal activity on dendritic remodeling. It was shown that blocking synaptic activity during development can prevent normal elaboration of dendritic arbors in spinal motor neurons (Kalb, 1994). Pharmacological blockade of NMDA receptors also leads to deficits in dendritic growth in the *Xenopus* optic tectal neurons (Rajan and Cline, 1998), in the supraoptic nucleus in vivo and in acute slices (Chavaleyre, et al., 2002). On the other hand, several studies have shown that blockade of NMDA receptors resulted in a more complex arborization of the dendritic tree and a substantial increase in synapse number in vivo in visual cortex (Rocha and Sur, 1995) and in hippocampal (Luthi et al., 2001) and cortical (McAllister et al., 1996) slice cultures. Thus, changes in synaptic input can greatly influence dendritic morphology, and vice versa changes in dendritic topology can have important consequences for synaptic transmission.

As it was described in section 3.2.1, Jacob overexpression in primary hippocampal neurons leads to drastic changes in dendritic morphology. Therefore, it was suggested that changes in dendritic cytoarchitecture induced by overexpression of different Jacob mutants can be accompanied by changes in number of synaptic contacts. To answer this question mature hippocampal neurons (DIV 11) were transfected with different Jacob mutants and the density of synaptic puncta was analyzed 12 hours after transfection. GFP-transfected neurons were used as a control. Synapses were visualized using immunocytochemical staining with the presynaptic marker Bassoon. Bassoon puncta were counted per 50 μm

length of each transfected neuron and 50 different neurons were used for each experimental group, the synaptic density then was expressed as number of synapses per 10 µm.

I.

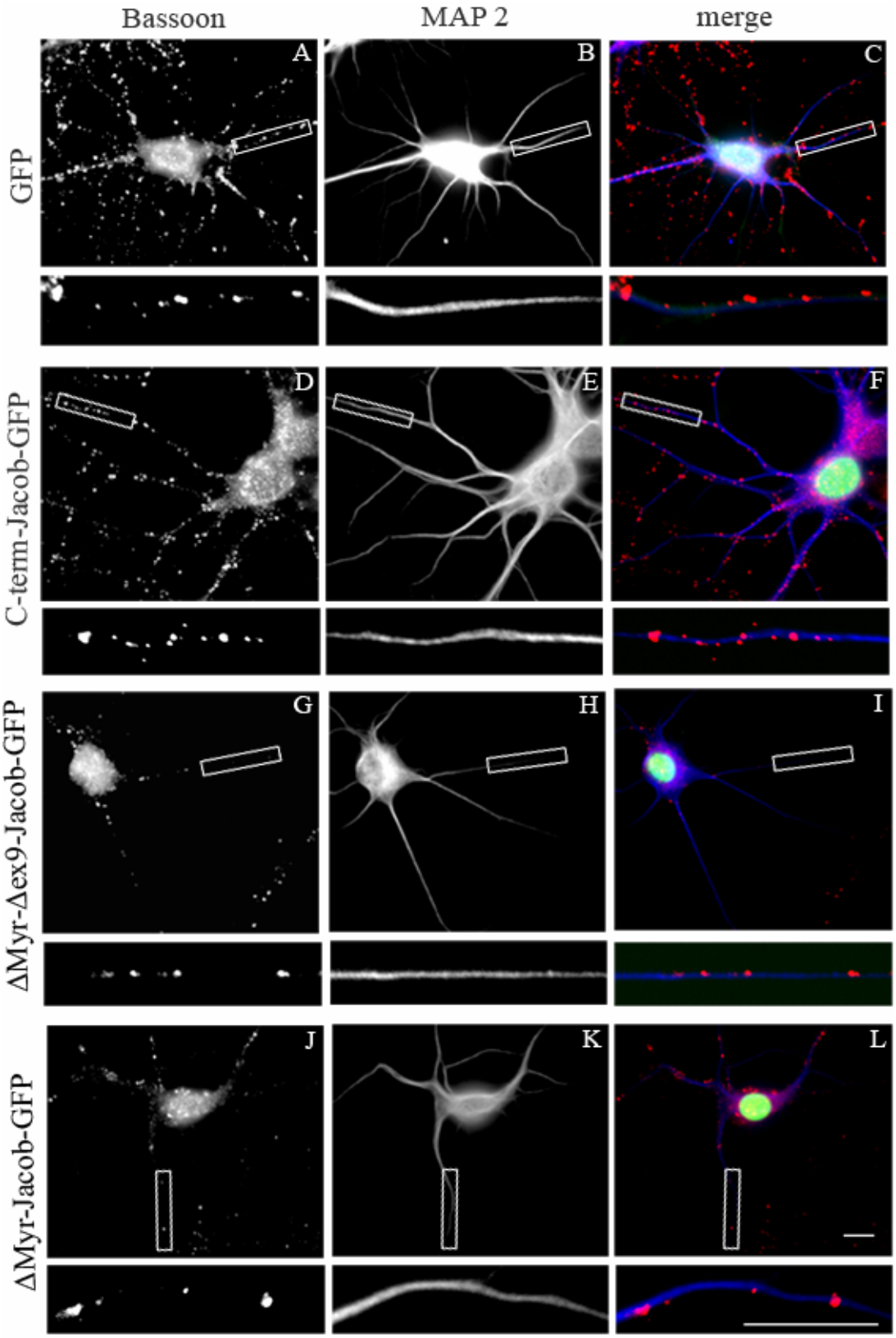

Fig. 7-I

See next page for legend

II

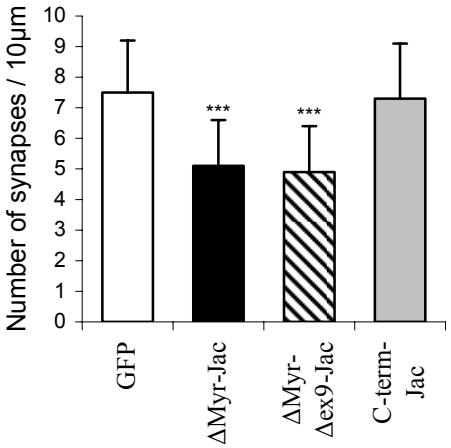

Fig. 7 Nuclear accumulation of different Jacob mutants has a differential effect on number of synaptic contacts.
I. 11-day-old hippocampal neurons were transfected with ΔMyr-Jacob-GFP (J-L), ΔMyr-Δexon9-Jacob-GFP (G-I), C-term-Jacob-GFP (D-F) or GFP-vector without insert (A-C). 12 hours later, cultures were fixed with 4% PFA and immunostained with anti-MAP2 antibodies to visualize dendritic processes (blue in the merged displays) and with Bassoon antibodies to visualize synapses (red in the merged displays). Inserts show higher magnification views. Scale bar: 10 µm.
II. Quantification of Bassoon puncta on dendrites of hippocampal neurons after overexpression of ΔMyr-Jacob-GFP (black column), ΔMyr-Δexon9-Jacob-GFP (hatched column), C-term-Jacob-GFP (gray column) or GFP-vector (white column). Quantification was done 12 h after transfection. Data are presented as a mean ± SEM. *** $p < 0{,}001$. 50 neurons were quantified per each time point in each group.

Neurons transfected with ΔMyr-Jacob-GFP mutant showed more than 30% decrease in density of synaptic puncta in comparison to control cells transfected with GFP (Fig. 7, I:A-C, J-L; II). Interestingly, this reduction in number of synaptic contacts occurs 12 hours after transfection and precedes a massive dendritic loss induced by ΔMyr-Jacob-GFP overexpression (Fig. 6, II-A), suggesting that stripping of synaptic contacts could contribute to dendritic retraction.

On the other hand, overexpression of wt-Jacob-GFP or ΔNLS-Jacob-GFP in hippocampal neurons had no effect on the number of synapses (data not shown). Note, that in contrast to wt-Jacob-GFP and ΔNLS-Jacob-GFP, ΔMyr-Jacob-GFP accumulates in the cell nuclei after overexpression. These data suggest that the reduction of synaptic contacts correlates with the nuclear localization of Jacob.

3.2.3 The C-terminus of Jacob is dispensable for its effect on synapto-dendritic cytoarchitecture

As it was shown in section 3.2.1 overexpression of different Jacob mutants in primary hippocampal neurons have a drastic effect on dendritic cytoarchitecture. Moreover, nuclear accumulation of Jacob resulted in stripping of synaptic contacts and retraction of dendritic processes (section 3.2.1; 3.2.2). But the molecular mechanisms underlying Jacob's regulation of synaptic number and dendritic growth and retraction needs to be solved. To answer this question it is required to know which part of Jacob is responsible for its effects on synapto-dendritic cytoarchitecture.

The Jacob gene displays a complex organization with 16 exons, most of which are smaller than 120 bp. Alternative splicing generates a multitude of different Jacob isoforms with different calculated molecular weights. One splice variant lacks exon 9 (Δex9-Jacob), and the deletion of exon 9 results in a frameshift in the coding sequence with a stop codon at position 1145-1147 and an open reading frame for a 337 amino acids (Daniela Dieterich, Ph.D. thesis, 2003). The resulting protein contains the myristoylation motif and NLS but lack large part of the carboxy-terminus. Therefore, this splice isoform has two motifs, which are important for subcellular localization of the protein and can potentially function as a regulator of synapto-dendritic cytoarchitecture. To prove this possibility and answer the question whether the N-terminal part of Jacob is sufficient for its effects on synapto-dendritic cytoarchitecture, a Δexon9-Jacob-GFP construct was generated (Fig. 8). Subsequently, hippocampal neurons were transfected with the Δexon9-Jacob-GFP construct to prove whether Jacob's N-terminal part is responsible for its morphogenetic effects. After overexpression Δexon9-Jacob-GFP showed a distribution pattern very similar to the wt-Jacob-GFP (Fig. 6), filling the whole cytoplasm, but it was also present in the cell nucleus. Moreover, Δexon9-Jacob-GFP transfected neurons showed drastic changes in dendritic cytoarchitecture comparable with changes observed in the case of wt-Jacob-GFP transfection: numerous short and less complex dendritic processes (Fig. 6; 7).

To investigate the effect of the nuclear accumulation of the N-terminal part of Jacob, a ΔMyr-Δexon9-Jacob-GFP construct was generated and transfected into primary hippocampal neurons. ΔMyr-Δexon9-Jacob-GFP accumulated exclusively in the nucleus after transfection and its overexpression resulted in a drastic reduction of dendritic complexity (Fig. 6; 7; 9). Moreover, the loss dendrites was preceded by stripping of synaptic contacts, similar to that observed after ΔMyr-Jacob-GFP overexpression (Fig. 8).

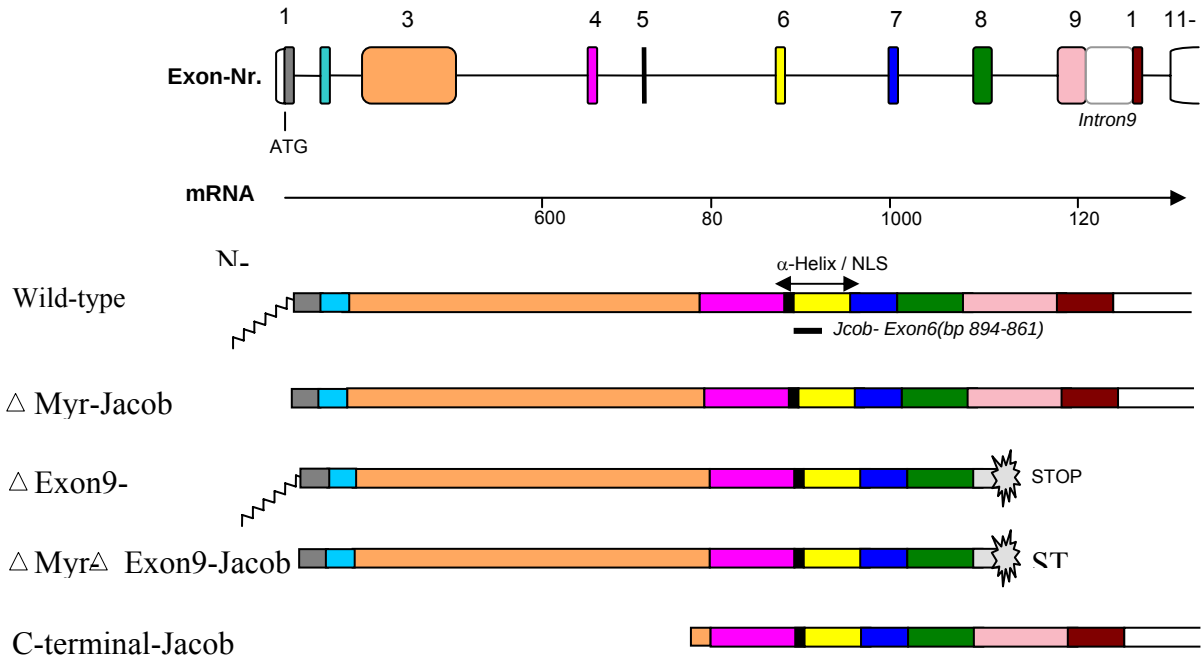

Fig. 8 Schematic illustration of the Jacob gene structure and different recombinant Jacob mutants used in this study.
Colored ellipsoids represent different exons (1-10) in schematic drawing of the Jacob gene primary structure (upper part). The scheme below illustrates different Jacob mutants. N-myristoylation is depicted in the scheme as a red oval and a star indicates the STOP codon in exon 10, which is due to a deletion of exon 9 (splice isoform Jacob-Δexon9).

These results suggest that the N-terminal part of Jacob is responsible for its effect on synapto-dendritic architecture. To directly test whether the C-terminus of Jacob is involved in the morphogenetic effects, a construct lacking the first 235 amino acids was generated (C-terminal-Jacob-GFP). This construct includes the entire C-terminal part of Jacob (exon5-exon16) and, therefore, harbors the NLS but lacks the myristoylation motif. After overexpression in hippocampal neurons C-term-Jacob-GFP accumulated exclusively in the cell nucleus but caused neither dendritic loss nor synaptic stripping (Fig. 8; 9). Neurons transfected with C-terminal-Jacob-GFP represent cytoarchitecture and synaptic density comparable with the control neurons transfected with empty GFP vector even 48 hours following transfection (Fig. 8; 9). Thus, the N-terminal half of Jacob is crucial and sufficient for its effects on synapto-dendritic cytoarchitecture.

I.

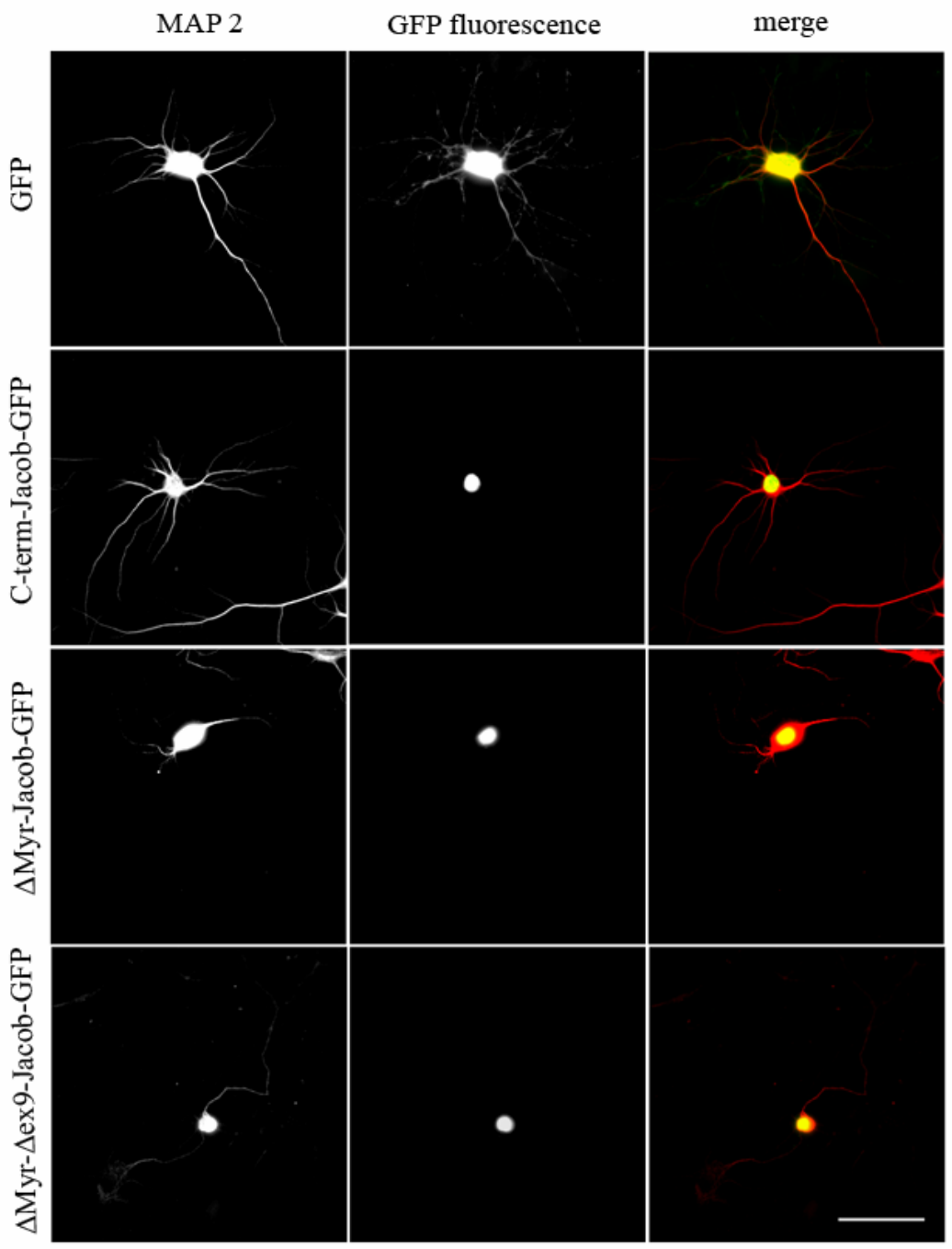

Fig. 9-I

See next page for legend

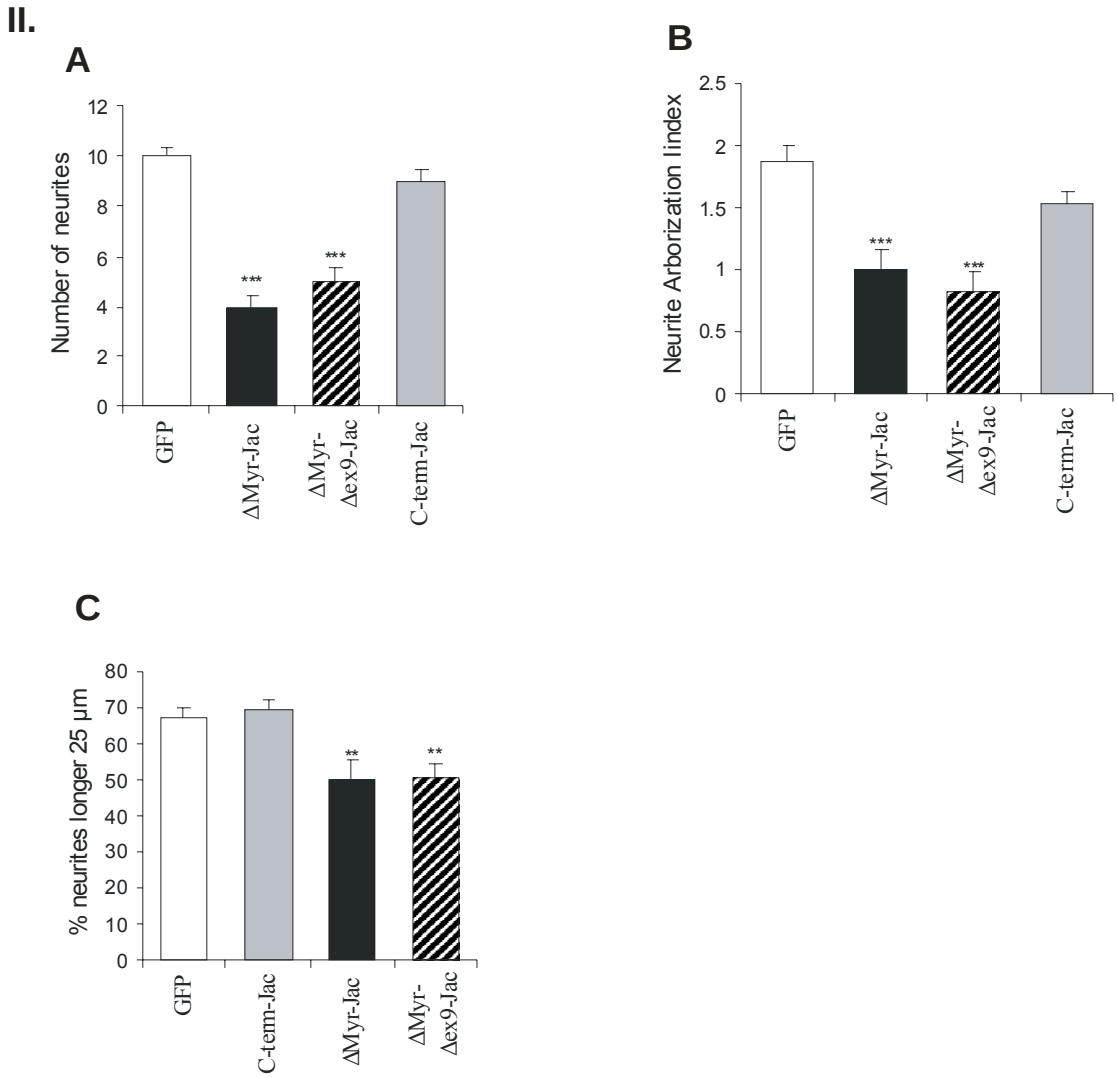

Fig. 9 The C-terminal part of Jacob is dispensible for its effect on dendritic cytoarchitecture.
Primary hippocampal neurons at DIV 11 were transfected with different Jacob-GFP constructs or with pEGFP-vector without insert (control). 48 hours after transfection, cultures were fixed and immunolabeled for MAP2.

I. Micrographs depicting MAP2 labeled (red in merged displays) hippocampal neurons 48 hours after transfection with different Jacob-constructs (as indicated to the left). Scale bar: 50 µm.

II. Morphological analysis of primary neurons after Jacob overexpression in primary hippocampal neurons.

Neurons transfected with ΔMyr-Jacob-GFP (black column) or with ΔMyr-Δexon9-Jacob-GFP (hatched column) showed a drastic decrease in dendritic complexity (B), neurite number (A) and length (C) in comparison to GFP-transfected neurons (white columns). No significant differences were found between GFP-transfected cells and neurons after C-term-Jacob-GFP overexpression (gray column). Quantifications were done 48 h after transfection. Data are presented as a mean ± SEM. **p< 0,01; *** p< 0,001. 50 neurons were quantified at each time point in each group.

3.2.4 Redistribution of endogenous Jacob affects synaptogenesis in primary hippocampal neurons

As shown previously by Dr. rer. nat. Daniela Dieterich and Dipl. Biol. Martin Kreutz (unpublished data), endogenous Jacob translocates to the nucleus in response to NMDA receptor activation. On the other hand, the nuclear accumulation of Jacob after overexpression leads to a decrease of synapse number in mature hippocampal neurons (see sections 3.2.2). To answer the question whether accumulation of endogenous Jacob will have a negative effect on synaptogenesis the following experiment was performed. Mature hippocampal neurons (DIV 13) were stimulated with 50 μM NMDA for 3 min and fixed after 4 hours following stimulation. Untreated cells were used as a control. After fixation neurons were immunostained with anti-Bassoon antibody to visualize synapses and with anti-MAP2 antibodies to visualize dendritic protrusions. Bassoon puncta were counted per 40 μm length of each randomly chosen neuron and 50 different neurons were used for each experimental group, the synaptic density then was expressed as number of synapses per 10 μm. In case of neurons stimulated with NMDA a reduction in synapse density was clearly observable and was about 25% less in comparison with control untreated cells (Fig. 10).

It is known that structural rearrangements that accompany synaptic plasticity require de novo protein synthesis and gene transcription (Alberini, 1999; Malenka, 2003; Thomas and Huganir, 2004), therefore, it was suggested that Jacob can directly or indirectly regulate transcription regulation after translocation to the nucleus. Moreover, it was shown previously by Dr. Karl-Heinz Smalla (unpublished data) that nuclear Jacob exclusively associated with the RNA-polymerase II-containing euchromatin. It is well known that structural aspects of chromatin are important factor in the control of gene expression. The packaging of DNA in nucleosomes and higher order structures represents an obstacle to the binding of specific proteins and RNA polymerases to control transcription initiation sites (Reyes et al., 1997). Heterochromatin consists of densely packed chromosome regions and most transcription occurs in regions of the lightly packed form of chromatin – euchromatin (Lodish et al., 2001). The enrichment of Jacob at active sites of nuclear gene transcription and mRNA processing supports the hypothesis proposed above that Jacob is involved in transcription regulation.

I.

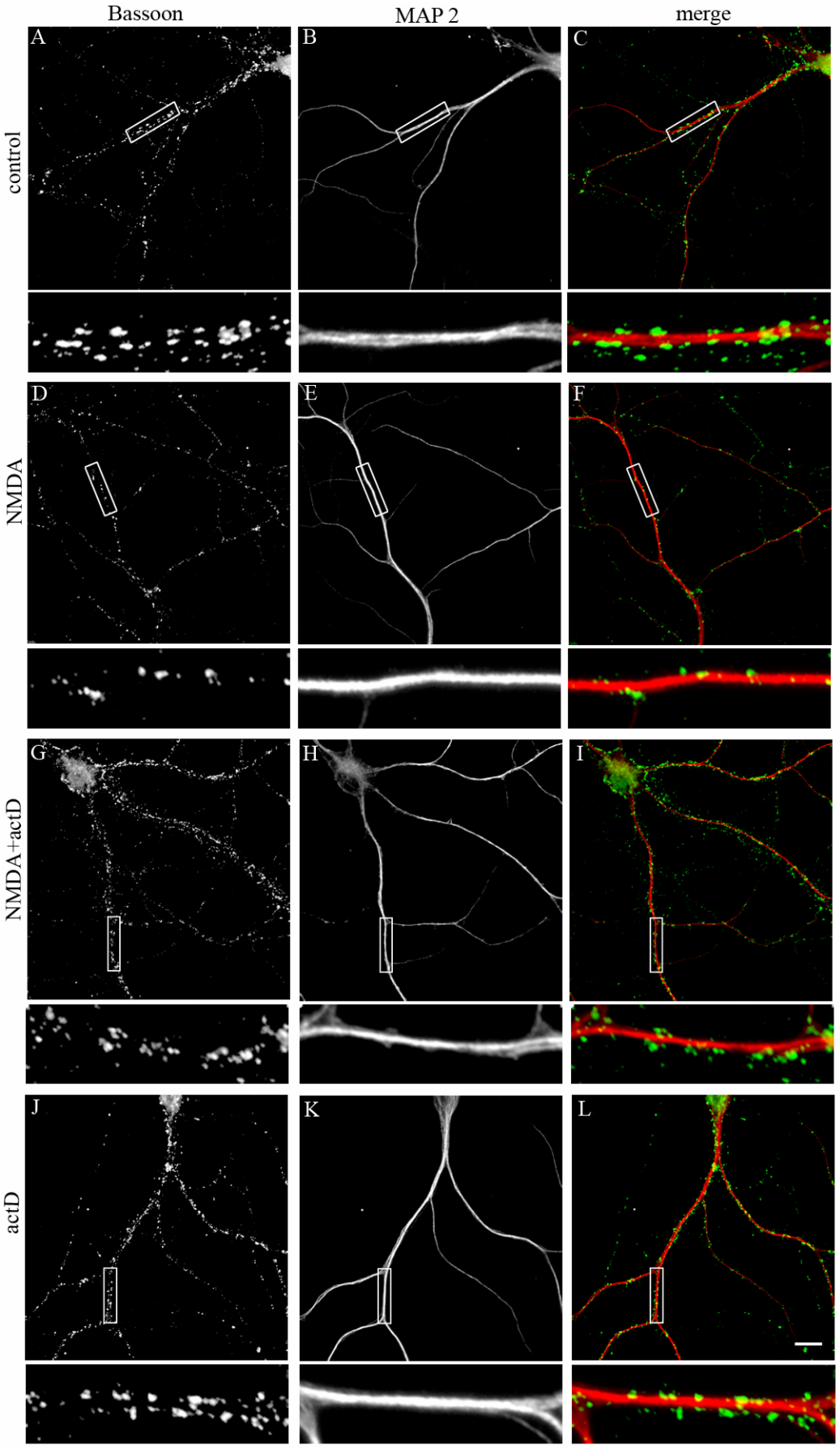

Fig. 10-I

See next page for legend

II.

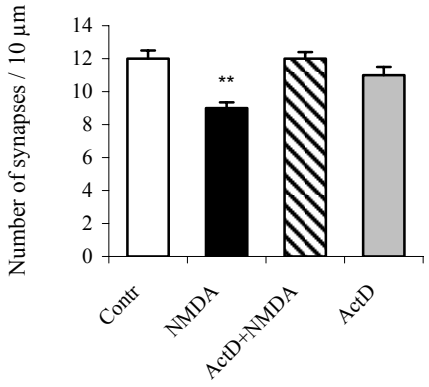

Fig. 10 NMDA receptor activation leads to reduction of synaptic density in primary hippocampal neurons.
I. Hippocampal neurons after 13 DIV were stimulated for 3 min with 50 µM NMDA (D-F); NMDA and actinomycin D (G-I); or with actinomycin D alone (J-L). 4 hours later cultures were fixed and immunostained with anti-MAP2 antibodies to visualize dendritic processes (red in merged displays) and with Bassoon antibodies to visualize synapses (green in merged displays). Inserts show higher magnification views. Scale bar: 10 µm.
II. NMDA-stimulation (black column) results in significant reduction of synaptic density in hippocampal neurons and this effect was abolished by application of actinomycin D (hatched column). No significant differences were found between untreated neurons (white column) and neurons incubated with actinomycin D alone (gray column). Data are presented as a mean ± SEM. **p< 0,01. 50 neurons were quantified per each experimental group.

To test this prediction, prior to stimulation with NMDA neurons were incubated with the transcription inhibitor actinomycin-D, and after washing out NMDA cells were kept in media contained actinomycin-D until fixation. Control cells were incubated in actinomycin-D-containing media but were not stimulated with NMDA. Treatment with actinomycin-D abolished the reduction in synapse numbers after NMDA stimulation and neurons stimulated with NMDA and treated with actinomycin-D showed no significant difference with control groups – untreated cells and treated only with actinomycin D (Fig. 10). These data support the idea proposed above that Jacob influence synaptogenesis via transcription regulation.

To further prove that Jacob's nuclear accumulation is responsible for the synaptic stripping after NMDA receptor stimulation the following experiment was performed. Primary hippocampal neurons (DIV 7) were transfected with small interfering RNA (siRNA) targeted to specifically inhibit all mRNAs corresponding to Jacob isoforms containing exon 6 and the NLS sequence (see Fig. 8) and therefore prevent nuclear accumulation of Jacob. Control cells were transfected with an empty pRNAt vector. 7 days following transfection (DIV 13) neurons were stimulated with 50 µM NMDA for 3 min. Unstimulated cells were

I.

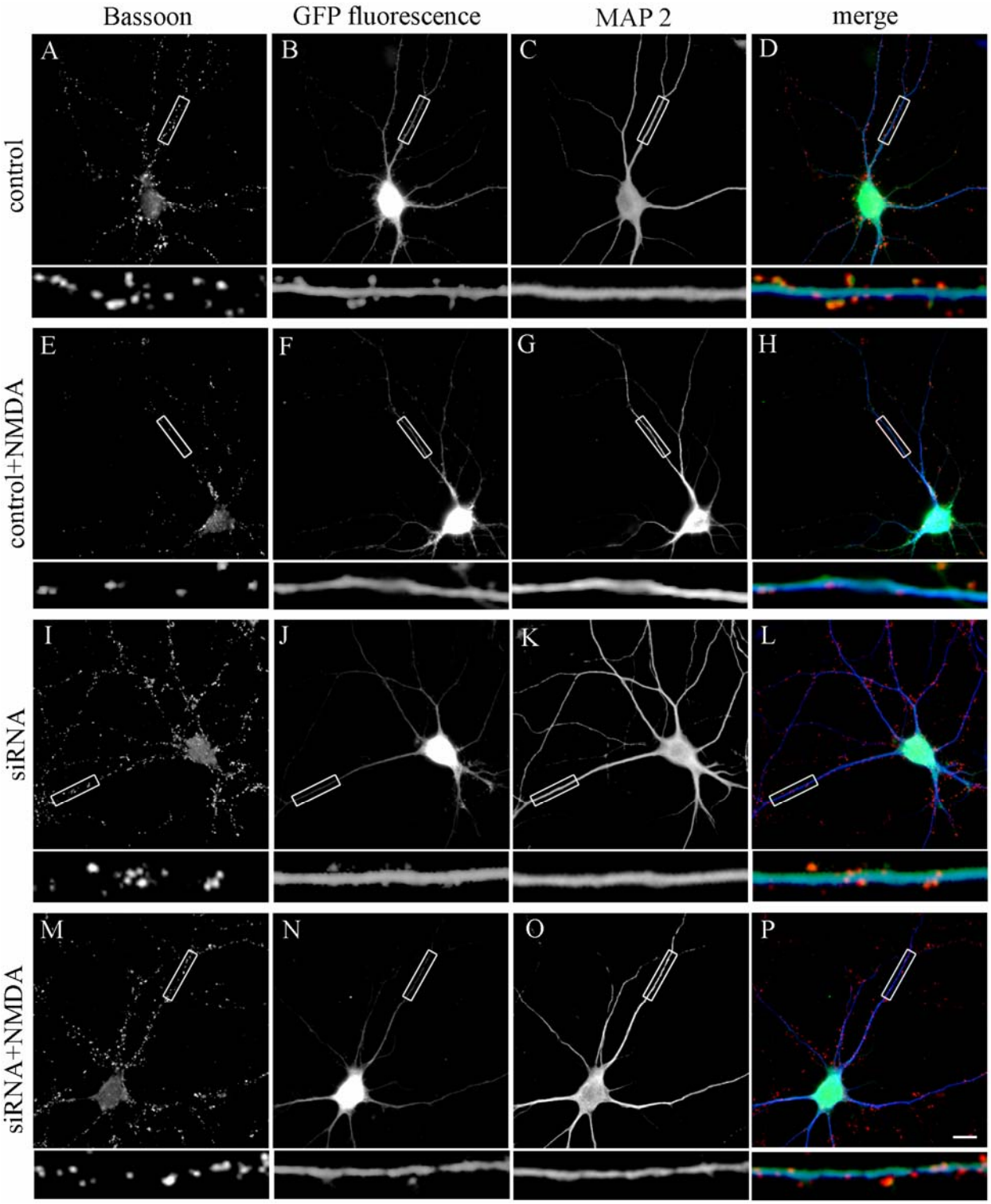

Fig. 11-I

See next page for legend

II.

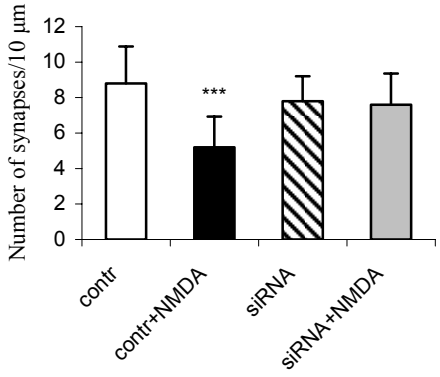

Fig. 11 Nuclear accumulation of endogenous Jacob upon NMDA receptor activation leads to stripping of synaptic contacts.
I. Hippocampal neurons after 7 DIV were transfected with siRNA (I-P) specifically knocking down the nuclear Jacob expression or empty pRNAt vector (A-H). 7 days after transfection neurons were stimulated for 3 min with 50 µM NMDA (E-H; M-P) and fixed 4 hours later and immunolabeled for Bassoon (A, E, I, M; red in merge) and MAP2 (C, G, K, O; blue in merge). Inserts show higher magnification of the boxed areas. Scale bar: 10 µm.
II. NMDA stimulation leads to significant reduction of synapse density in hippocampal neurons transfected with empty pRNAt vector (black column), but no reduction was observed in siRNA transfected neurons (grey column). No significant differences were found between unstimulated neurons transfected with empty pRNAt vector (white column) and neurons transfected with siRNA (hatched column). Data are presented as a mean ± SEM. **p< 0,01. 50 neurons were quantified per each experimental group.

used as a control. Four hours later neurons were fixed and immunostained with anti-Bassoon antibody to visualize synapses and with anti-MAP2 antibodies to visualize dendritic protrusions. Bassoon puncta were counted per 50 µm length of each randomly chosen neuron and then was expressed as number of synapses per 10 µm. Altogether 50 different neurons were used for each experimental group.

Similar to results described above, neurons transfected with empty pRNAt vector and stimulated with NMDA showed significant reduction in synapse density in comparison to unstimulated control cells (Fig. 10, 11). However, no reduction in synapse density was found after NMDA stimulation in neurons transfected with the siRNA. Thus, knocking down the nuclear Jacob expression by siRNA abolished the reduction of synapse numbers after NMDA stimulation. Taken together, these results suggest that the nuclear translocation of Jacob upon NMDA receptor activation has a negative effect on synaptogenesis depending on gene transcription.

3.3 Jacob links extrasynaptic NMDA receptors and CREB dephosphorylation

3.3.1 Extrasynaptic NMDA receptor activation induced massive nuclear translocation of Jacob

As described in sections 3.2.1 and 3.2.2 Jacob translocates to the nucleus in response to NMDA receptor activation and the nuclear accumulation of Jacob has a strong negative pleiomorphic effect on neurite and synapse number in hippocampal neurons. The number of studies indicates that there are marked differences in cellular responses induced by different populations of NMDA receptors: synaptic and extrasynaptic (Hardingham et al., 2002; Hardingham and Bading, 2002, 2003; Vanhoutte and Bading, 2003). Calcium entry through synaptic NMDARs strongly promotes CREB activity and CREB-dependent gene expression; in direct contrast, activation of extrasynaptic NMDARs triggers a dominant CREB shut-off signal that acts via inducing rapid dephosphorylation of CREB on serine-133 (Hardingham et al., 2002; Hardingham and Bading, 2002, 2003; Vanhoutte and Bading, 2003). The transcription factor CREB is thought to be central to certain aspects of adaptive responses by the neuron, controls the expression of a number of pro-survival genes and has been shown to be important in determining neuronal survival/death (Tao et al., 1998; Riccio et al., 1999; Walton and Dragunow, 2000; Finkbeiner, 2000; Mantamadiotis et al., 2002).

To determine which type of NMDA receptors is responsible for nuclear translocation of Jacob, synaptic or extrasynaptic NMDA receptors were stimulated in primary hippocampal cultures. Two hours after stimulation the neurons were fixed, immunostained with anti-Jacob antibodies, and the level of Jacob immunoreactivity in the cell nuclei was determined.

As hippocampal cultures contain inhibitory interneurons (~10%) that impose a tonic inhibition on the neuronal network, blocking $GABA_A$ (γ-aminobutyric acid) receptor function causes the neurons to fire synchronous bursts of action potentials. The GABA receptor antagonist bicuculline induces bursts of action potentials, which are associated with synaptic NMDA receptors activity (Hardingham et al., 2001a). Simultaneous treatment with 2.5 mM 4-aminopyridine (4-AP), a weak potassium-channel blocker, converts the bicuculline-induced ‘oscillation type’ calcium signals into elevated ‘plateau-type’ calcium signals and markedly increases the burst frequency (Hardingham et al., 2002). Therefore,

biccuculine/4-AP treatment was used as first experimental conditions to activate synaptically located NMDA receptors.

In the second set of experimental conditions, synaptic NMDA receptors were selectively inactivated using MK-801 in conjunction with bicuculline and 4-AP. Because MK-801 is an open channel blocker and binds only activated NMDA receptors, the population of NMDA receptors not stimulated by bicuculline-induced firing (those not located at synapses) were left unblocked (Hardingham et al., 2002). This population of extrasynaptic NMDA receptors was then activated by adding 100 µM NMDA to the medium (third experimental conditions).

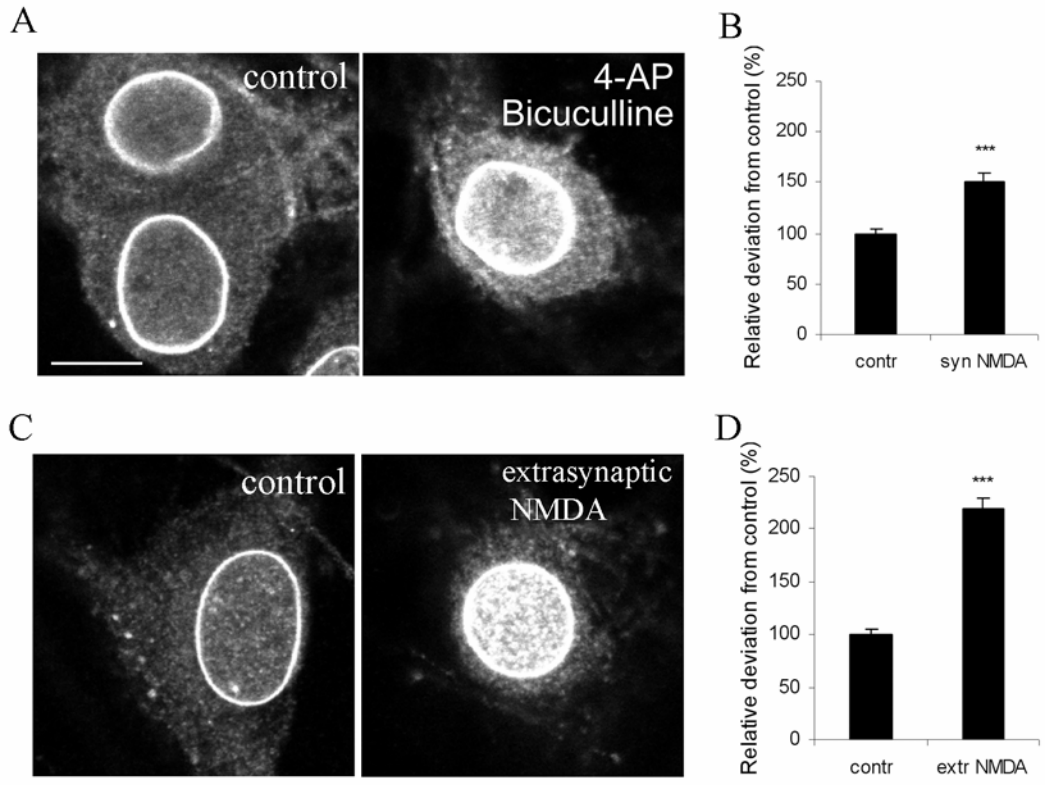

Fig. 12 Stimulation of extrasynaptic NMDA receptors rather than synaptic NMDA receptors is responsible for nuclear Jacob translocation. I. Neurons after 16 DIV were treated with 50 µM bicuculline and 2.5 mM 4-AP to induce activation of synaptic NMDA receptors (A right) or with 50 µM bicuculline, 2.5 mM 4-AP, 10 µM MK-801 and 30 min later (after washing) 100 µM NMDA for 3 min to induce activation of extrasynaptic NMDA receptors (C right). Untreated cells (A, C left) were used as a control. After washing cultures were incubated for 30 min and then fixed and immunostained with anti-Jacob antibodies. Scale bar: 10 µm.
II. Quantitative analysis of nuclear Jacob immunofluorescence.
Data are presented as percent deviation from unstimulated control cells. Synaptic NMDA receptor activation induces 50% increase of Jacob immunoreactivity in the nuclei in comparison with control cells (A). In contrast, activation of extrasynaptic NMDA receptors resulted in a 120% increase of nuclear Jacob immunoreactivity (B). Data are presented as a mean ± SEM. ***p< 0,001. 20-30 neurons were quantified per each experimental group.

Confocal laser scan microscopy and statistical analyzes were performed together with Dr. Anna Karpova, the special laboratory for electron- and laserscanning microscopy, Leibniz

Institute for Neurobiology, Magdeburg. Calcium flux through synaptic NMDA receptors, triggered by bicuculline exposure, induced 50% increase of Jacob immunoreactivity in neuronal nuclei in comparison to untreated cells (Fig. 12). However, activation of extrasynaptic NMDA receptors resulted in much higher – 120% - increase of nuclear Jacob immunoreactivity (Fig. 12). These results suggest that Jacob nuclear translocation is dominantly triggering by activation of extrasynaptic population of NMDA receptors.

3.3.2 Nuclear Jacob has a negative regulatory effect on CREB phosphorylation

Activation of extrasynaptic NMDA receptors triggers CREB shut-off pathway that acts via induction of rapid dephosphorylation of CREB on serine-133 (Hardingham et al., 2002; Hardingham and Bading, 2003). On the other hand, activation of extrasynaptic NMDA receptors triggers massive Jacob nuclear translocation and as it was shown in sections 3.2.4 Jacob might be involved in transcription regulation. Based on these data we can assume that Jacob might link extrasynaptic NMDA receptors and CREB dephosphorylation. To test this hypothesis and investigate whether Jacob nuclear accumulation will affect the CREB phosphorylation primary hippocampal neurons were transfected with ΔMyr-Jacob-GFP – the mutant which accumulates exclusively in the cell nucleus – or with empty GFP vector, 10 hours after transfection the cells were fixed and immunostained with anti-phosphor-CREB (Ser-133) antibody to assess the level of phosphorylated CREB in transfected neurons.

Overexpression of ΔMyr-Jacob-GFP resulted in a drastic reduction of phosphorylated CREB in neuronal nuclei in comparison with untransfected cells (Fig. 13). No significant differences in the level of CREB phosphorylation was found between GFP transfected control and untransfected neurons (Fig. 13).

These data support the idea that Jacob couples the extrasynaptic NMDA receptors and CREB dephosphorylation.

To provide a direct test of the hypothesis that Jacob plays an important role in CREB shut-off pathway, primary hippocampal neurons (DIV 8) were transfected with siRNA specifically targeted to mRNAs corresponding to Jacob isoforms that contain exon 6 sequence and therefore prevent nuclear translocation of Jacob; 7 days following transfection (DIV 15) extrasynaptic NMDA receptors were stimulated as described in the previous section. Neurons transfected with an empty pRNAt vector were used as a control. 15 minutes after stimulation, neurons were fixed and immunostained with anti-phosphor-

CREB (Ser-133) antibody and levels of phosphorylated CREB in the nuclei of transfected neurons were analyzed.

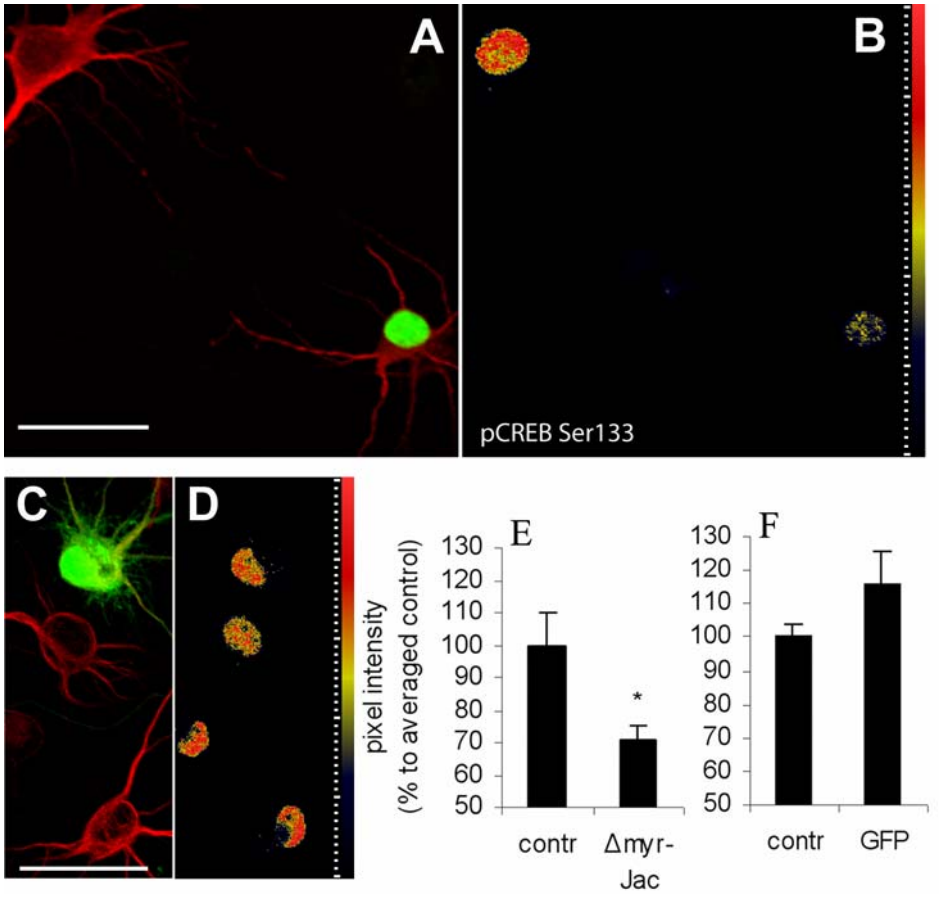

Fig. 13 Nuclear Jacob overexpression induces CREB dephosphorylation. Hippocampal neurons after 11 DIV were transfected with ΔMyr-Jacob-GFP (A, B) or GFP-vector without insert (C, D). Ten hours later transfected cultures were fixed and immunostained with antibodies against phosphorylated CREB on Ser-133 (pCREB Ser133; B, D). Fluorescence changes in phosphor-CREB levels were quantified from averaged confocal image stacks acquired using ImageJ software in nuclei regions. Colored bars represent pixel intensity in range from 0 (black) to 255 (red). Scale bar: 50 μm. Overexpression of nuclear Jacob significantly decrease level of phosphorylated CREB (A, B, E) in comparison with untransfected neurons; whereas no significant differences was found in phosphor-CREB level between untransfected and GFP-transfected neurons (C, D, F). Data are presented as a percent deviation from untransfected cells (mean ± SEM). * p< 0,1. 20-30 neurons were quantified per each experimental group.

Stimulation of the extrasynaptic population of NMDA receptors leads to significant reduction in phosphor-CREB levels in neurons transfected with empty pRNAt vector in comparison with unstimulated control cells (Fig. 14). However, no significant decrease in phopho-CREB levels was found after extrasynaptic NMDA receptor activation in neurons transfected with the siRNA. Thus knocking down the nuclear Jacob expression by siRNA abolishes the negative effect of extrasynaptic NMDA receptor activation on CREB

phosphorylation (Fig. 14). These results indicate that Jacob play a crucial role in the CREB shut-off pathway initiated by extrasynaptic NMDA receptors.

A

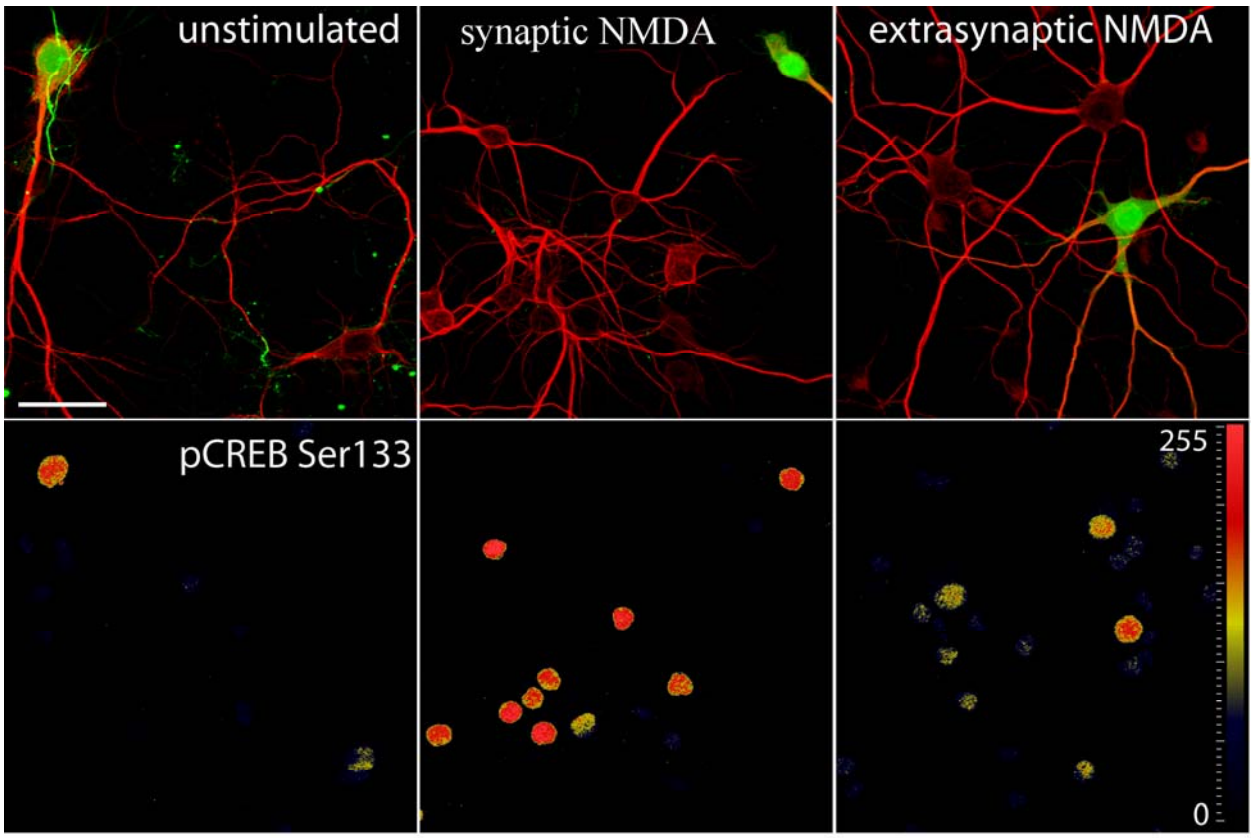

B

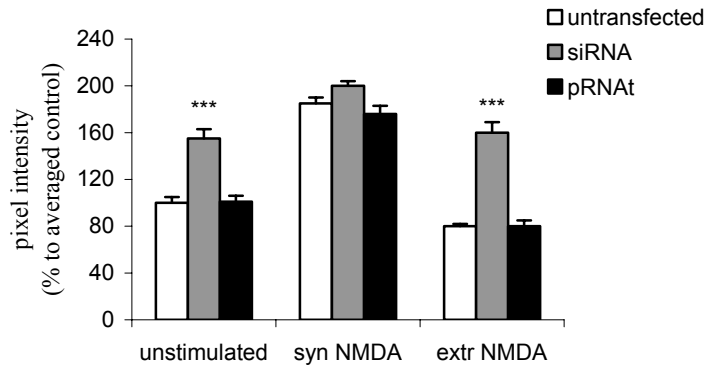

Fig. 14 Nuclear knockdown of Jacob prevents CREB shut-off after extrasynaptic NMDA receptor activation. A. Primary hippocampal neurons were transfected with siRNA (DIV 8) (green in merge, upper panel) to knock down levels of nuclear Jacob. At DIV 15 synaptic or extrasynaptic NMDA receptors were stimulated, neurons were incubated after stimulation for 30 min and then fixed and immunostained with anti-MAP2 antibody (red in merge, upper panel) to confirm their neuronal identity; and with anti-phosphor-CREB (Ser133) antibody (lower panel) to assess level of phosphorylated CREB. Colored bars represent pixel intensity in range from 0 (black) to 255 (red). Scale bar: 30 µm.**B.** Quantitative analysis of phosphor-CREB level. Knockdown of nuclear Jacob by siRNA transfection significantly decreased levels of CREB dephosphorylation after extrasynaptic NMDA receptor activation in comparison with untransfected neurons or neurons transfected with empty pRNAt vector.

3.3.3 Nuclear accumulation of Jacob triggers cell death

The transcription factor CREB controls the expression of a number of pro-survival genes like NGF and BDNF (Tao et al., 1998; Riccio et al., 1999; Vanhoutte and Bading, 2003). Mice lacking CREB in the CNS during development show extensive neuronal apoptosis (Mantamadiotis et al., 2002). Postnatal disruption of the CREB gene leads to progressive neurodegeneration in the hippocampus and dorsolateral striatum (Mantamadiotis et al., 2002). Extrasynaptic NMDA receptors are specifically coupled to a dominant CREB shut-off pathway that causes CREB dephosphorylation of its activator site (Ser133) that can lead to cell death (Hardingham et al., 2002). Similarly, apoptosis caused by the blockade of synaptic NMDARs in the developing brain (Ikonomidou et al., 1999) could be in part due to a reduction in synaptic NMDAR-dependent CREB activity. Since Jacob nuclear translocation seems to play an important role in the mechanism by which extrasynaptic NMDA receptors down-regulate CREB phosphorylation (section 3.3.1, 3.3.2), it was assumed that disturbance of Jacob nuclear trafficking may efficiently prevent neuronal death. To prove this prediction primary hippocampal neurons were transfected with siRNA (DIV 8) to knock down levels of Jacob which can be transported to the nucleus or with empty pRNAt vector and then stimulated (DIV 15) with 100 μM NMDA for 3 min or with 300 μM NMDA for 5 min. 24 hours after NMDA exposure total and dead cells were determined by nuclei staining with 100 ng/ml 4',6-diamidino-2-phenylindole (DAPI) and propidium iodide (PI) (10 μM), respectively. After 30 min incubation with DAPI and PI neurons were fixed and ration between dead and total number of cells was determined (Fig. 15). Furthermore, to determine apoptotic cells, neurons were fixed 24 hours after NMDA exposure and then were stained by using a ApopTag® Red Apoptosis Detection Kit (Fig. 16).

Treatment of the hippocampal cultures with high dose of NMDA resulted in massive cell death: more than 60% of cells transfected with the empty pRNAt vector demonstrate positive PI and apoptotic staining (Fig. 15, 16). However, knock down of nuclear Jacob by siRNA significantly diminish cell death weather monitored by PI or ApopTag assay. These data strongly suggest that Jacob nuclear accumulation triggers cell death.

Taken together, these studies indicate that after extrasynaptic NMDA receptor activation Jacob translocates to the nucleus where it contributes to the CREB shut-off pathway via induction of rapid CREB dephosphorylation and cell death.

A.

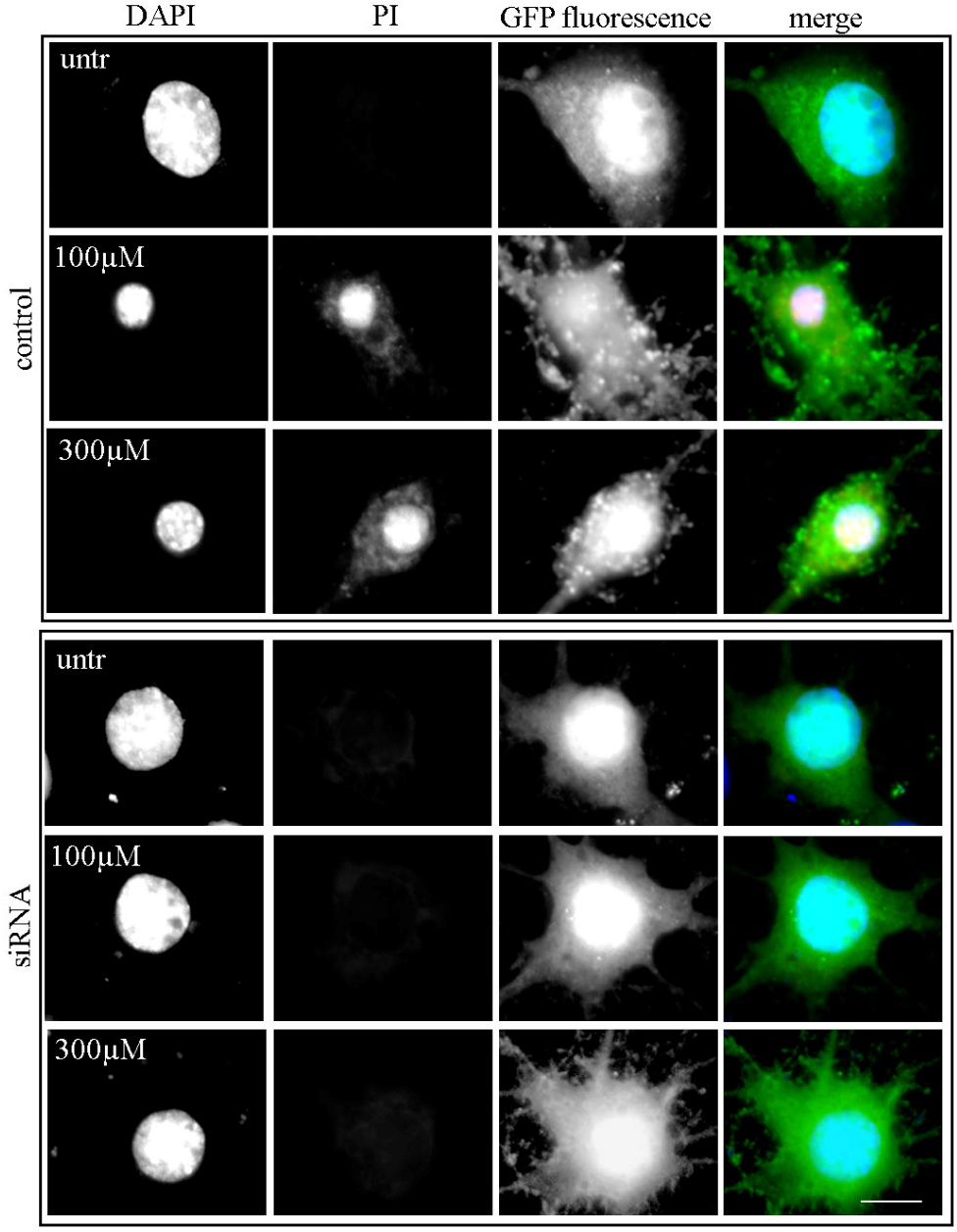

B.

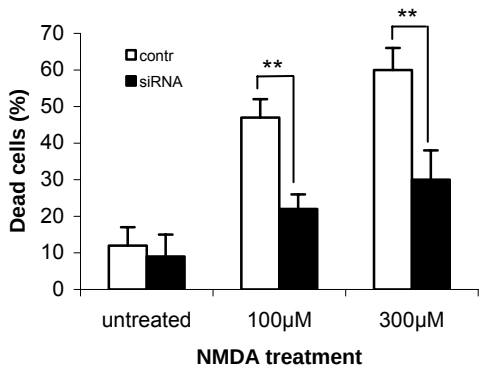

Fig. 15

See next page for legend

Fig. 15 Knockdown of nuclear Jacob attenuates NMDA-induced neuronal cell death. A. Hippocampal neurons after 8 DIV were transfected with siRNA to knock down levels of nuclear Jacob (lower panel) or with empty pRNAt vector (upper panel). 7 days later (DIV 15) transfected cultures were stimulated with 100 µM NMDA for 3 min or with 300 µM NMDA for 5 min (as indicated to the left), untreated cells were used as a control. After washing cultures were incubated for 24 hours and then DAPI (blue in merged displays) and PI (red in merged displays) were added for 30 min to the culture medium. Then neurons were fixed and examined under fluorescence microscope. Cell viability was determined as the ration of dead cells (PI-positive) to total number of transfected neurons (B). Data are presented as a mean ± SEM. **p< 0,01. 40 neurons were quantified per in each group. Scale bar: 10 µm.

A.

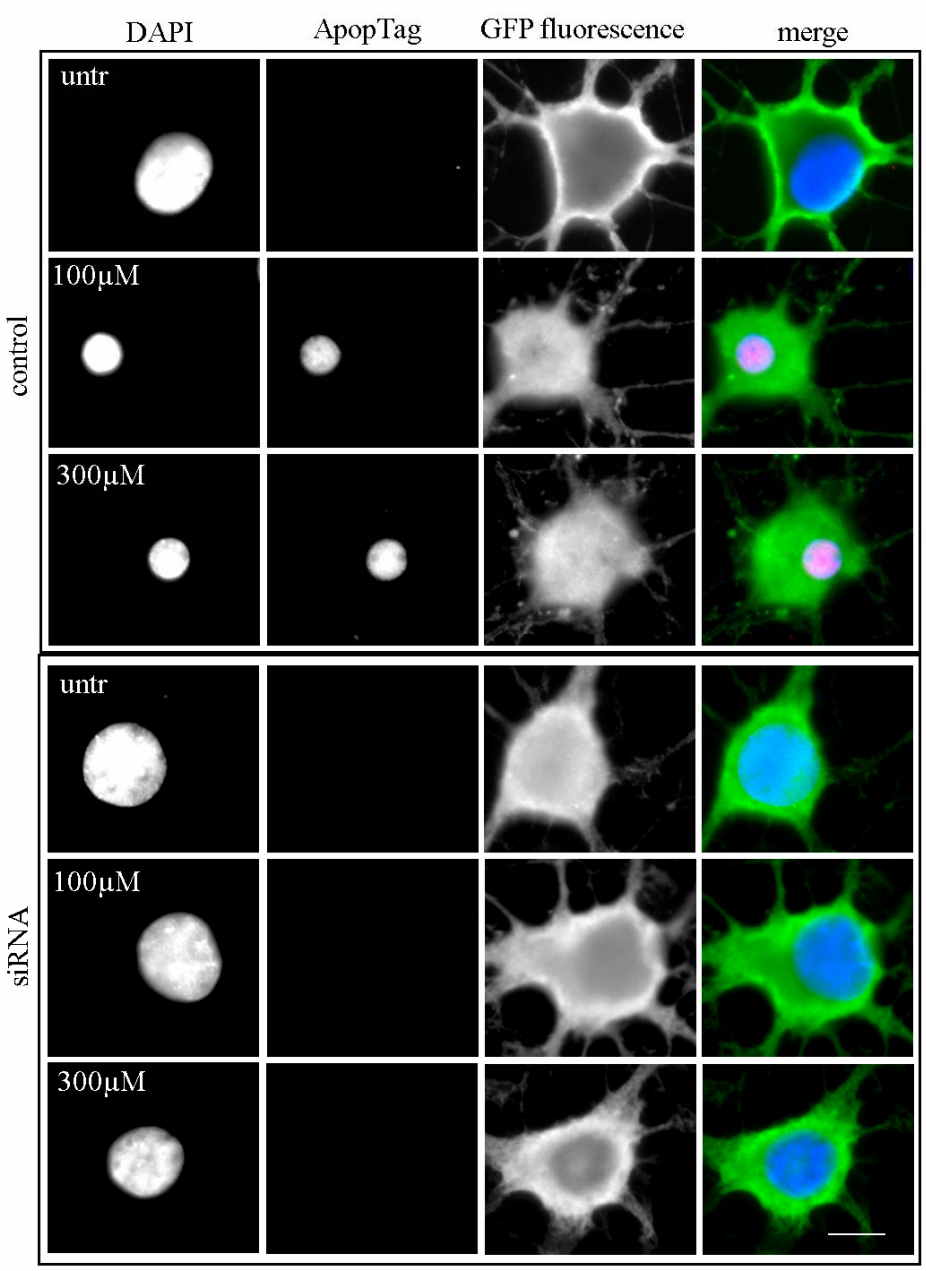

Fig. 16

See next page for legend

B.

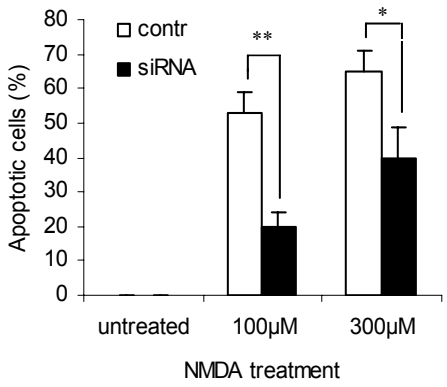

Fig. 16 Knockdown of nuclear Jacob diminishes NMDA-induced apoptotic cell death. A. Primary hippocampal neurons were transfected with siRNA (DIV 8) to knock down the level of nuclear Jacob (lower panel) or with empty pRNAt vector (upper panel). At DIV 15 transfected neurons were stimulated with 100 µM NMDA for 3 min or with 300 µM NMDA for 5 min (as indicated to the left), untreated cells were used as a control. 24 hours after NMDA exposure neurons were fixed and stained by using a ApopTag® Red Apoptosis Detection Kit to determine apoptotic cells (red in merged displays). Neuronal nuclei were counterstained with DAPI (blue in merged displays). Cell viability was determined as the ration of dead cells to total number of transfected neurons (B). Data are presented as a mean ± SEM. * p< 0,1; **p< 0,01. 40 neurons were quantified in each group. Scale bar: 10 µm.

3.3.4 The C-terminal part of Jacob is dispensable for its negative effect on CREB phosphorylation

As it was shown in section 3.2.3 the N-terminal part of the Jacob protein is responsible and sufficient for its strong negative effect on synapto-dendritic architecture. On the other hand, Jacob's C-terminus is dispensable for its morphogenetic effects. This suggested that C-terminal part of Jacob is not involved in the transcription regulation and CREB shut-off pathway.

To test this prediction primary hippocampal neurons were transfected with C-term-Jacob-GFP or with ΔMyr-Jacob-GFP, fixed 10 hours following transfection and immunostained with anti-phosphor-CREB (Ser133) antibody to assess levels of phosphorylated CREB in transfected neurons.

ΔMyr-Jacob-GFP overexpression leads to 30 % reduction of phosphor-CREB level in comparison with untransfected cells (Fig. 17) whereas no significant differences were found in the level of CREB phosphorylation between untransfected neurons and cells transfected with C-term-Jacob-GFP (Fig. 17). These findings are consistent with the previous observations that the C-terminal part of Jacob is inessential for its morphogenetic

effect and confirm the hypothesis that Jacob's C-terminus is dispensable for regulation of CREB phosphorylation.

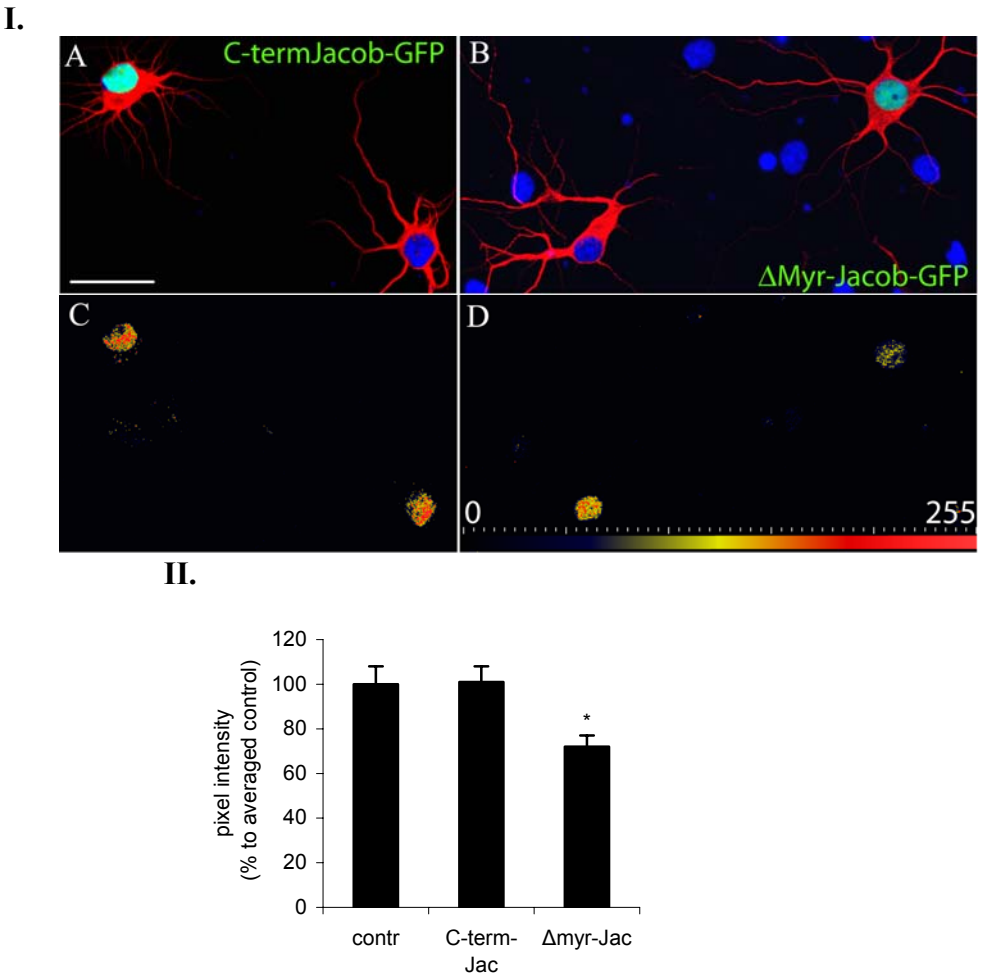

Fig. 17 The C-terminal part of Jacob is dispensable for its negative effect on CREB phosphorylation.
Hippocampal neurons after 11 DIV were transfected with C-term-Jacob-GFP (A, C) or with ΔMyr-Jacob-GFP (B, D). Ten hours later transfected cultures were fixed and immunostained with anti-phosphor-CREB (Ser-133) antibody (C, D). Neuronal nuclei were counterstained with DAPI (blue). Changes in fluorescence intensity of phosphor-CREB levels were quantified from averaged confocal image stacks acquired using ImageJ software in nuclei regions. Colored bars represent pixel intensity in range from 0 (black) to 255 (red). Scale bar: 30 μm. Overexpression of nuclear Jacob significantly decrease the level of phosphorylated CREB (D, II) in comparison with untransfected neurons; whereas no significant differences were found in phosphor-CREB levels between untransfected and C-term-Jacob-GFP-transfected neurons (C, D, F). Data are presented as percentage deviation from untransfected cells (mean ± SEM). * p< 0,1. 20-30 neurons were quantified per each experimental group.

3.4 Caldendrin regulates Jacob distribution in neurons

At resting conditions, Jacob is present in the somato-dendritic compartment and demonstrates significant overlap with the distribution of Caldendrin in dendritic processes and spines. In contrast to Caldendrin, Jacob translocates to the nucleus in response to

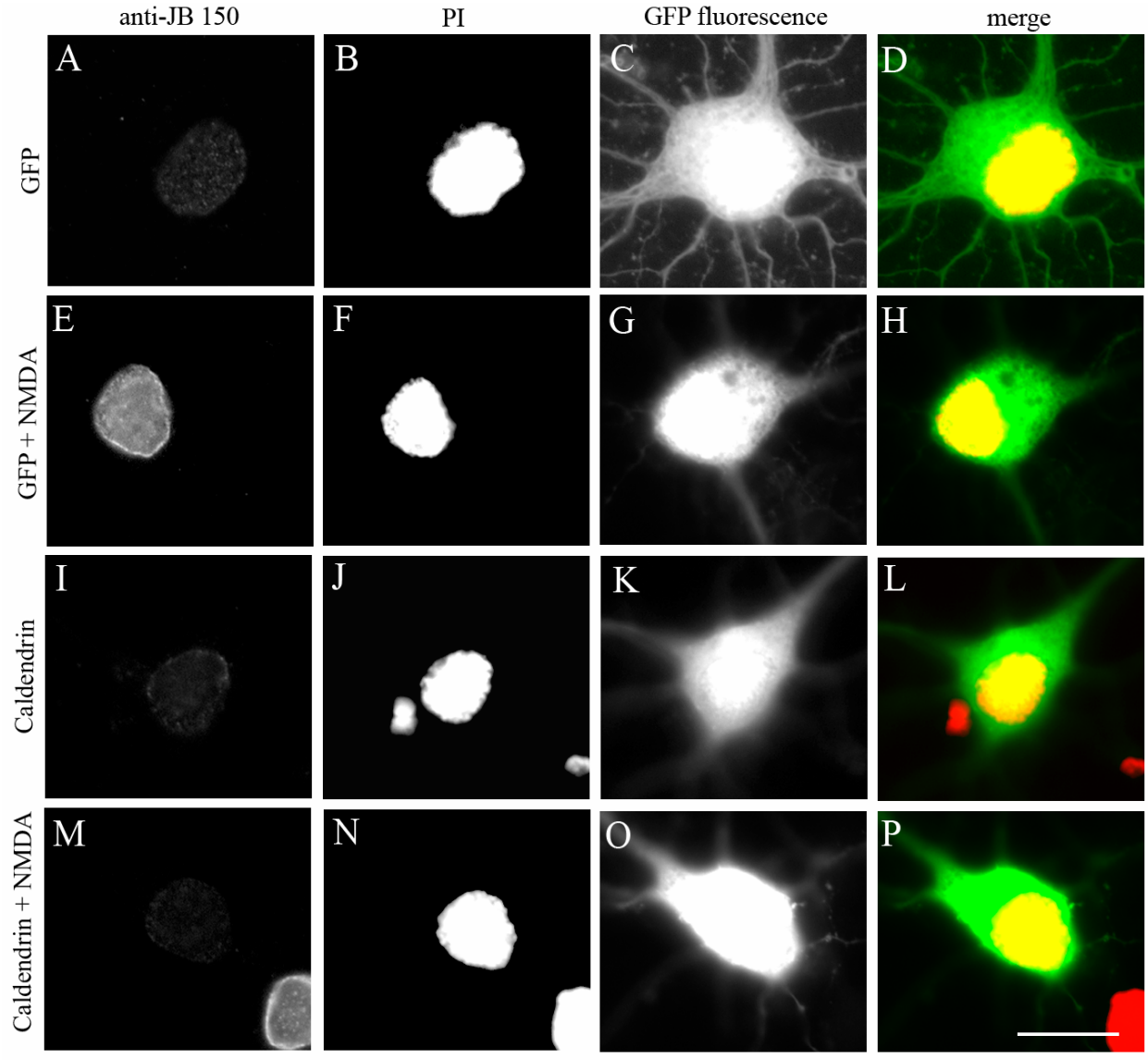

II

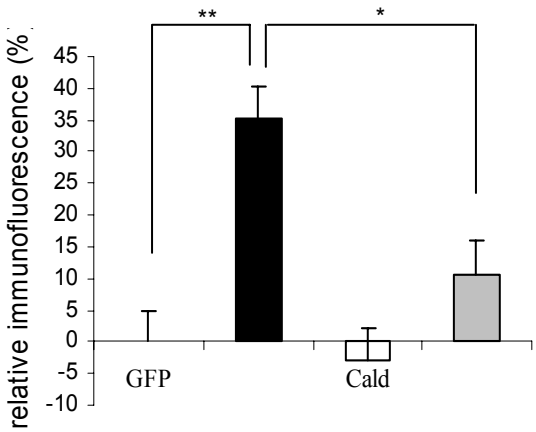

Fig. 18

See next page for legend

Fig. 18 Caldendrin overexpression prevents nuclear accumulation of Jacob upon NMDA receptor activation.
I. Hippocampal neurons after 11 DIV were transfected with wt-Caldendrin-GFP (I-P) or GFP-vector without insert (A-H). 24 hours later transfected cultures were stimulated for 3 min with 100 μM NMDA (E-H; M-P). After washing cultures were incubated for 2 hours and then fixed and immunostained with antibodies against the endogenous Jacob (JB 150) and neuronal nuclei were counterstained with propidium iodide (PI; red in merged displays). Scale bar: 10 μm.
II. Quantitative analysis of nuclear Jacob immunofluorescence.
Data are presented as a percent deviation from unstimulated GFP-transfected cells. After NMDA application Jacob immunofluorescence significantly increase in nuclei of GFP-transfected neurons (black column) but no increase of nuclear Jacob immunoreactivity in response to NMDA receptor activation was detected after wt-Caldendrin overexpression (gray column). Data are presented as a mean ± SEM. * p< 0,1; **p< 0,01. 50 neurons were quantified per each experimental group.

NMDA receptor activation and the NLS of Jacob is essential for this translocation (section 3.1). Moreover, it was shown previously by Dr. Michael R. Kreutz (unpublished data) that Jacob's NLS is a binding site for importin-α, a well-studied adapter which mediates nuclear import of proteins that carry a classical NLS (Weis, 2002). Like Jacob importin-α translocates from dendrites to the nucleus upon NMDA receptor activation (Thompson et al., 2004) and recruits importin-α-bound Jacob to the nucleus (Dr. Michael R. Kreutz, unpublished data). However, at high calcium which can be achieved after enhanced synaptic activation, Caldendrin competes with importin-α for Jacob binding and can prevent its nuclear translocation (Dr. Michael R. Kreutz, unpublished data). Therefore, it was predicted, that after synaptic activation Caldendrin will bind Jacob and mask Jacob's NLS, and thereby interfere with Jacob's nuclear recruitment.

To confirm this hypothesis and investigate how Caldendrin binding affects the intracellular localization of Jacob after synaptic activation the following experiment was performed: Hippocampal neurons (DIV 11) were transfected with full-length GFP-Caldendrin or with GFP alone and 24 hours later transfected cultures were stimulated for 3 min with 100 μM NMDA. To assess Jacob's distribution, neurons were fixed 2 hours following stimulation and immunostained with antibodies against the endogenous Jacob (Fig. 18). Expectedly, overexpression of Caldendrin led to a significant reduction of Jacob immunoreactivity in neuronal nuclei in comparison with GFP transfected cells (Fig. 18). Thus, the interaction with the calcium-sensor Caldendrin seems to mask the bipartite NLS of Jacob in vivo. This points to a regulatory function of the protein-protein interaction in nuclear trafficking of Jacob after enhanced synaptic activation that is most likely related to the competitive accessibility of Jacob's NLS for either Caldendrin or nuclear transport factor importin-α binding.

3.5 Extranuclear Jacob has a drastic effect on synapse formation

3.5.1 Overexpression of Jacob mutants induces formation of huge synapses in mature hippocampal neurons

Overexpression of ΔNLS-Jacob-GFP in primary hippocampal neurons resulted in 30% of transfected cells in formation of huge protrusions disposed around the cell body and along the dendrites (see section 3.1, Fig. 5). Moreover, the overexpressed ΔNLS-Jacob-GFP protein accumulated mainly in these protrusions. The same phenotype was observed after Δexon9-Jacob-GFP overexpression in primary hippocampal neurons. Furthermore, after Δexon9-Jacob-GFP overexpression almost all transfected neurons exhibited the 'protrusions phenotype'.

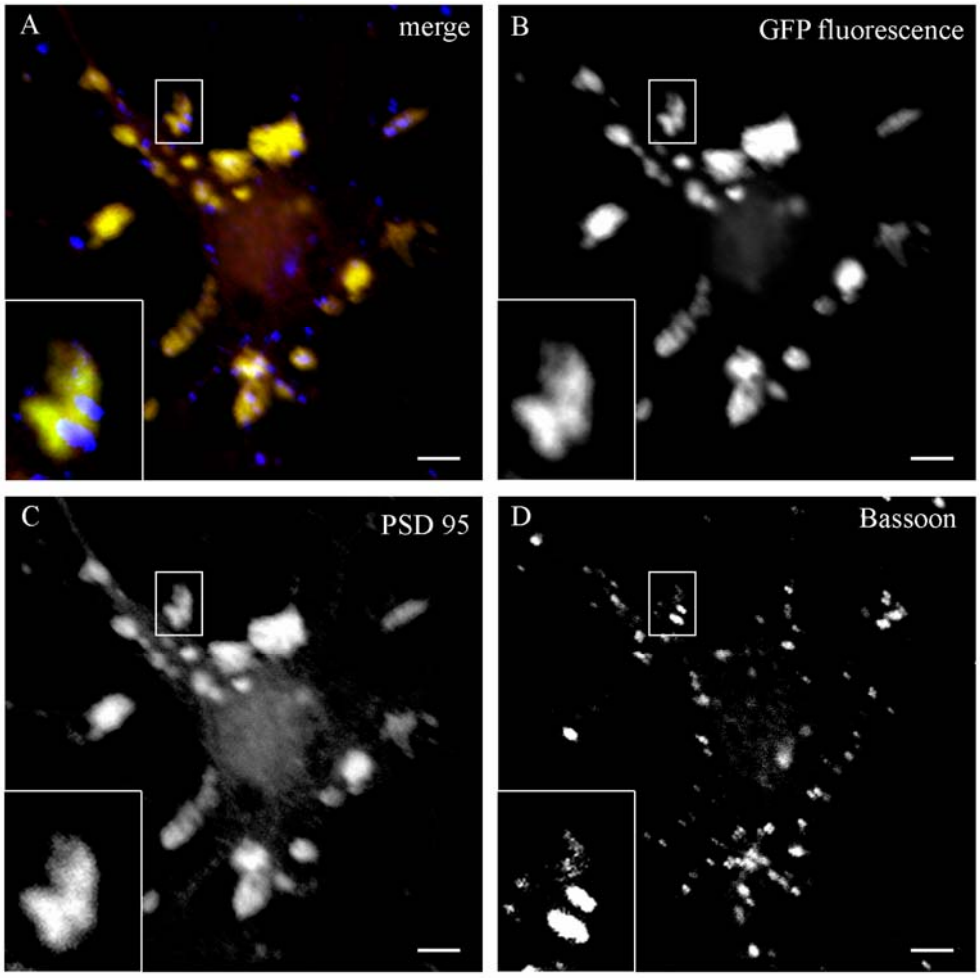

Fig. 19 Immunolocalization of endogenous PSD95 and Bassoon in mature hippocampal cultures transfected with Δexon9-Jacob-GFP.
Hippocampal neurons after 11 DIV were transfected with Δexon9-Jacob-GFP, 24 hours later the cultures were fixed and immunostained with anti-PSD95 antibodies (C; red in merge) and anti-Bassoon antibodies (D; blue in merge). **B** represents GFP fluorescence of overexpressed Δexon9-Jacob-GFP; **A** shows the merged images. Inserts represent higher magnifications of the boxed areas.

Immunostaining performed in neurons transfected with Δexon9-Jacob-GFP revealed intense immunolabeling for postsynaptic density-95 protein (PSD95; also known as synapse-associated protein SAP90) and proline-rich synapse-associated protein-2 (ProSAP2; also known as Shank3) in all the protrusions (Fig. 19, 20). It is well known that PSD95 and ProSAP2 are key components of the postsynaptic density (PSD), a membrane-associated structure of electron dense material that is found at the synaptic junction of excitatory synapses (Nimchinsky, et al., 2002). The PSD consists of neurotransmitter receptors, ion channels, adapter and scaffolding proteins as well as signaling molecules and couples presynaptic activity to postsynaptic signaling cascades (Kornau, 1997; Sheng, 1996; Sheng and Kim, 2000; Boeckers et al., 2001; Ehlers, 2002; Nimchinsky, et al., 2002). Therefore, it was suggested that the huge protrusions found in the Δexon9-Jacob-GFP transfected neurons might contain one or more functional synaptic contacts.

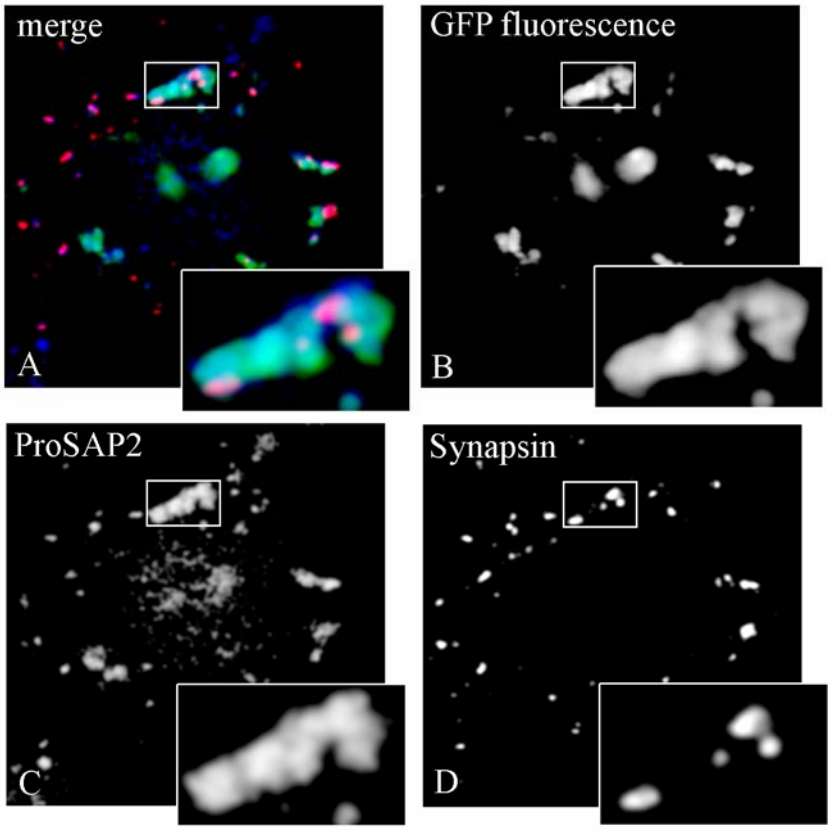

Fig. 20 Immunolocalization of endogenous ProSAP2 and Synapsin in mature hippocampal cultures transfected with Δexon9-Jacob-GFP.
Primary hippocampal neurons (DIV 11) were transfected with Δexon9-Jacob-GFP and fixed 24 hours after transfection. Transfected neurons were immunolabeled for ProSAP2 (C; blue in merge) and Synapsin (D; red in merge). **B** represents GFP fluorescence of overexpressed Δexon9-Jacob-GFP; **A** shows the merged images. Inserts represent higher magnifications of the boxed areas.

To determine whether the protrusions in Δexon9-Jacob-GFP transfected neurons contain neurotransmitter receptors, as a very important constituent of the functional synapse, immunofluorescence staining with antibodies directed against NMDA receptor (NMDAR) subunits 2a and 2b; and AMPA receptor subunit GluR2 was carried out. Double-immunofluorescence confocal laserscan micrographs demonstrated significant overlap between NMDAR 2a, NMDAR 2b, GluR2 immunolabeling and Δexon9-Jacob-GFP fluorescence in the protrusions (Fig. 21). These results support the hypothesis that the protrusions that arise in neurons after Δexon9-Jacob-GFP overexpression contain functional synapses.

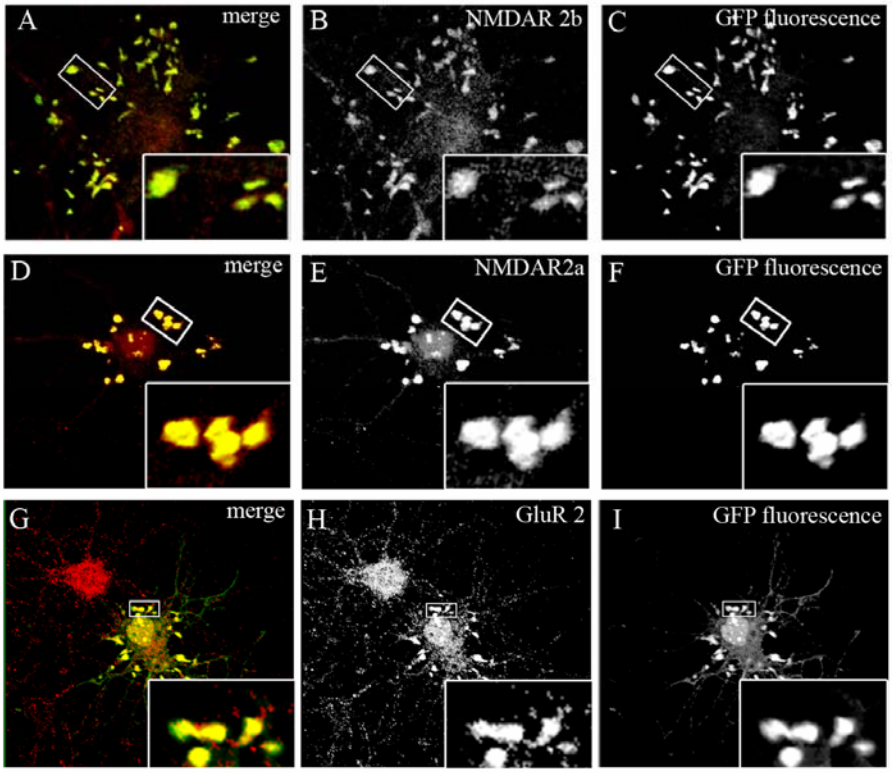

Fig. 21 Immunolocalization of endogenous NMDAR NR2B, NR2A and AMPA receptor GluR2 subunits in mature hippocampal neurons transfected with Δexon9-Jacob-GFP.
Hippocampal neurons (12 DIV) transfected with Δexon9-Jacob-GFP were fixed 24 hours after transfection and then immunostained with antibodies against the endogenous NMDA receptors NR2B subunit (B; red in merged image A), NR2A subunit (E; red in merged image D) or against AMPA receptor subunit GluR2 (H; red in merged image G). C, F and I micrographs represent GFP fluorescence signal corresponding to overexpressed Δexon9-Jacob-GFP. Inserts represent higher magnifications of the boxed areas.

To further prove the hypothesis, it needs to be addressed whether these protrusions make a contact with presynaptic terminals. To answer this question hippocampal neurons transfected with Δexon9-Jacob-GFP were immunostained with anti-Bassoon or anti-Synapsin antibody to visualize the presynaptic terminals and with anti-PSD95 (or

ProSAP2) antibodies to visualize the PSD. Confocal laserscan micrographs demonstrated that in most cases single GFP-positive protrusions overlapped with a single continuous PSD95 (or ProSAP2) immunopositive spots but with several separated Basson or Synapsin puncta (Fig. 19; 20; 22). Based on these data it was suggested that the protrusions in exon9-Jacob-GFP transfected neurons include one huge PSD and make contacts with several presynaptic terminals.

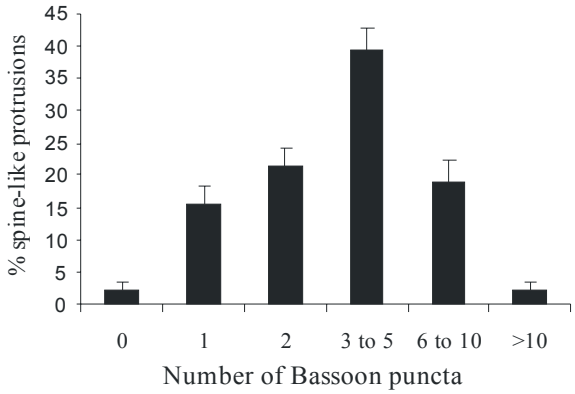

Fig. 22 Huge protrusions in Δexon9-Jacob-GFP transfected neurons make contacts with several presynaptic terminals.
11 DIV primary hippocampal neurons were transfected with Δexon9-Jacob-GFP, 24 hours later cultures were fixed and immunolabeled for Bassoon. Number of Bassoon puncta overlapping or contiguous to each GFP fluorescent spot corresponding to overexpressed Δexon9-Jacob-GFP was quantified. Single-plane confocal images were used for the quantification. Data are presented as a mean ± SEM.

Since Caldendrin can play a crucial role in the subcellular localization of Jacob (see sections 3.4) it was predicted that both proteins will exhibit a similar distribution in Δexon9-Jacob-GFP transfected neurons. Indeed, endogenous Caldendrin displayed a localization pattern overlapping closely with overexpressed Δexon9-Jacob-GFP (Fig. 23).

To visualize the morphology of the protrusions scanning electron microscopy (SEM) was carried out. All SEM experiments were performed in collaboration with Dr. Heiner Sann (the special laboratory for electron- and laserscanning microscopy, Leibniz Institute for Neurobiology, Magdeburg). SEM revealed that neurons transfected with Δexon9-Jacob-GFP have huge round-shaped structures disposed around the cell body and along the dendrites (Fig. 24).

Since Caldendrin can play a crucial role in the subcellular localization of Jacob (see sections 3.4) it was predicted that both proteins will exhibit a similar distribution in

Δexon9-Jacob-GFP transfected neurons. Indeed, endogenous Caldendrin displayed a localization pattern overlapping closely with overexpressed Δexon9-Jacob-GFP (Fig. 23).

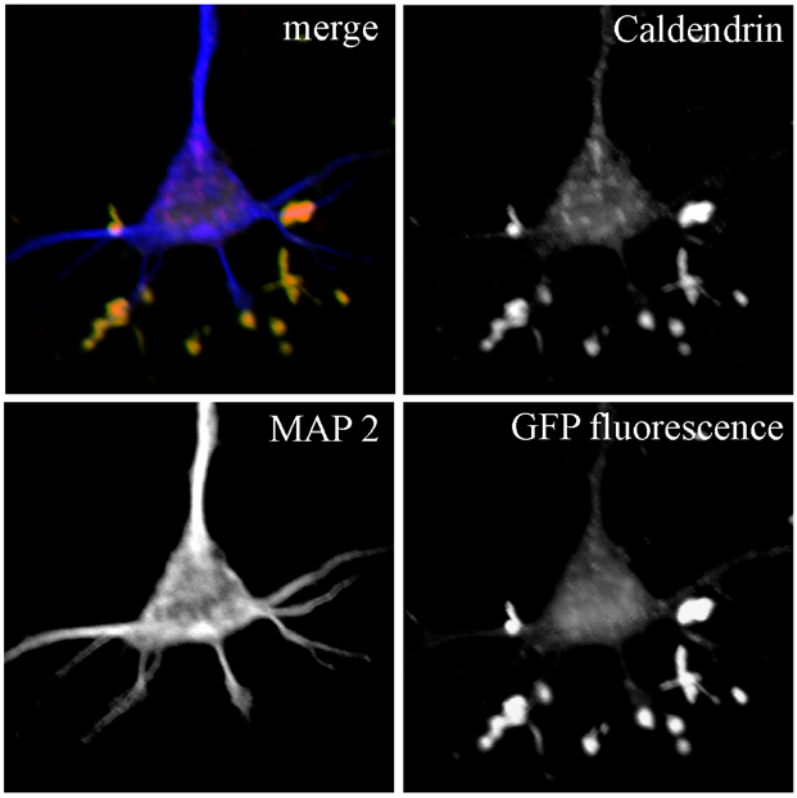

Fig. 23 Caldendrin and Δexon9-Jacob-GFP colocalizing in mature hippocampal neurons.
Primary hippocampal neurons after 11 DIV were immunostained with anti-Caldendrin (red in merge) and anti-MAP2 antibodies (blue in merge). GFP fluorescence signal correspond to overexpressed Δexon9-Jacob-GFP. Colocalization appears in yellow in merged image.

To visualize the morphology of the protrusions scanning electron microscopy (SEM) was carried out. All SEM experiments were performed in collaboration with Dr. Heiner Sann (the special laboratory for electron- and laserscanning microscopy, Leibniz Institute for Neurobiology, Magdeburg). SEM revealed that neurons transfected with Δexon9-Jacob-GFP have huge round-shaped structures disposed around the cell body and along the dendrites (Fig. 24).

To determine whether overexpression of Δexon9-Jacob-GFP in neurons caused the formation of these structures the following procedure was performed: confocal laserscan micrographs and SEM micrographs were taken from the same Δexon9-Jacob-GFP transfected cell and were compared. All structures on SEM micrographs that correspond to the protrusions visible as GFP-positive blobs on the laserscan micrographs were identified. All others structures on SEM micrographs comparable with the protrusions in shape and size were quantified.

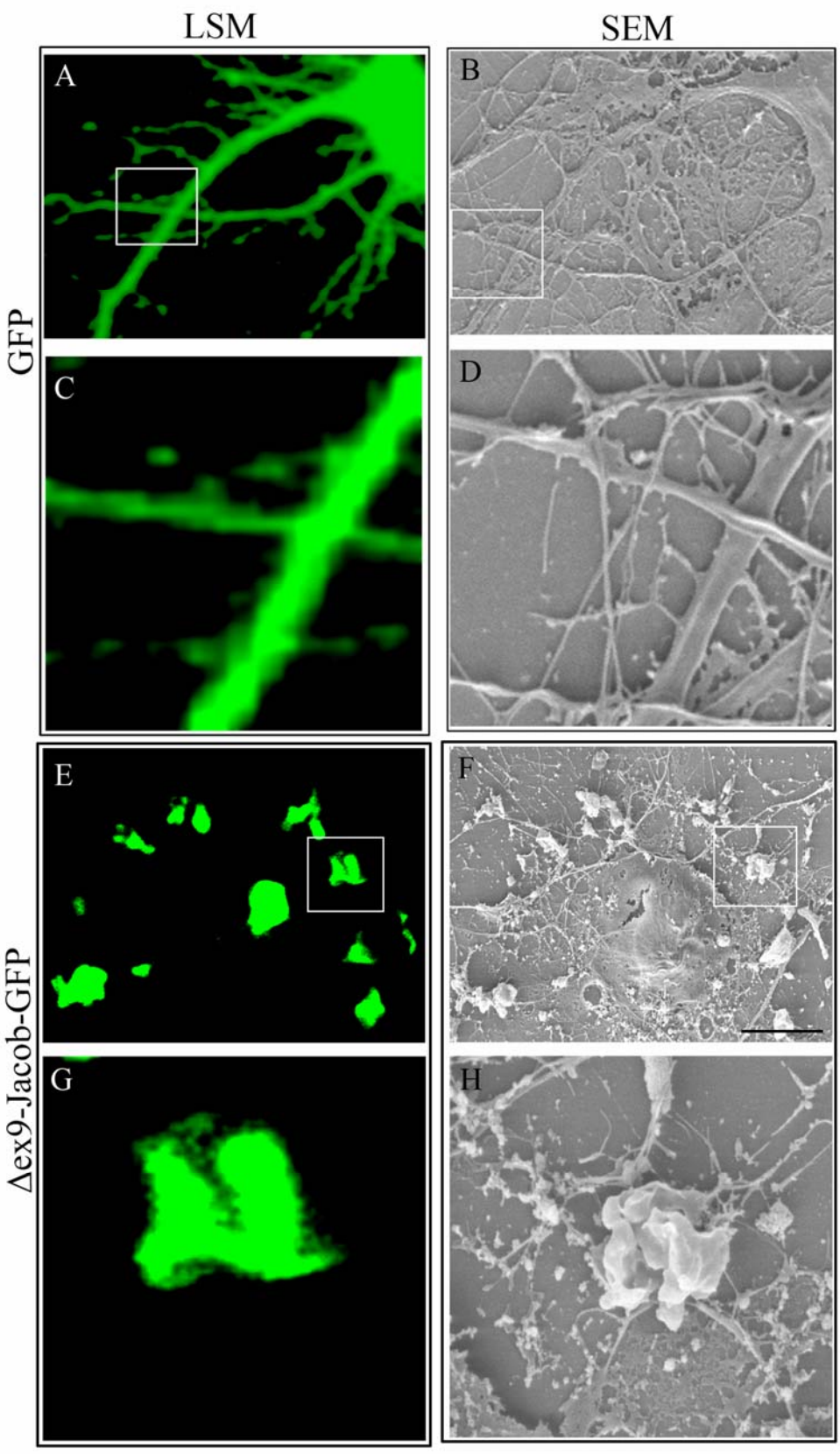

Fig. 24 Overexpression of Δexon9-Jacob-GFP in mature primary hippocampal neurons causes formation of huge protrusions.
Hippocampal neurons after 11 DIV were transfected with Δexon9-Jacob-GFP (E-H) or GFP-vector without insert (A-D). After 24 hours neurons were fixed and confocal laserscan (left panel) and scanning electron images (right panel) were taken. C, D and G, H represent higher magnifications of the boxed areas in A, B and E, F micrographs respectively. Scale bar: 10 μm.

Finally, it was found that 85% of all round-shaped structures on the SEM micrographs correspond to the GFP-positive protrusions (Fig. 25). No similar structures were found in case of GFP-transfected neurons (Fig. 24). Based on these data it was concluded that overexpression of Δexon9-Jacob-GFP in neurons results in the formation of huge membranous protrusions from the neuronal surface.

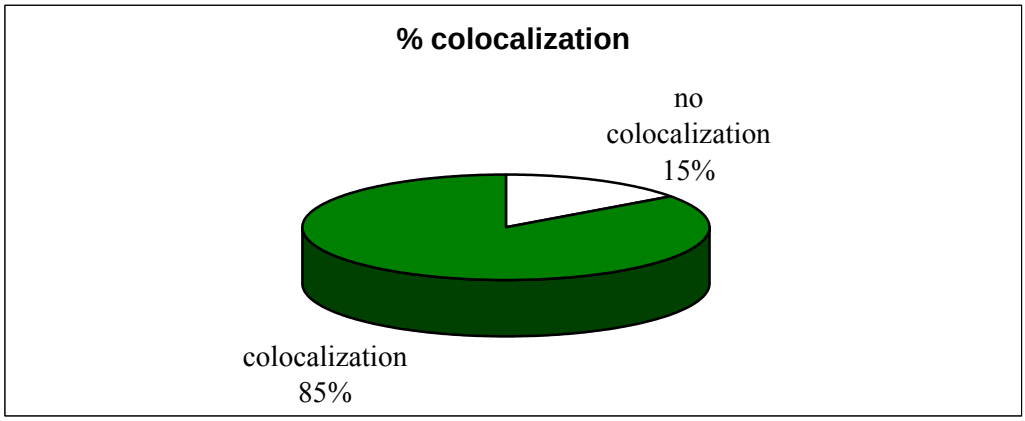

Fig. 25 Overexpressed Δexon9-Jacob-GFP accumulates in the huge protrusions in primary hippocampal neurons.
Confocal laserscan and scanning electron images were taken from Δexon9-Jacob-GFP transfected hippocampal neurons 24 hours after transfection. Then laserscan and SEM micrographs corresponding to the same cell were compared and all structures on SEM micrographs that correspond to the GFP-spot on the laserscan micrographs were identified.
All others structures comparable in size on SEM micrographs were quantified. 85 % of all round-shaped structures on SEM micrographs correspond to the GFP spots.

As it was described above, double-immunofluorescence staining with antibodies directed against PSD95 and GFP after Δexon9-Jacob-GFP overexpression demonstrated significant overlap in the protrusions (Fig. 19). Moreover, PSD95 immunolabeling was present as a single continuous spot and its size and shape more or less correspond to the GFP-positive protrusion (Fig. 19). Therefore, it was suggested that the protrusions have one large continuous PSD. To confirm this hypothesis the following experiment was performed: hippocampal neurons transfected with Δexon9-Jacob-GFP and GFP empty vector were fixed with 4% PFA and treated with buffer containing 0.3% Triton X-100 to destroy all membranous structure. Extraction of the plasma membrane with Triton X-100 removes the lipid bilayer, leaving the proteins associated with the insoluble cytoskeleton (Horst, et al., 1987). After that samples were immunostained for PSD95 and confocal laserscan micrographs and SEM micrographs were taken. SEM revealed that neurons transfected with Δexon9-Jacob-GFP had a huge Triton X-100 insoluble structure which corresponded to the PSD95 immunolabeled protrusions on laserscan micrographs (Fig. 26-I).

I.

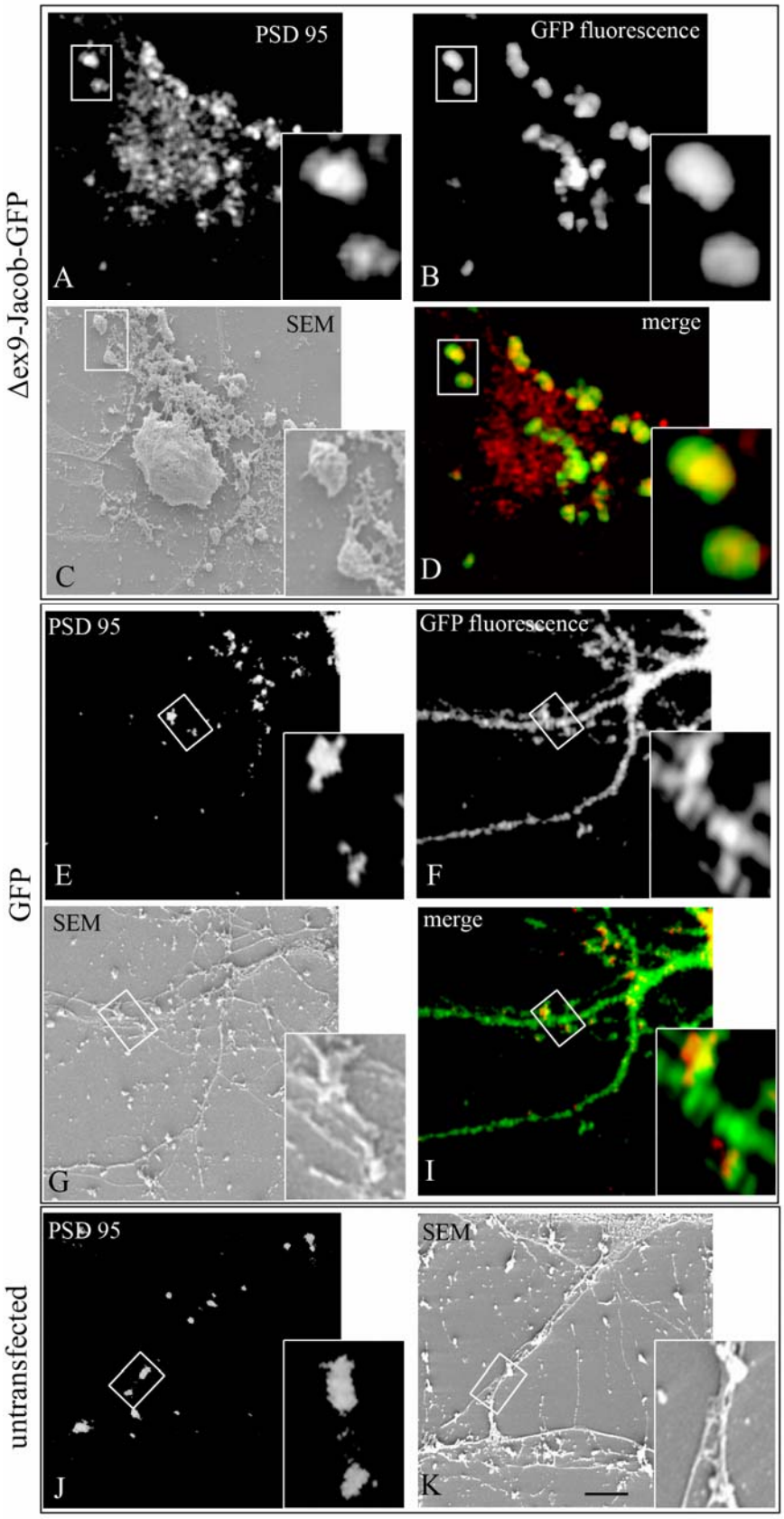

Fig. 26-I

See next page for legend

II.

III. **A** **B**

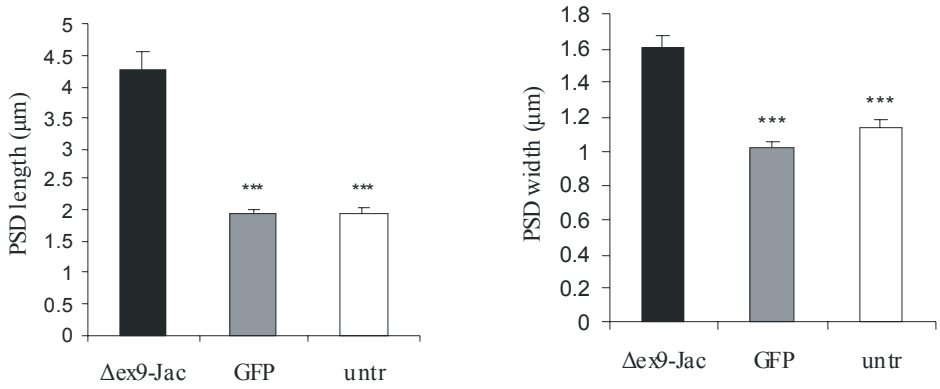

Fig. 26 Overexpression of Δexon9-Jacob induces formation of huge PSDs.

I. Hippocampal neurons after 11 DIV were transfected with Δexon9-Jacob-GFP (A-D) or GFP empty vector without insert (E-I). 24 hours after transfection neurons were fixed with 4% PFA and immunostained with anti-PSD95 antibodies to visualize PSDs (A, E, J; red in merge). The samples were treated with buffer containing 0.3% Triton X-100 during the immunostaining to remove membranous structures. Confocal laserscan and scanning electron micrographs (C, G, K) were taken. **B** and **F** represent GFP fluorescence of overexpressed Δexon9-Jacob-GFP and GFP, respectively. **D** and **I** show the merged images. The structures on SEM micrographs that correspond to the PSD95 spots on laserscan images were identified. Inserts represents higher magnification of the boxed areas. Scale bar: 5 µm.

II. Schematic drawing of the synapse and PSD (blue oval). The length of the longest Y- and X-axis of the PSDs on the SEM micrographs was measured and taken as a PSD length and width, respectively.

III. Neurons transfected with Δexon9-Jacob-GFP (black columns) have significantly larger PSD length (A) and width (B) than GFP transfected cells (grey columns) or untransfected control neurons (white columns). Data are presented as a mean ± SEM. *** $p < 0{,}001$. 5 - 8 neurons and 60 – 90 PSDs were quantified per each group.

The size and shape of these Triton X-100 insoluble structures were equal to the size and shape of the corresponding PSD95-positive spot on confocal micrographs. Based on this observation, Triton X-100 insoluble structures on SEM micrographs were determined as a PSD. The length of the longest Y- and X-axis of the PSDs was measured (Fig. 26-II). The longest Y-axis was taken as a PSD length and X-axis as a PSD width. Neurons transfected

with GFP vector and untreated cells were used as a control. It was found that protrusions in Δexon9-Jacob-GFP transfected neurons have almost 2.5 times longer and 1.6 times thicker PSDs than GFP transfected or untransfected neurons (Fig. 26-III). No significant differences concerning the PSD size were found between of GFP transfected neurons and untreated cells.

These data confirmed that huge protrusions induced by Δexon9-Jacob-GFP overexpression contain continuous PSDs several times exceeding the size of PSDs in untransfected or GFP transfected cells.

3.5.2 Overexpression of Jacob mutant result in the formation of huge PSD-like protrusions in young hippocampal neurons

It is well known that development of mature synapses is a quite prolonged process, requiring two to three weeks in rodents, a period equivalent to the entire period of prenatal development (Hall, 1992). Dissociated hippocampal neuronal cultures used in the present work were prepared from rat embryos (embryonic day 18) and synapse formation in these cultures starts around day 7 and until this time neurons do not have functional synapses (Papa et al., 1995; Boyer et al., 1998). Since overexpression of Δexon9-Jacob has a drastic effect on synapse formation in mature hippocampal neurons (section 3.5.1), the next aim was to investigate if Δexon9-Jacob also has impact on synaptogenesis in young neurons. For this purpose, 3-day-old primary hippocampal cultures were transfected with Δexon9-Jacob-GFP, fixed 24 hours later and immunolabeled for postsynaptic protein PSD95 and the presynaptic protein Bassoon (Fig. 27). All transfected neurons develop the same protrusion phenotype which was observed in mature hippocampal neurons after Δexon9-Jacob-GFP overexpression. Moreover, confocal laserscan micrographs demonstrated that all GFP fluorescence spots, which correspond to the overexpressed Δexon9-Jacob-GFP, clearly overlap with intense immunolabeling for PSD95 (Fig. 27). At the same time no PSD95 puncta were visible along the dendrites in young neurons transfected with GFP or untransfected neurons (Fig. 27).

These data suggest that Δexon9-Jacob-GFP overexpression provoke formation of huge clusters of the main component of the postsynaptic density - PSD95 - in young hippocampal neurons.

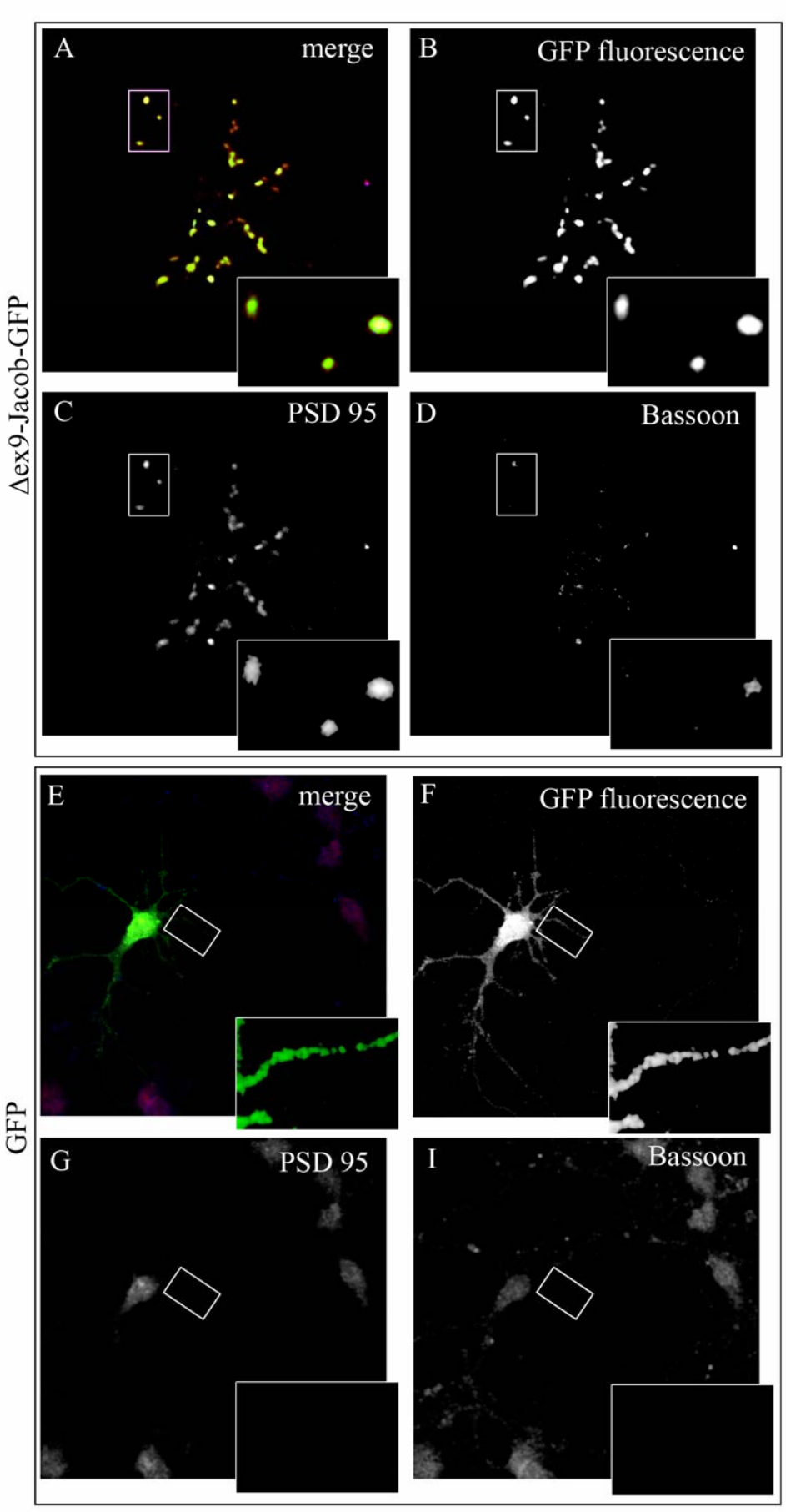

Fig. 27

See next page for legend

Fig. 27 Immunolocalization of endogenous PSD95 and Bassoon in young hippocampal cultures.
DIV3 hippocampal neurons were transfected with Δexon9-Jacob-GFP (A-D) or with GFP-vector without insert (E-I), 24 hours later the cultures were fixed and immunostained with anti-PSD95 antibodies (C, G; red in merged displays: A, E) and anti-Bassoon antibodies (D, I; blue in merged displays: A, E). **B** and **F** represent GFP fluorescence of overexpressed proteins. Inserts represent higher magnifications of the boxed areas.

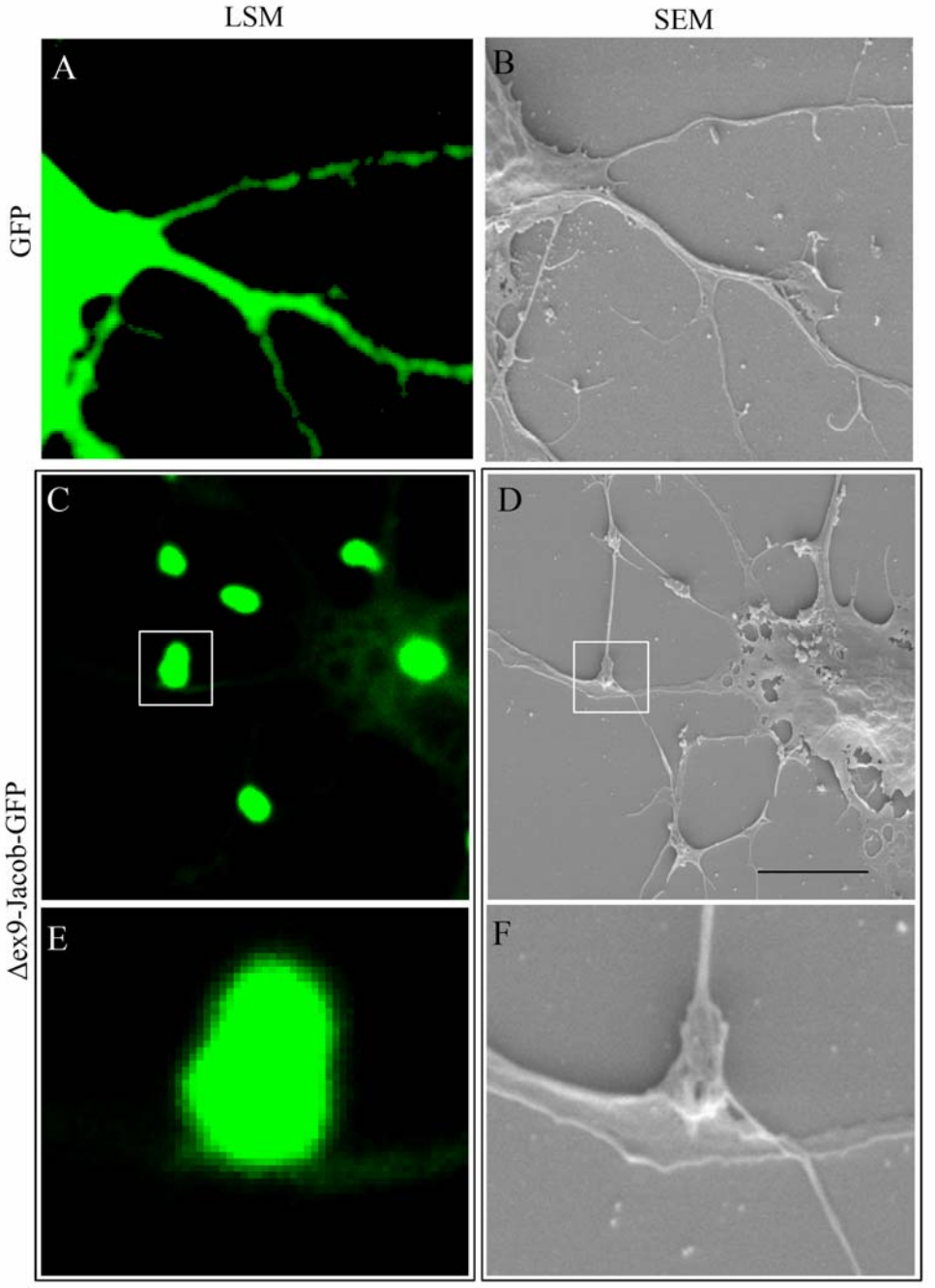

Fig. 28 Overexpression of Δexon9-Jacob-GFP resulted in formation of huge protrusions in young primary hippocampal neurons.
Hippocampal neurons after 3 DIV were transfected with Δexon9-Jacob-GFP (C-F) or GFP-vector without insert (A, B) and fixed 24 hours after transfection. Confocal laserscan (left panel) and scanning electron images (right panel) were taken. E and F represent higher magnifications of the boxed areas in C and D micrographs respectively. Scale bar: 10 μm.

This phenomenon may indicate that overexpression of Δexon9-Jacob-GFP induce formation of huge synapses in young hippocampal neurons. Moreover, confocal laserscan micrographs showed that some of the PSD95 and GFP fluorescent spots overlapped with Bassoon puncta (Fig. 27) as it was shown for mature hippocampal neurons transfected with Δexon9-Jacob-GFP (section 3.5.1, Fig. 18, 19, 21).

To visualize the structure of the protrusions developed by young hippocampal neurons after Δexon9-Jacob-GFP overexpression SEM was carried out. SEM revealed that Δexon9-Jacob-GFP accumulated in huge varicosities (protrusions) of the dendritic processes (Fig. 28) and no similar structures were found in case of GFP-transfected neurons. Moreover, clearly visible tiny processes connected most of the varicosities between each other. These tiny processes could represent self-connection between some of protrusions of the same neuron. This finding is in line with data obtained from immunofluorescence confocal laserscan micrographs which revealed presynaptic labelling with Bassoon on the protrusions (Fig. 27).

Taken together these data suggest that overexpression of Δexon9-Jacob-GFP in young primary hippocampal neurons resulted in formation of huge protrusions enriched with PSD95 and possible established contacts with presynaptic terminals.

3.5.3 Jacob overexpression causes similar effects in hippocampal and cortical neurons

The nervous system is composed of a number of different types of neurons. All of them respond differently to the same factors, including such important regulatory molecules as neurotransmitters, growth factors, neuropeptides and cytokines. A part of this flexibility is probably due to intrinsic differences between the various types of neuronal cells, for example, different stimuli induce distinct programmes of downstream gene expression in different types of neurons (Bartel et al., 1989; Mayr et al., 2001; West et al., 2002).

As shown in sections 3.5.1 and 3.5.2, overexpression of Δexon9-Jacob in primary hippocampal neurons has a drastic effect on synapse formation. To check whether this effect was cell type-specific or whether Jacob performs similar regulatory functions in different types of neuronal cells; primary cortical neurons were transfected with Δexon9-Jacob-GFP. 24 hours after transfection 90-100 % of transfected cortical neurons exhibited a similar protrusion phenotype, as that typically seen in hippocampal neurons transfected with Δexon9-Jacob-GFP (Fig. 29). However, protrusions developed in cortical neurons were smaller in size and larger in number than in case of hippocampal neuronal cells.

Moreover, Δexon9-Jacob-GFP overexpression in cortical neurons resulted in a larger number of neurites (Fig. 29). A similar increase in neurite number was observed in primary hippocampal neurons transfected with Δexon9-Jacob-GFP (Fig. 6). Therefore, these observations suggest that Jacob can play a similar regulatory role in different types of neuronal cells.

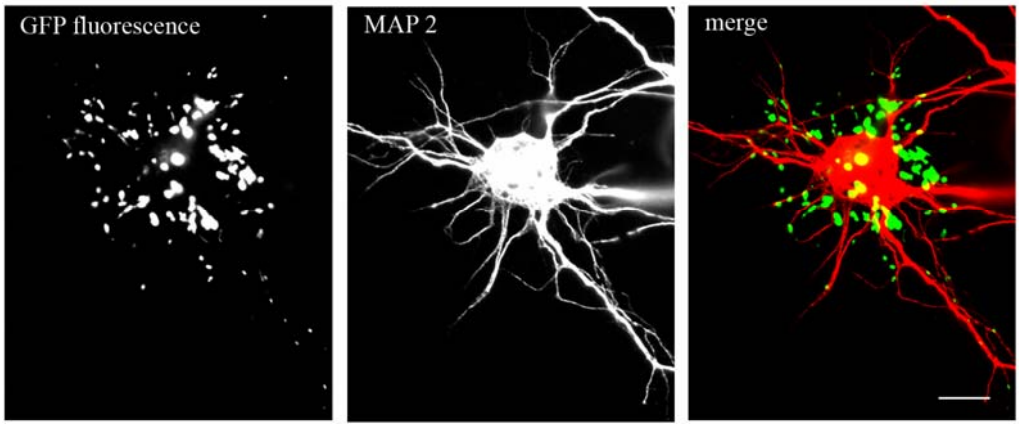

Fig. 29 Overexpression of Δexon9-Jacob induces formation of huge protrusions in cortical neurons. Cortical neurons after 10 DIV were transfected with Δexon9-Jacob-GFP and fixed 24 hours after transfection. Transfected cells were immunolabeled for MAP2 (red in merge) to confirm their neuronal identity.

4 Discussion

4.1 NMDA receptor activation triggers Jacob / importin binding and their nuclear translocation

Proper growth and branching of dendrites is crucial for nervous system function since the patterns of dendritic arborization determine the nature and amount of innervation that a neuron receives (Jan and Jan, 2003; Miller and Kaplan, 2003). Dendritic development is a highly dynamic process that is regulated by both activity-independent and activity-dependent signals. There is now compelling evidence that during postnatal development, neuronal activity is a key determinant of dendritic growth and branching (McAllister et al., 1996; Rajan and Cline, 1998; Redmond et al., 2002; Sin et al., 2002; Konur and Gosh, 2005). The time of maximal dendrite growth and remodeling is concurrent with that of afferent innervation suggesting that afferent activity can play an important role in dendritic development (Wu et al., 1996, 1999; Wong and Ghosh, 2002). A broad range of studies suggest that calcium is the pivotal messenger coupling synaptic activity to nuclear gene transcription and calcium-dependant signaling from synapses to the nucleus results in long-lasting changes in dendritic cytoarchitecture (Berridge 1998; Milner et al., 1998; Carafoli et al., 2001; Miller and Kaplan, 2003; Konur and Ghosh, 2005). It also has been shown that calcium signaling from synapse to nucleus propagates independently of global increases in calcium-concentrations (Deisseroth et al., 2003; Hardingham et al., 2001b). How are calcium-transients reliably encoded in the intracellular-signaling machinery? The newly identified protein Jacob is well suited to couple synaptic activity-dependent calcium signals to the cell nucleus and this novel synapto-nuclear signaling results in long-lasting changes in the cytoarchitecture of the dendrites and the number of synapses.

The requirement for transcription during long-lasting plasticity indicates that signals generated at the synapse must be transported to the nucleus where they are converted into changes in gene expression. Little is known about the cellular mechanisms that target and transport synaptically activated second messengers and transcription factors to the nucleus. The extreme polarity of neurons presents a special set of challenges for intracellular signal transduction, because the distance between the synapse and nucleus can be extremely large. Thus, a signal from a distal synapse must first travel the length of the axon or dendrite and then must be transported through the nuclear envelope. Cytoplasmic proteins bearing nuclear localization signals are targeted to the nucleus and

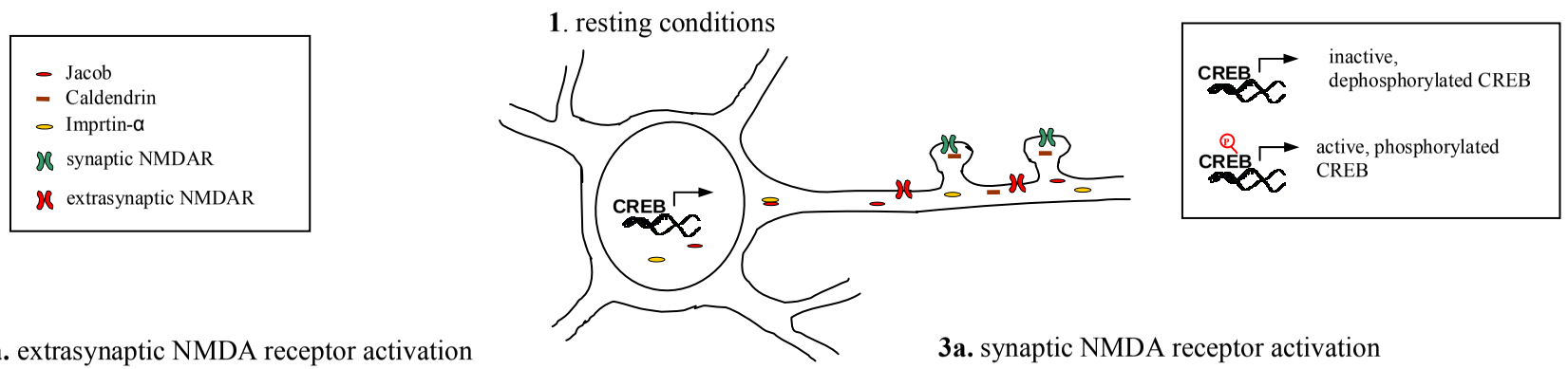

2a. extrasynaptic NMDA receptor activation

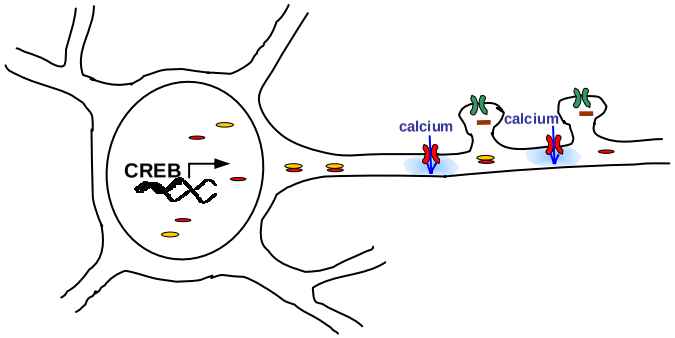

2b. CREB shut-off and simplification of synapto-dendritic architecture

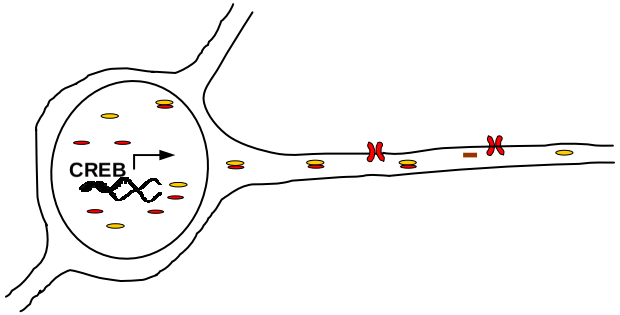

3a. synaptic NMDA receptor activation

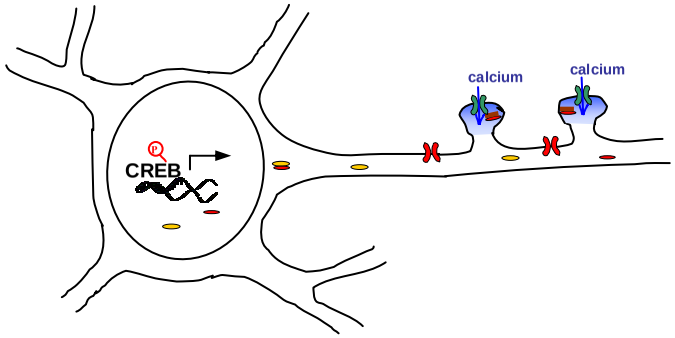

3b. strenthening of synapses

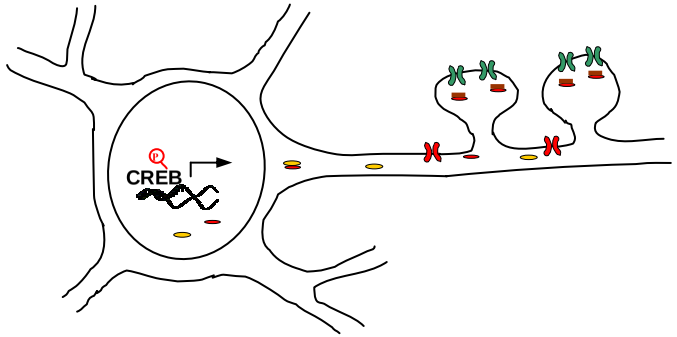

See next page for legend

Fig.30

Fig. 30 Schematic model showing the mechanism for activity-driven synapto-dendritic rempdeling. At resting conditions (1) Jacob is present extranuclearly in an either importin-α bound or unbound state. (2a) Activation of extrasynaptic NMDA receptors leads to nuclear translocation of importin-α and therefore, importin-α-bound Jacob. (2b) Nuclear translocation of Jacob, in turn, induces CREB dephosphorylation and simplification of synapto-dendritic architecture. (3a) However, in presence of high Ca^{2+}-levels, which can be achieved in Ca^{2+} microdomains such as postsynaptic spines after synaptic activation, Caldendrin compete with importin-α for Jacob's NLS binding and prevent its nuclear translocation. (3b) Jacob recruited via Caldendrin in the extensively activated synapses and this leads to stabilization of existing spines.

transported through the nuclear pores by a large family of soluble nuclear transport factors known as importins or karyopherins (Weis, 2002). The newly identified protein Jacob harbors a well-conserved bipartite nuclear localization signal and as it was shown in the present work Jacob's NLS is essential for nuclear import of the protein. Furthermore, it was shown previously by Dr. Michael R. Kreutz (unpublished data) that importin-α binds Jacob and the NLS of Jacob is a binding region for importin- α .

Thompson and colleagues (2004) have shown that importin-α is present in distal hippocampal neuronal processes including synaptic compartments and NMDA receptor activation triggers its translocation from synapses into the nucleus. Therefore, importin-α may bind NLS-containing cargos at the synapse and transport it to the nucleus in an activity-dependent manner. It was shown previously that Jacob translocates to the nucleus in response to NMDA receptor activation (Dr. rer. nat. Daniela Dieterich and Dipl. Biol. Martin Kreutz, unpublished data) and therefore Jacob can be the first identified cargo for importin-α.

At resting conditions, extranuclear Jacob can be present in an either importin-α-bound or unbound state and as NMDA receptor activation leads to nuclear translocation of importin-α, it was proposed that importin-α-bound Jacob will be recruited from dendrites into the nucleus. Fig. 30 shows a schematic drawing of this scenario. The region of Jacob that harbors the bipartite NLS is necessary for importin binding and nuclear translocation of Jacob (Dr. Michael R. Kreutz, unpublished data); at the same time the NLS is a binding site for Caldendrin, an EF-hand calcium-binding protein (Daniela Dieterich, Ph.D. thesis, 2003). Therefore, it could be predicted that Caldendrin binding can mask the bipartite NLS of Jacob in competition with importin-α and thereby prevent its nuclear trafficking. Consistent with this idea, overexpression of Caldendrin in primary hippocampal neurons attenuates the Jacob's nuclear translocation after NMDA receptor activation. However, it was shown previously that Caldendrin binds Jacob only in presence of elevated calcium levels which can be achieved only after enhanced synaptic activation (Daniela Dieterich,

Ph.D. thesis, 2003). Moreover, only in the presence of calcium there is a competition between Caldendrin and importin-α for binding to Jacob (Dr. Michael R. Kreutz, unpublished data).

Since Jacob, Caldendrin and importin-α are similarly distributed in dendritic processes at resting conditions, it can be predicted that the presence or absence of Caldendrin in the respective synapto-dendritic compartment, the strength of synaptic activation and, therefore, local calcium-transients will determine whether Jacob will be bound by Caldendrin or by importin-α, and whether Jacob shuttles to the nucleus or stays in the postsynaptic compartment (Fig. 30).

4.2 Jacob couples extrasynaptic NMDA receptors to a CREB shut-off pathway

Most electrical activity-dependent adaptations in the mammalian central nervous system are triggered by rapid, signal-induced changes in the intracellular concentration of calcium (Berridge, 1998; Carafoli, 2001). Intracellular calcium signals in neurons can lead to a range of alterations in neuronal function lasting from seconds to days. The number of potential calcium-regulated biological responses are diverse, ranging from gene regulation, plasticity and learning, to survival and death (Milner, 1998; Carafoli, 2001). How do neuronal cells control multiple processes using a single second messenger? The diversity of events controlled by calcium must partly be a consequence of the distinct types of calcium-signals that differ spatially, temporally and in magnitude (Bito et al., 1996; Fields et al., 1997; Hardingham et al., 1997, 1999, 2001a; 2001b; Bading, 2000; Chawla and Bading, 2001). The different outcomes can also be a consequence of the actions of a range of calcium-sensor proteins that transduce calcium-signals into specific changes in cellular function (Burgoyne, 2007). The NMDA subtype of glutamate receptors is responsible for a substantial fraction of the total calcium influx in response to synaptic activity. NMDA receptors are linked via the C-termini of their subunits to large complexes of cytoplasmic proteins. These include scaffolding, adaptor, cell adhesion and cytoskeletal proteins, as well as components of signal transduction pathways (Sheng and Pak, 2000). Therefore, calcium entry through NMDA receptors will occur in special molecular environment distinct from that in other parts of the cell. The emerging picture is that different channels associate with different signaling molecules or adapters, which may therefore be specifically or at least more efficiently, activated when calcium flows in

through that particular channel. Thus, the site of calcium entry can determine the biological outcome of the signal.

An example of calcium entry site-specific differences is the regulation of gene transcription mediated by the CRE-binding protein CREB. CREB activation involves a crucial step: phosphorylation on serine 133. Calcium entry through synaptic NMDARs strongly promotes CREB phosphorylation and CREB-dependent gene expression. In direct contrast, activation of extrasynaptic NMDARs triggers a dominant CREB shut-off signal that acts via inducing rapid dephosphorylation of CREB on serine 133 (Hardingham and Bading, 2002). The marked difference in cellular responses induced by synaptic versus extrasynaptic NMDA receptors is likely due to differences in the receptor signaling complexes. However, the exact nature of the CREB shut-off pathway and the mechanism by which extrasynaptic NMDA receptors activate it was not discovered until now.

The activation of extrasynaptic NMDARs requires the access of glutamate diffusing from synaptic release sites (spillover); this is possible when transmitter release is high enough for glutamate to diffuse to the extrasynaptic space from adjacent synaptic boutons and to reach concentrations sufficient to activate extrasynaptic receptors (Kullmann and Asztely 1998; Carter and Regehr 2000; Chen and Diamond 2002; Clark and Cull-Candy 2002). Due to their location outside synapses, extrasynaptic NMDA receptors may be involved in sensing ambient levels of glutamate (Lachamp et al., 2005). Therefore, the activation of the extrasynaptic NMDA is attributed mainly to global release of glutamate occurring at pathological conditions including hypoxic/ischaemic insults, traumas, and epileptic brain damage (Lipton, 1999; Arundine and Tymianski, 2004). In agreement with these findings, it was shown that differences in the degree of receptor activation (giving rise to different size calcium transients) account for the directly opposing effects on cell fate, with low or moderate stimulation of the receptor promoting survival and over-activation inflicting neuronal damage (Choi, 1992; Lipton and Rosenberg, 1994; Hardingham and Bading, 2003; Bossy-Wetzel et al., 2004).

In the present work, it was shown that activation of extrasynaptic NMDA receptors is mainly responsible for the nuclear trafficking of Jacob. On the other hand, Caldendrin competes with importin-α for binding to Jacob (Dr. Michael R. Kreutz, unpublished data) and therefore controls Jacob's extra-nuclear localization. This competition requires high calcium levels, which presumably can easily be achieved in calcium microdomains such as postsynaptic spines, but not in the synapto-dendritic region after extrasynaptic NMDA receptor activation. Thus, the finding that extrasynaptic NMDA receptor activation leads to a massive nuclear translocation of Jacob is in line with the hypothesis that the calcium

concentration in the respective synapto-dendritic compartment determines whether Jacob will be bound by Caldendrin or by importin-α, and therefore decides Jacob's subsequent localization.

Since extrasynaptic NMDA receptor activation triggers the CREB shut-off pathway (Hardingham and Bading, 2002), it was suggested that Jacob can be involved in this process. Indeed, nuclear accumulation of overexpressed Jacob prevents CREB phosphorylation in hippocampal neurons without NMDA receptor stimulation. Furthermore, nuclear knock-down of Jacob diminishes NMDA-induced CREB dephosphorylation. Based on these data it has been suggested that translocation of Jacob into the nucleus, initiated by calcium transients through extrasynaptic NMDA receptors might play a key role in the regulation of CREB phosphorylation and therefore CREB-dependent gene transcription. A model for this scenario is illustrated in Fig. 30.

It was shown previously that nuclear accumulation of endogenous Jacob occurs within 2 hours and is already visible 30 minutes after NMDA-receptor activation (Daniela Dieterich, Ph.D. thesis, 2003). This time course of Jacob's nuclear accumulation also is in favour for a role in the regulation of gene transcription (Bading, 2000). Furthermore, it was shown previously (Dr. Karl-Heinz Smalla, unpublished data) that Jacob exclusively associated with the RNA-polymerase II-containing euchromatin. It is well known that unfolding the structure of euchromatin allows regulatory proteins and RNA polymerase complexes to bind to the DNA sequence and initiate the transcription process (Lodish et al., 2001). The Jacob localization at sites of active nuclear gene transcription is highly suggestive for a role in transcription regulation.

Taken together these data suggest a new mechanism of gene regulation by glutamatergic synaptic transmission: nuclear accumulation of Jacob initiated by calcium flux through extrasynaptic NMDA receptors triggering CREB shut-off pathway and in consequence negatively regulate CREB target gene expression (Fig. 30).

It is well known that many of the molecules, which control neuronal survival are regulated through the activation of CREB. For example, NGF-induced survival of sympathetic neurons is achieved via the CREB-dependent activation of the anti-apoptotic gene bcl-2 (Riccio, et al., 1999). The expression of brain-derived neurotrophic factor (BDNF) is also regulated by CREB and is robustly induced by synaptic NMDA receptor activity (Tao et al., 1998; Hardingham et al., 2002). Similarly, apoptosis caused by blockade of synaptic NMDA receptors in the developing brain could be in part due to a reduction in synaptic NMDA receptor-dependent CREB activity (Ikonomidou et al., 1999). Therefore, synaptic NMDA receptor activation promotes nuclear signaling to CREB and activates anti-

apoptotic pathways; whereas calcium influx through extrasynaptic NMDA receptors antagonizes nuclear signaling to CREB, blocks induction of pro-survival genes, and leads to cell death (Hardingham et al., 2002).

Since extrasynaptic NMDA receptor activation triggers nuclear trafficking of Jacob and Jacob in turn suppresses CREB phosphorylation, it was hypothesized that Jacob nuclear accumulation can play a crucial role in blocking pro-survival activity. Indeed, the knock down of nuclear Jacob by siRNA transfection diminishes cell death in primary hippocampal cultures after NMDA exposure. Thus, Jacob could be a link between extrasynaptic NMDA receptors, CREB dephosphorylation and cell death (Fig. 30).

Taken together all these data suggest a novel mechanism of synapse-to-nucleus communication, which links the activity of NMDA receptors to nuclear signalling events involved in long-lasting changes in synapto-dendritic architecture and determination of cell fate: survival versus death.

4.3 Jacob controls the number of synaptic contacts and dendritic arborization via transcription regulation

Dendrites serve a critical role in neuronal information processing as sites of synaptic integration. The morphological diversity of dendritic architecture reflects specialized strategies that neurons have evolved to detect and process incoming information and patterns of dendritic arborization determine the nature and amount of innervation that a neuron receives (Jan and Jan, 2003; Miller and Kaplan, 2003). Recent observations suggest that synaptic activity exert an important influence on neuronal morphology by regulating the growth and branching of dendrites and the formation of dendritic synapses (Wong and Ghosh, 2002; Konur and Ghosh, 2005). It was shown that much of the effect on dendritic branching is mediated by NMDA receptors, and NMDA receptor activation is required for activity-dependent dendritic development (Rajan and Cline, 1998; Sin et al., 2002). Many studies indicate that calcium signaling in neurons can regulate dendritic growth and remodeling, and likely is a key mediator of structural plasticity in the developing brain (Sin et al., 2002; Konur and Ghosh, 2005; Lohmann and Wong, 2005).

As it was described above, calcium transients through NMDA receptors play an essential role in the regulation of Jacob's subcellular localization and this can determine the cell fate: survival versus death. To investigate functional consequences of the nuclear and extranuclear localization of Jacob in detail different mutants and wt-Jacob cDNA were transfected in neuronal cells. Overexpression of nuclear Jacob resulted in drastic changes

in synapto-dendritic architecture of the hippocampal neurons: nuclear accumulation of Jacob had a profound negative effect on dendrite elongation, branching and spine formation. Moreover, the dendritic retraction was preceded by a stripping of synaptic contacts, suggesting that reduction of synaptic input can be an initial trigger for the dendritic loss and that Jacob is mainly in control of synapse number. There are many evidences that dendritic morphology is regulated by synaptic input and that dendrites that lose contact with presynaptic terminals are not maintained: in somatosensory and visual systems, dendrites dramatically reorganize in response to synaptic/afferent input; activity deprivation experiments also suggest that loss of normal activity during development leads to lasting deficits in dendritic development (Wiesel and Hubel, 1963; Coleman and Riesen, 1968; Feng and Rogowski, 1980; Lund et al., 1991; Sin et al., 2002); pharmacological blockade of synaptic activity in vitro and in vivo leads to deficits in dendritic growth (McAllister et al., 1996; Rajan and Cline, 1998; Redmond et al., 2002). Synapto-dendritic remodelling after Jacob overexpression is very rapid suggesting that synapses are actively destabilized and dendritic processes are actively retracted after nuclear accumulation of Jacob. Long-lasting structural changes in a cell require de novo protein synthesis and mRNA formation. Therefore, Jacob could either block an essential nuclear signaling event required to prevent the removal of synaptic input or regulate the expression of genes that will destabilize synapses.

In contrast extranuclear Jacob overexpression leads to an increased number of dendrites and formation of PSD-like structures that eventually promote formation of dendritic protrusions with active synaptic contacts (this aspect will be discussed below in more detail). Thus, the effect of Jacob overexpression suggests that Jacob signalling to the nucleus could have an important regulatory influence on the specification of dendritic morphology in mature neurons.

Since Jacob translocates to the nucleus in response to NMDA receptor activation (Daniela Dieterich, Ph.D. thesis, 2003), it was suggested that nuclear accumulation of endogenous Jacob after NMDA receptor stimulation can also lead to synaptic stripping as it was observed after nuclear accumulation of overexpressed Jacob mutants. Indeed, NMDA bath application resulted in a reduction of the number of synaptic contacts in hippocampal neurons; however, pretreatment of the cultures with the transcription inhibitor actinomycin-D abolishes this effect. These findings further confirm the hypothesis that nuclear Jacob controls synaptogenesis via transcription regulation (Fig. 30). Furthermore, the effect of synaptic stripping after NMDA receptor activation was rescued by a specific

knock down of nuclear Jacob, confirming that Jacob plays a central role in coupling synaptic activity to changes in gene expression and synapto-dendritic remodeling.

4.4 Jacob determines the size of PSDs in neurons

A specific set of molecules including glutamate receptors is targeted to the postsynaptic specialization of excitatory synapses in the brain, gathered in a structure known as the postsynaptic density. The proteins in the PSDs are assembled in highly ordered arrays attached to the cytoplasmic surface and create an interface between clustered membrane-bound receptors, cell adhesion molecules and the actin-based cytoskeleton. In neuronal excitatory synapses, glutamate receptors – NMDA- and AMPA-type - are cardinal components of the postsynaptic specialization and are highly concentrated in the PSD. A great variety of scaffolding proteins in the PSD are involved in the regulation of synaptic function. Key components among these are proteins of the MAGuKs and ProSAP/Shanks families. Many of the scaffolding proteins in the PSD bind directly or indirectly to NMDA or AMPA receptors forming a highly organized biochemical apparatus attached to the cytosolic surface of the postsynaptic membrane (Kennedy, 2000; Boeckers, 2006).

As it was shown in the present work overexpression of one of the splice variants of Jacob lacking the C-terminal part triggers formation of large protrusions. Major PSD-scaffolding proteins like PSD95, ProSAP/Shank and different receptor types - NMDARs and AMPARs - are highly enriched in these protrusions. Moreover, after extraction of membranous structures with Triton X-100, insoluble continuous structures are visible in the scanning electron microscope and these structures are immuno-positive for the major components of PSDs. These data suggest that overexpression of a Jacob splice isoform lacking the C-terminal part triggers formation of large PSD-like structures, which are located in huge protrusions. Furthermore, immunocytochemical analysis revealed that in most cases a single protrusion overlaps with several Bassoon or Synapsin puncta suggesting that these protrusions form multiple contacts with a presynaptic terminal. Consistent with this, several tiny processes connected with a single huge Jacob-induced protrusion are visible on scanning electron micrographs. Probably, these tiny structures represent axonal terminals making presynaptic contacts with the protrusions. The presence of key components of the PSD, receptors and connections with presynaptic terminals suggest that huge protrusions induced by Jacob overexpression contain functional synapses.

There is a lack of data about the size of a typical PSD in neurons because of the difficulties of quantitative measurement. Disk-like structures around 30–50 nm thick and up to a few hundred nm wide can be purified with nonionic detergents by differential centrifugation from cerebral cortex (Carlin et al., 1980). However, it is known that the area of a PSD correlates well with the spine volume (Harris and Stevens, 1989), since the typical mature spine in the mammalian brain has a single synapse located at its head and most synapses have a single continuous PSD per spine (Hering and Sheng, 2001; Nimchinsky et al., 2002). Dendritic spines come in a wide variety of shapes and sizes, ranging in volume from less than 0.01 μm^3 to 1.5 μm^3. A similar range of PSD sizes was found in the present study in hippocampal neurons, using scanning electron microscopy. However, overexpression of the Jacob isoform lacking the C-terminal part leads to dramatic increase in PSD sizes: almost 2.5 times increase in PSD width and 1.6 times increase in thickness in comparison with control GFP-transfected or untransfected neurons.

There are many studies, which demonstrate changes in the morphology of spines, such as enlargement of the spine head (and PSD size respectively). Activity pattern that induce long-term potentiation (LTP) - high frequency synaptic stimulation and chemical treatments - causes spine heads enlargement (Matsuzaki et al., 2004; Okamoto et al., 2004; Otmakhov et al., 2004; Zhou et al., 2004; Kopec et al., 2006). In contrast, low-frequency stimulation, which is known to induce long-term depression (LTD), causes some spines to shrink and, in some cases, to even disappear (Okamoto et al., 2004; Zhou et al., 2004). It is not known whether the extent of spine shrinkage depends on spine size; however, it was shown that the extent of LTP-dependent spine enlargement depends on the initial size of the spine: small spines enlarge, while large spines do not. As a result, the larger a spine becomes, the harder it is for subsequent enlargement to occur (Matsuzaki, 2006). There is a suggestion that this property may protect stable retention of memory against changes induced by further activity and experiences (Fusi et al., 2005). These phenomena arise the question whether the spine and the PSD have a limited maximal size to grow? It was shown that LTP-dependent PSD growth followed by formation of discontinuous or ‘perforated’ PSDs (completely partitioned PSDs on one spine) and finally bifurcation of spines and formation of two (or more) spines contacting the same presynaptic terminal. Thus, large spines and PSDs break apart, forming at first perforated synapses and finally new separated spines (Calverley and Jones, 1990; Trommald et al., 1990; Toni et al., 1999, 2001).

In contrast with this, PSD-like structures induced by overexpression of Jacob can grow up to huge sizes exceeding the size of typical PSDs in several times. Moreover, Jacob overexpression triggers formation of the huge PSD-like structures in immature hippocampal neurons before synaptogenesis take place and only small part of these protrusions make presynaptic contacts. Therefore, it is plausible to assume that Jacob can trigger formation and growth of the PSDs in neurons and presynaptic contacts are not necessary for this process. Furthermore, overexpressed Jacob accumulates almost exclusively in the protrusions and all of the protrusions contain Jacob.

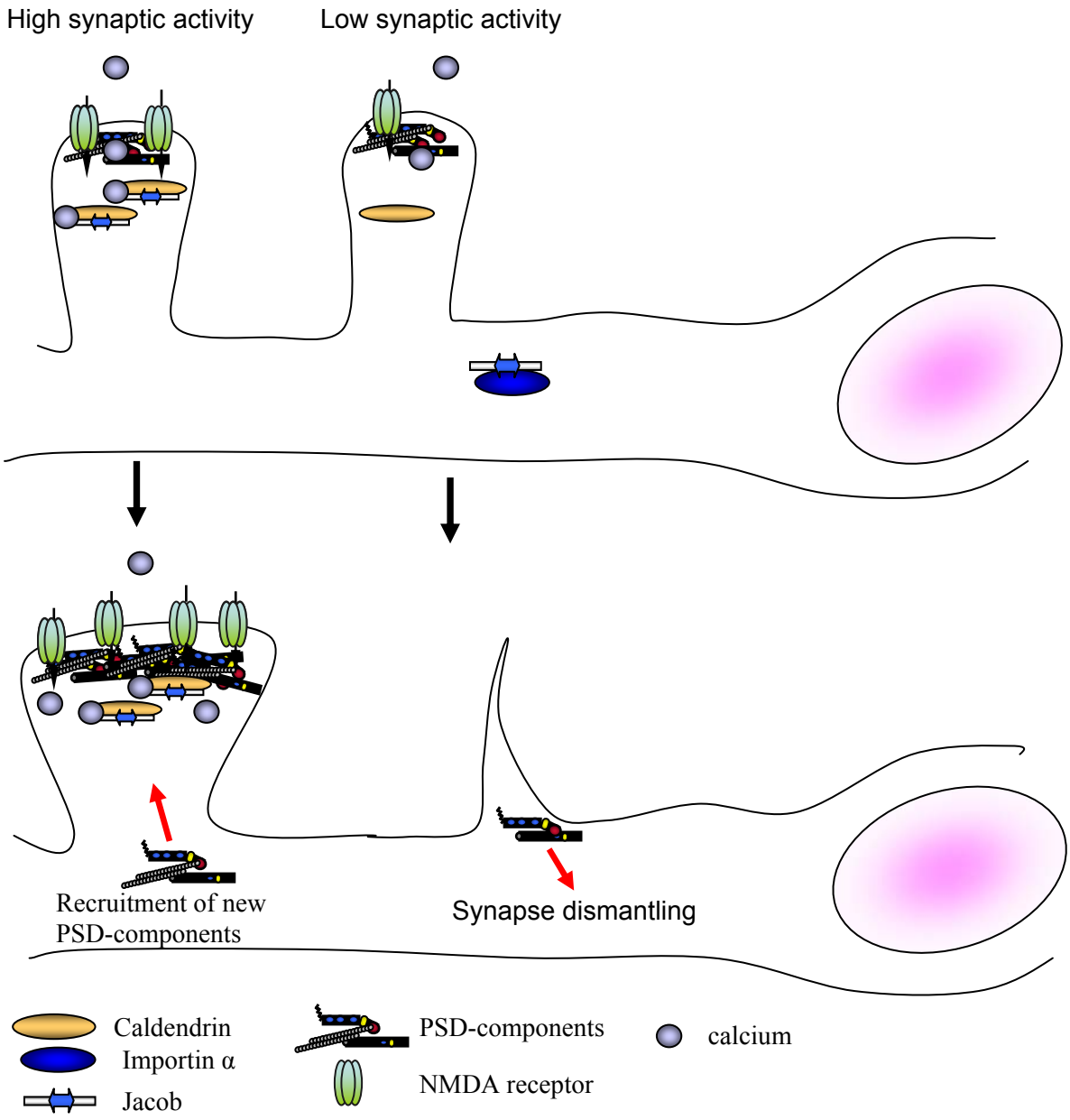

Fig. 31 Jacob determines stabilization and growth of PSDs in neurons.
Jacob recruited via Caldendrin in the extensively activated synapses and this leads to stabilization of existing PSD and/or recruit new PSD proteins in the synapse.

Taken together these observations raise the hypothesis that Jacob might be a nucleation factor and/or a stabilizing factor for the PSD, in other words, presence of Jacob in the synapse could stabilize existing PSD and/or recruit new PSD proteins in the synapse (Fig. 31).

Interestingly, huge blob-like protrusions, which arise after Jacob overexpression in hippocampal neurons at DIV 4-11, could not be found at later stages: overexpression of Jacob in hippocampal neurons at DIV 20-24 resulted in spine enlargement but the effect is not as prominent as it was shown for younger neurons (Marina Mikhaylova, personal communications). As it was proposed above, Jacob can be recruited via Caldendrin binding only in the extensively activated synapses and this recruitment will lead to stabilization of the synapses. Consistently, immunocytochemical analysis demonstrated that Caldendrin is enriched in the protrusions induced by Jacob overexpression (Fig. 31).

Therefore, it can be hypothesized that in neurons with many established synaptic contacts (at DIV 20-24) Jacob is distributed more or less equally between functional synapses. In turn, the presence of Jacob in the synapse will lead to stabilization of existing PSD and strengthening of the synapse (Fig. 31). On the other hand, in young neurons there are very few established synaptic contacts, and Jacob accumulates in these 'hot sports' and seems to recruit all available PSD proteins to these sites. The distribution of all sources of PSD proteins of the cell between a few number of synapses may lead to formation of huge PSD-like structures which can be observed after Jacob overexpression in hippocampal neurons at DIV 4-11.

However, Jacob does not affect synaptogenesis, since Jacob overexpression does not induce formation of new synapses in young neurons.

Different types of neurons show distinct responses to a variety of environmental signals, like interaction with neighboring cells, synaptic activity, and growth factors. Part of this flexibility is probably due to the ability of different stimuli to induce distinct programs of downstream gene expression (Bartel et al., 1989; Mayr et al., 2001; West et al., 2002). To investigate whether Jacob has a similar regulatory function in other types of neurons, the splice isoform of Jacob, that induces the formation of huge PSD-like structures in hippocampal neurons, was overexpressed also in primary cortical cultures. Transfected cortical neurons exhibited a similar protrusion phenotype which was observed for hippocampal neurons. Therefore, Jacob overexpression had a similar effect on cortical and hippocampal neurons suggesting that Jacob provide the same regulatory mechanism in different types of neuronal cells.

5 References

Alberini, C.,M. (1999). Genes to remember. J. Exp. Biol. 202, 2887–2891.

Antonova, I., Arancio, O., Trillat, A.C., Wang, H.G., Zablow, L., Udo, H., Kandel, E.R., Hawkins, R.D. (2001) Rapid Increase in Clusters of Presynaptic Proteins at Onset of Long-Lasting Potentiation. Science 294, 1547-1550.

Arundine, M., Tymianski, M. (2004) Molecular mechanisms of glutamate-dependent neurodegeneration in ischemia and traumatic brain injury. Cell Mol Life Sci *61*, 657–668.

Ausubel, F.M., Brent, R., Kingston, R.E. (1999) Short Protocols in Molecular Biology. 4th ed.: Wiley John & Sons Inc.

Bading, H., Ginty, D.D., Greenberg, M.E. (1993) Regulation of gene expression in hippocampal neurons by distinct calcium signaling pathways. Science 260, 181-186.

Bading, H. (2000) Transcription-dependent neuronal plasticity: the nuclear calcium hypothesis. Eur. J. Biochem. *267,* 5280–5283.

Bartel, D.P., Sheng, M., Lau, L.F., Greenberg, M.E. (1989) Grofth factors and membrane depolarization activate distinct programs of early response gene expression: dissociation of *fos* and *jun* induction. Genes Dev. *3*, 304-313.

Berridge, M.J. (1998) Neuronal calcium signaling. Neuron 21, 13-26.

Bito, H., Deisseroth, K., Tsien, R. W. (1996) CREB phosphorylation and dephosphorylation: a calcium and stimulus duration–dependent switch for hippocampal gene expression. *Cell 87,* 1203–1214.

Boeckers, T.M., Mameza, M.G., Kreutz, M.R., Bockmann, J., Weise, C., Buck. F., Richter, D., Gundelfinger, E.D., Kreienkamp, H.J. (2001) Synaptic scaffolding proteins in rat brain. Ankyrin repeats of the multidomain Shank protein family interact with the cytoskeletal protein alpha-fodrin. J Biol Chem *276*, 40104–40112.

Boeckers, T.M. (2006) The postsynaptic density. Cell Tissue Res *326*, 409-422.

Bootman, M.D., Lipp, P., Berridge, M.J. (2001) The organization and functions of local calcium signals. J. Cell Sci. 114, 2213-2222.

Bossy-Wetzel, E., Schwarzenbacher, R., Lipton, S.A. (2004) Molecular pathways to neurodegeneration. Nat. Med. *10*, S2–S9.

Boyer, C., Schikorski, T., Stevens, C. (1998) Comparison of hippocampal dendritic spines in culture and in brain. J Neurosci, *18*(14), 5294–300.

Boulikas T. (1993) Nuclear localization signals (NLS). Crit Rev Eukaryot Gene Expr. 3(3):193-227.

Braunewell, K.H., Gundelfinger, E.D. (1999) Intracellular neuronal calcium sensor proteins: a family of EF-hand calcium-binding proteins in search of a function. Cell Tissue Res. 295, 1-12.

Burgoyne, R.D., Weiss, J.L. (2001). The neuronal calcium sensor family of calcium-binding proteins. Biochem. J. 353, 1-12.

Burgoyne, R.D., O'Callaghan, D.W., Hasdemir, B., Haynes, L.P., and Tepikin, A.V. (2004). Neuronal calcium-sensor proteins: multitalented regulators of neuronal function. Trends Neurosci. 27, 203-209.

Carafoli, E., Santella, L., Branca, D., Brini, M. (2001) Generation, control, and processing of cellular calcium signals. *Crit. Rev. Biochem. Mol. Biol. 36,* 107–260.

Carrion, A.M., Link, W.A., Ledo, F., Mellstrom, B., Naranjo, J.R. (1999) DREAM is a calcium-regulated transcriptional repressor. Nature 398, 80-84.

Carter, A.G., Regehr, W.G. (2000) Prolonged synaptic currents and glutamate spillover at the parallel fiber to stellate cell synapse. J Neurosci *20*, 4423–4434.

Chavaleyre, V., Moos, F.C., Desarmenien, M.G. (2002) interplay between presynaptic and postsynaptic activities is required for dendritic plasticity and synaptogenesis in the supraoptic nucleus. J.Neurosci. 22, 265-273.

Chawla, S., Bading, H. (2001) CREB/CBP and SRE-interacting transcriptional regulators are fast on–off switches: duration of calcium transients specifies the magnitude of transcriptional responses. *J. Neurochem. 79,* 849–858.

Chen, S., Diamond, J.S. (2002) Synaptically released glutamate activates extrasynaptic NMDA receptors on cells in the ganglion cell layer of rat retina. J Neurosci *22*, 2165–2173.

Choi, D.W. (1992). Excitotoxic cell death. J. Neurobiol. *23*, 1261–1276.

Clark, B.A., Cull-Candy, S.G. (2002) Activity-dependent recruitment of extrasynaptic NMDA receptor activation at an AMPA receptoronly synapse. J Neurosci *22*, 4428–4436.

Cline, H.T. (2001). Dendritic arbor development and synaptogenesis. Curr. Opin. Neurobiol. 11, 118–126.

Coleman, P.D., Riesen, A.H. (1968) Evironmental effects on cortical dendritic fields. I. Rearing in the dark. J Anat.*102*,363-74.

Daoudal, G., Debanne, D. (2003) Long-Term Plasticity of Intrinsic Excitability: Learning Rules and Mechanisms. Learn. Mem. 10, 456-465.

Deisseroth, K., Bito, H., Tsien, R.W. (1996) Signaling from synapse to nucleus: postsynaptic
CREB phosphorylation during multiple forms of hippocampal synaptic plasticity. Neuron 16, 89-101.

Deisseroth, K., Heist, E.K., Tsien, R.W. (1998) Translocation of calmodulin to the nucleus supports CREB phosphorylation in hippocampal neurons. Nature 392, 198-202.

Deisseroth, K., Mermelstein, P.G., Xia, H., Tsien, R.W. (2003) Signaling from synapse to nucleus: the logic behind the mechanisms. Curr. Opin. Neurobiol. 13, 354–365.

Dolmetsch, R.E., Pajvani, U., Fife, K., Spotts, J.M., Greenberg, M.E. (2001) Signaling to the nucleus by an L-type calcium channel-calmodulin complex through the MAP kinase pathway. Science 294, 333-339.

Dresbach, T., Hempelmann, A., Spilker, C., tom Dieck, S., Altrock, W., Zuschratter, W., Garner, C., Gundelfinger E. (2003) Functional regions of the presynaptic cytomatrix protein Bassoon: significance for synaptic targeting and cytomatrix anchoring. *Mol Cell Neuroscience*, *23*, 279-291.

Ehlers, M.D. (2002) Molecular morphogens for dendritic spines. Trends Neurosci *25*, 64–67.

Engert, F., Bonhoeffer, T. (1999) Dendritic spine changes associated with hippocampal long-term synaptic plasticity. Nature 399, 66-70.

Euler, T., and Denk, W. (2001). Dendritic processing. Curr. Opin. Neurobiol. 11, 415–422.

Feng, A., Rogowski, B. (1980) Effects of monaural and binaural occlusion on the morphology of neurons in the medial superior olivary nucleus of the rat. Brain Res *189*, 530 –534.

Fields, R. D., Esthete, F., Stevens, B., Itoh, K. (1997) Action potential–dependent regulation of gene expression: temporal specificity in calcium, cAMP-reponsive element binding proteins, and mitogen-activated protein kinase signalling. *J. Neurosci. 17,* 7252–7266.

Finkbeiner, S. (2000) CREB couples neurotrophin signals to survival messages. Neuron 25, 11–14.

Gao, F.B., Bogert, B.A. (2003). Genetic control of dendritic morphogenesis in Drosophila. Trends Neurosci. 26, 262–268.

Goslin, K., Asmussen, H., Banker, G. (1998) Rat hippocampal neurons in low-density culture, in: Banker, G., Goslin, K. (eds.), Culturing nerve cells, 2nd ed., pp. 339-370. MIT Press, MIT Press, Cambridge, MA.

Graef, I.A., Mermelstein, P.G., Stankunas, K., Neilson, J.R., Deisseroth, K., Tsien R.W., Crabtree, G.R. (1999). L-type calcium channels and GSK-3 regulate the activity of NFATc4 in hippocampal neurons. Nature 401,703-708.

Haeseleer, F, Sokal, I., Verlinde, L.M.J., Erdjumen-Bromage, H., Tempst, P., Pronin, A.N., Benovic, J.L., Fariss, R.N., and Palczewski, K. (2000). Five members of a novel

calcium-binding protein (CaBP) subfamily with similarity to calmodulin. J. Biol. Chem. 275, 1247-1260.

Hall, Z.,H. (1992) An introduction to molecular neurobiology. Sunderland, Massachusetts. 428-438.

Hardingham, G. E., Chawla, S., Johnson, C. M., Bading, H. (1997) Distinct functions of nuclear and cytoplasmic calcium in the control of gene expression. Nature 385, 260–265.

Hardingham, G. E., Chawla, S., Cruzalegui, F. H., Bading, H. (1999) Control of recruitment and transcription-activating function of CBP determines gene regulation by NMDA receptors and L-type calcium channels. Neuron 22, 789–798.

Hardingham, G. E., Arnold, F. J. L., Bading, H. (2001a) Nuclear calcium signaling controls CREB-mediated gene expression triggered by synaptic activity. Nat. Neurosci. 4, 261–267.

Hardingham, G.E., Arnold, F.J., Bading, H. (2001b) A calcium microdomain near NMDA receptors: on switch for ERK-dependent synapseto-nucleus communication. Nat. Neurosci. 4, 565-566.

Hardingham, G.E., Fukunaga, Y., Bading, H. (2002) Extrasynaptic NMDARs oppose synaptic NMDARs by triggering CREB shut-off and cell death pathways. Nat Neurosci. 5, 389-90.

Hardingham, G.E., Bading, H. (2002) Coupling of extrasynaptic NMDA receptors to a CREB shut-off pathway is developmentally regulated Biochim Biophys Acta. 4, 148-153.

Hardingham, G.E., Bading, H. (2003) The Yin and Yang of NMDA receptor signaling. TRENDS in Neurosci 26, 81-89.

Harris, K.M., Stevens, J.K. (1989) Dendritic spines of CA1 pyramidal cells in the rat hippocampus: serial electron microscopy with reference to their biophysical characteristics. J. Neurosci. 9, 2982–97.

Hausser, M., Mel, B. (2003). Dendrites: bug or feature? Curr. Opin. Neurobiol. 13, 372–383.

Hering, H., Sheng, M. (2001) Dendritic spines: structure, dynamics and regulation. Nature Rev 2, 881-887.

Horst, C.J., Forestner, D.M., Besharse, J.C. (1987) Cytoskeletal-membrane interactions: a stable interaction between cell surface glycoconjugates and doublet microtubules of the photoreceptor connecting cilium. The Journal of Cell Biology 105, 2973-298

Ikonomidou, C., Bosch, F., Miksa, M., Bittigau, P., Vockler, J., Dikranian, K., Tenkova, T.I., Stefovska, V., Turski, L., Olney, J.W. (1999) Blockade of NMDA receptors and apoptotic neurodegeneration in the developing brain. Science *283*, 70–74.

Ikura. M. (1996) Calcium binding and conformational response in EF-hand proteins. Trends Biochem. Sci. 21, 14-17.

Jan, Y.N., Jan, L.Y. (2001). Dendrites. Genes Dev. 15, 2627–2641.

Jan, Y.N., Jan, L.Y. (2003) The Control of Dendrite Development. Neuron 40, 229–242.

Kalb, R.G. (1994) Regulation of motor neuron dendrite growth by NMDA receptor activation. Development 120, 3063-3071.

Konur, S., Ghosh, A. (2005) Calcium signaling and the control of dendritic development. Neuron *46*, 401-405.

Kornau, H.-C., Seeburg, P. H., Kennedy, M. B. (1997) Interaction of ion channels and receptors with PDZ domain proteins. Curr. Opin. Neurobiol. *7*, 368-373.

Kullmann, D.M., Asztely, F. (1998) Extrasynaptic glutamate spillover in the hippocampus: evidence and implications. Trends Neurosci *21*, 8–14.

Lachamp, Ph., Balland, B., Tell, F., Baude, A., Strube, C., Crest, M., Kessler, J. (2005) Early expression of AMPA receptors and lack of NMDA receptors in developing rat climbing fibre synapses. J Physiol *564*, 751-763.

Laube, G., Seidenbecher, C.I., Richter, K., Dieterich, D.C., Hoffmann, B., Landwehr, M., Smalla, K.H., Winter, C., Böckers, T.M., Wolf, G., Gundelfinger, E.D., and Kreutz, M.R. (2002). The neuron-specific calcium-binding protein caldendrin: gene structure, splice isoforms and expression in the rat central nervous system. Mol. Cell. Neurosci. 19, 459-475.

Lipscombe, D., Madison, D.V., Poenie, M., Reuter, H., Tsien, R.W., Tsien, R.Y. (1988) Imaging of cytosolic calcium transients arising from calcium stores and calcium channels in sympathetic neurons. Neuron 1,355-365.

Lipton, P. (1999). Ischemic cell death in brain neurons. Physiol Rev *79*, 1431–1568.

Lipton, S.A., Rosenberg, P.A. (1994). Excitatory amino acids as a final common pathway for neurologic disorders. N. Engl. J. Med. *330*, 613–622.

Lodish, H., Berk, A., Zipursky, S.L., Matsudaira, P., Baltimore, D., Darnell, J. (2001) Molecular cell biology. W.H.Freeman and Company pp. 320-332.

Lohmann, C., Wong, R.O. (2005) Regulation of dendritic growth and plasticity by local and global calcium dynamics. Cell Calcium 37, 403-409.

Lohmann, C., Myhr, K.L., Wong, R.O.L. (2002) Transmitter-evoked local calcium release stabilizes developing dendrites. Nature 418, 177-181.

Lund, J.S., Holbach, S.M., Chung, W. (1991) Postnatal development of thalamic recipient neurons in the monkey striate cortex. II. Influence of afferent driving on spine acquisition and dendritic growth of layer 4c spiny stellate neurons. J Comp Neurol *309*,129 –140.

Luthi, A., Schwyzer, L., Mateos, J.M., Gahwiler, B.H., McKinney, R.A. (2001) NMDA receptor activation limits the number of synaptic connections during hippocampal development. Nat. Neurosci. 11, 1102-1107.

Malenka, R.C. (2003). The long-term potential of LTP. Nat. Rev. Neurosci. *4*, 923-926.

Mantamadiotis, T., Lemberger, T., Bleckmann, S.C., Kern, H., Kretz, O., Villalba, A.M., Tronche, F., Kellendonk, C., Gau, D., Kapfhammer, J., Otto, C., Schmid, W., Schutz, G. (2002) Disruption of CREB function in brain leads to neurodegeneration. Nature Genetics *31*, 47–54.

Martin, S.J., Grimwood, P.D., and Morris, R.G. (2000). Synaptic plasticity and memory: an evaluation of the hypothesis. Annu. Rev. Neurosci. 23, 649–711.

Mayr, B.M., Canettieri, G., Montminy, M.R. (2001) Distinct effects of cAMP and mitogenic signals on CREB-binding protein recruitment impart specificity to target gene activation via CREB. Proc. Natl Acad Sci USA 98, 10936-10941.

McAllister, A.K., Katz, L.C., Lo, D.C. (1996). Neurotrophin regulation of cortical dendritic growth requires activity. Neuron *17*, 1057– 1064.

McAllister, A.K. (2000). Cellular and molecular mechanisms of dendrite growth. Cereb. Cortex 10, 963–973.

Mermelstein, P.G., Deisseroth, K., Dasgupta, N., Isaksen, A.L., Tsien, R.W. (2001) Calmodulin priming: nuclear translocation of a Calmodulin complex and the memory of prior neuronal activity. Proc. Natl. Acad. Sci. USA 98, 15342-15347.

Milner, B., Squire, L. R., Kandel, E. R. (1998) Cognitive neuroscience and the study of memory. *Neuron 20,* 445–468.

Miller, F.D., Kaplan, D.R. (2003). Signaling mechanisms underlying dendrite formation. Current Opinion in Neurobiology 13, 391–398.

Nimchinsky, E.A., Sabatini, B.L., Svoboda, K. (2002) Structure and function of dendritic spines. Annu.Rev. Physiol. *64*, 313-353.

Osawa, M., Tong, K.I., Lilliehook, C., Wasco, W., Buxbaum, J.D., Cheng, H.Y., Penninger, J.M., Ikura, M., Ames, J.B. (2001) Calcium-regulated DNA binding and oligomerization of the neuronal calciumsensing protein, calsenilin/DREAM/KChIP3. J Biol. Chem. 276, 41005-41013.

Papa, M., Bundman, M., Greenberger, V., Segal, M. (1995) Morphological analysis of dendritic spine development in primary cultures of hippocampal neurons. J Neurosci, *15*, 1–11.

Rajan, I., Cline, H.T. (1998) Glutamate receptor activity is required for normal development of tectal cell dendrites in vivo. J. Neurosci. 18, 7836-7846.

Redmond, L., Kashani, A.H., Ghosh, A. (2002). Calcium regulation of dendritic growth via CaM kinase IV and CREB-mediated transcription. Neuron *34*, 999–1010.

Resh, M.D. (1999) Fatty acylation of proteins: new insights into membrane targeting of myristoylated and palmitoylated proteins. Biochim Biophys Acta. 1451, 1-16.

Reyes, J.C., Muchardt, C., Yaniv, M. (1997) Components of the human SWI/SNF complex are enriched in active chromatin and are associated with the nuclear matrix. J. Cell Biol. *137*, 263-274.

Riccio, A., Ahn, S., Davenport, C.M., Blendy, J.A., Ginty, D.D. (1999) Mediation by a CREB family transcription factor of NGF-dependent survival of sympathetic neurons. Science *286*, 2358–2361.

Rocha, M., Sur, M. (1995) Rapid acquisition of dendritic spines by visual thalamic neurons after blocade of N-methyl-D-aspartate receptors. Proc. Natl. Acad. Sci. USA 92, 8026-8030.

Sambrook, J., Fritsch, E.F., Maniatis, T. (1989) Molecular cloning: a laboratory manual, 2nd edition. Cold Spring Harbor Laboratory Press, Cold Spring Harbor, NY.

Scott, E.K., and Luo, L. (2001). How do dendrites take their shape? Nat. Neurosci. 4, 359–365.

Seidenbecher, C.I., Langnäse, K., Sanmarti-Vila, L., Böckers, T.M., Smalla, K.H., Sabel, B.A., Garner, C.C., Gundelfinger, E.D., and Kreutz, M.R. (1998). Caldendrin, a novel neuronal calcium-binding protein confined to the somato-dendritic compartment. J. Biol. Chem. 273, 21324-21331.

Seidenbecher, C.I., Reissner, C., and Kreutz, M.R. (2002). Caldendrins in the inner retina. Adv. Exp. Med. Biol. 514,451-463.

Sheng, M. (1996) PDZs and Receptor/Channel Clustering: Rounding Up the Latest Suspects. Neuron *17*, 575-578.

Sheng, M., Kim, E. (2000) The Shank family of scaffold proteins. J Cell Sci *113*, 1851–1856.

Sheng, M., Pak, D.T. (2000) Ligand-gated ion channel interactions with cytoskeletal and signaling proteins. Annu. Rev. Physiol. 62, 755–778.

Sin, W.C., Haas, K., Ruthazer, E.S., Cline, H.T. (2002). Dendrite growth increased by visual activity requires NMDA receptor and Rho GTPases. Nature 419, 475-480.

Spacek, J., Harris, K.M. (1997) Tree-dimentional organization of smooth endoplasmatic reticulum in hippocampal CA1 dendrites and dendritic spines of the immature and mature rat. J. Neurosci. 17, 190-203.

Tao, X., Finkbeiner, S., Arnold, D.B., Shaywitz, A.J, Greenberg, M.E. (1998) calcium influx regulates BDNF transcription by a CREB family transcription factor-dependent mechanism Neuron *20*, 709–726.

Thomas, G.M., and Huganir, R.L. (2004). MAPK cascade signalling and synaptic plasticity. Nat. Rev. Neurosci. *5*, 173-183.

Thompson, K.R., Otis, K.O., Chen, D.Y., Zhao, Y., O'Dell, T.J., Martin, K.C. (2004) Synapse to nucleus signaling during long-term synaptic plasticity; a role for the classical active nuclear import pathway. Neuron. *44*, 997-1009.

Vaillant, A.R., Zanassi, P., Walsh, G.S., Aumont, A., Alonso, A., Miller, F.D. (2002) Signaling mechanisms underlying activity-dependent dendrite formation. Neuron 34, 985-998.

Walton, M.R., Dragunow, M. (2000) Is CREB a key to neuronal survival? Trends in Neurosciences *23*, 48–53.

Weis, K. (2002). Nucleocytoplasmic transport: cargo trafficking across the border. Curr. Opin. Cell Biol. 14, 328–335.

West, A.E., Griffith, E.C., Greenberg, M.E. (2002) Regulation of transcription factors by neuronal activity. Nat. Rev. Neurosci. 3, 921-931.

Whitford, K.L., Dijkhuizen, P., Polleux, F., and Ghosh, A. (2002). Molecular control of cortical dendrite development. Annu. Rev. Neurosci. 25, 127–149.

Wong, W.T., Wong, R.O. (2001). Changing specificity of neurotransmitter regulation of rapid dendritic remodeling during synaptogenesis. Nature Neurosci. 4, 351-352

Wong, R.O., Ghosh, A. (2002). Activity-dependent regulation of dendritic growth and patterning. Nat. Rev. Neurosci. 3, 803–812.

Wu, G., Malinow, R., Cline, H.T. (1996). Maturation of a central glutamatergic synapse. Science 274, 972–976.

Wu, G.Y., Zou, D.J., Rajan, I., Cline, H. (1999). Dendritic dynamics in vivo change during neuronal maturation J. Neurosci. 19, 4472–4483.

Wu, G.Y., Deisseroth, K., Tsien, R.W. (2001a) Activity-dependent CREB phosphorylation: convergence of a fast, sensitive Calmodulin kinase pathway and a slow, less sensitive mitogen- activated protein kinase pathway. Proc Natl. Acad. Sci. USA 98, 2808-2813.

Wu, G.Y., Deisseroth, K., Tsien, R.W. (2001) Spaced stimuli stabilize MAPK pathway activation and its effects on dendritic morphology. Nat. Neurosci. 4, 151-158.

6 Abbreviations

The single letter code was used for amino acids and nucleotides

aa	amino acid(s)
actD	actinomycin-D
AMPA	a-amino-3-hydroxy-5-methyl-4-isoxazole propionic acid
bp	base pairs
BDNF	brain-derived neurotrophic factor
BSA	bovine serum albumin
CaM	Calmodulin
CaMKIV	Calmodulin-dependent protein kinase IV
CaN	calcineurin
CaBP1	Caldendrin
cAMP	cyclic AMP
cDNA	complementary DNA
CICR	Ca^{2+}-induced Ca^{2+} release
CMV	cytomegalovirus
CNS	central nervous system
CRE	Ca2+/cAMP-responsive element
CREB	Ca2+/cAMP-responsive element binding protein
C-terminus	carboxy terminus
DIV	days in vitro
DMEM	Dulbecco's modified Eagle's medium
DMSO	dimethylsulfoxide
DNA	desoxyribonucleic acid
dNTPs	deoxyribonucleoside triphosphates
DRE	downstream regulatory element
DREM	downstream regulatory element antagonistic modulator
E. coli	Escherichia coli
Fig.	figure
GFP	green fluorescent protein
GluR	glutamate receptor subunit
HEPES	N-2-hydroxyethylpiperanzine-N'-2-ethanesulfonic acid
HBSS	Hank's balanced salt solution
HS	horse serum
IgG	immunglobulin G
IF	immunofluorescence
$Ins(1,4,5)P_3$	inositol-1,4,5-triphosphate
kb	kilo bases
LB	Luria-Bertani
LSM	laserscan micrographs
LTD	long-term depression
LTP	long-term potentiation
MAGuK	membrane associated guanylate kinase
MAP	mitogen-activated protein
MAP2	microtubule-associated protein 2
MAPK	mitogen-activated protein kinase
Myr	myristoylation
n	number of scored cells
nAChR	nicotinic cholinergic receptors
NCS	neuronal Ca^{2+}-sensor (protein)

NFATc4	nuclear factor of activated T-cells c4
NLS	nuclear localization signal
NMDA	N-methyl-D-aspartate
NR	NMDA receptor subunit
N-terminus	amino terminus
PBS	phosphate-buffered saline
PCR	polymerase chain reaction
PDZ	postsynaptic density-95/discs-large/zona occludens 1
PFA	paraformaldehyde
pH	potentium hydrogenii
PKA	protein kinase A
ProSAP	proline-rich Synapse Associated protein
PSD	postsynaptic density
PSD95	postsynaptic density protein 95
Ref.	reference
RNA	ribonucleic acid
rpm	rounds per minute
RT	room temperature
SAP90	synapse-associated protein
SDS	sodium dodecyl sulphate
SEM	scanning electron microscopy
SEM	standard error of the mean
TAE	Tris-Acetate-EDTA
Tris	Tris(hydroxymethyl)-aminomethane
Tris –HCl	Tris(hydroxymethyl)-aminomethanhydrochloride
tRNA	transfer RNA
U	unit
VGCC	voltage-gated calcium channels
WB	western blot
wt	wild type

Curriculum Vitae

Name: Irina Zdobnova

Birthday: 15 July 1977

Place of birth: Ryzan, Russia

Nationality: Russian

Education & Experience:

2002 – 2007	PhD student, Leibniz Institute for Neurobiology, Department of Neurochemistry and Molecular Biology, Magdeburg
2000 – 2002	Practical training in the Department of Functional Biochemistry, Institute of Higher Nervous Activity and Neurophysiology, Moscow, Russia
1995 – 2000	Master of science in physiology from Moscow State University, Biology Department, Moscow, Russia
1985 –1995	High School, Ryzan, Russia

Scientific publications

- Dieterich, D.C., Karpova, A., Mikhaylova, M., Zdobnova, I., König, I., Landwehr, M., Kreutz, M., Smalla, K-H., Richter, K., Landgraf, P., Reissner, C., Böckers, T., Zuschratter, W., Spilker, C., Seidenbecher, C.I., Garner, C.C., Gundelfinger, E.D., Kreutz, M.R. Caldendrin – Jacob: A Protein Liaison that Controls NMDA Receptor Signalling to the Nucleus. PLoS Biology, in press.

- Stepanichev, M., Zdobnova, I., Zarubenko, I., Lazareva, N., Gulyaeva, N.V. (2006a) Differential effects of tumor necrosis factor-alpha co-administered with amyloid beta-peptide (25-35) on memory function and hippocampal damage in rat. Behav Brain Res. 175(2):352-361.

- Stepanichev, M., Zdobnova, I., Zarubenko, I., Lazareva, N., Gulyaeva, N.V. (2006b) Studies of the effects of central administration of beta-amyloid peptide (25-35): pathomorphological changes in the Hippocampus and impairment of spatial memory. Neurosci Behav Physiol. 36(1):101-106.

- Stepanichev, M., Zdobnova, I., Zarubenko, I., Moiseeva, Y.V., Lazareva, N., Onufriev, M.V., Gulyaeva, N.V. (2004) Amyloid-beta(25-35)-induced memory impairments correlate with cell loss in rat hippocampus. Physiol Behav. 80(5):647-655.

- Stepanichev, M., Zdobnova, I., Yakovlev, A.A., Onufriev, M.V., Lazareva, N., Zarubenko, I., Gulyaeva, N.V. (2003) Effects of tumor necrosis factor-alpha central administration on hippocampal damage in rat induced by amyloid beta-peptide (25-35). J Neurosci Res. 71(1):110-120.